**DOKUZ EYLÜL UNIVERSITY**

**GRADUATE SCHOOL OF NATURAL AND APPLIED SCIENCES**

# ANALYSIS OF SOME DRUGS IN COMPLEX MATRICES BY MICROEXTRACTION TECHNIQUES COUPLED WITH CHROMATOGRAPHIC TECHNIQUES

**by**

**Mahmood Saad Abdulwahid ALDOORI**

**April, 2023**

**İZMİR**

# ANALYSIS OF SOME DRUGS IN COMPLEX MATRICES BY MICROEXTRACTION TECHNIQUES COUPLED WITH CHROMATOGRAPHIC TECHNIQUES

**A Thesis Submitted to the**
**Graduate School of Natural and Applied Sciences of Dokuz Eylül University**
**In Partial Fulfillment of the Requirements for the Degree of Doctor of Philosophy in Chemistry, Analytical Chemistry Program**

**by**
**Mahmood Saad Abdulwahid ALDOORI**

**April, 2023**
**İZMİR**

**Ph.D. THESIS EXAMINATION RESULT FORM**

We have read the thesis entitled **"ANALYSIS OF SOME DRUGS IN COMPLEX MATRICES BY MICROEXTRACTION TECHNIQUES COUPLED WITH CHROMATOGRAPHIC TECHNIQUES"** completed by **MAHMOOD SAAD ABDULWAHID ALDOORI** under supervision of **PROF.DR. MELEK MERDİVAN** and we certify that in our opinion it is fully adequate, in scope and in quality, as a thesis for the degree of Doctor of Philosophy.

Prof. Dr. Melek MERDİVAN

Supervisor

Prof. Dr. Delia T. SPONZA

Thesis Committee Member

Prof. Dr. Serap SEYHAN BOZKURT

Thesis Committee Member

Prof. Dr. Müşerref ARDA

Examining Committee Member

Prof. Dr. Süleyman İNAN

Examining Committee Member

Prof. Dr. Okan FISTIKOĞLU

Director

Graduate School of Natural and Applied Sciences

## ACKNOWLEDGMENTS

I would like to express my gratitude to my thesis supervisor Prof. Dr. Melek MERDİVAN for her support, encouragement, guidance, and advice at all stages of this thesis study.

I gratefully want to thank Doç. Dr. Aylin ALTINIŞIK TAĞAÇ for helping me during laboratory studies, discussions and for her valuable contributions.

I would like to thank Prof. Dr. Serap SEYHAN BOZKURT and Dr. Taşkın MUMCU for their help during my chromatographic analysis.

Finally, I would like to express my deepest gratitude to my parents, Raya ALDOORI and Saad ALDOORI, who raised and supported me with patience and love. And of course, I am grateful to my lovely sisters, Shahad, Teba and Rasha ALDOORI for their encouragement.

Mahmood Saad Abdulwahid ALDOORI

**ANALYSIS OF SOME DRUGS IN COMPLEX MATRICES BY MICROEXTRACTION TECHNIQUES COUPLED WITH CHROMATOGRAPHIC TECHNIQUES**

## ABSTRACT

In this study, enrichment methods were developed for two different drug groups. In the first study, metal organic frameworks-based clay materials were synthesized for the extraction of sulfonamide and penicillin antibiotic drugs. By using these materials as adsorbent, antibiotics were extracted by dispersive micro solid phase extraction before analysis by high performance liquid chromatography. Sorbent materials prepared including montmorillonite and metal organic frameworks with copper nitrate and benzene-1,3,5-tricarboxylic acid were characterized. Before chromatographic determination of twelve selected antibiotics, dispersive micro solid phase extraction method parameters such as adsorbent amount, pH, extraction time and ionic strength were optimized. Analytical parameters were determined for both antibiotic groups. The accuracy and applicability of the developed methods were examined by studying real milk samples and synthetic urine solutions.

In another study, inflammatory drugs by high performance liquid chromatography and gas chromatography were determined after solid phase microextraction. Metal organic frameworks and montmorillonite based coating material containing copper nitrate and benzene-1,4-dicarboxylic acid for fiber was prepared and characterized. Analytes selected for determination by gas chromatography were derivatized because they were polar. Both chromatographic methods were optimized separately for the extraction method (extraction time, extraction temperature, pH, ionic strength) and desorption method (elution solvent type/volume and elution time, desorption time and desorption temperature). The analytical performances of the developed methods were examined. The applicability of tap water, wastewater, drug and synthetic urine samples

and the accuracy of the method by spiking the studied drugs were examined by recovery. High recoveries were obtained in both studies.

**Keywords:** Dispersive-micro-solid phase extraction, metal organic frameworks, drug, solid phase microextraction, GC, HPLC

# KROMATOGRAFİK TEKNİKLER İLE BİRLEŞTİRİLMİŞ MİKROEKSTRAKSİYON TEKNİKLERİ KULLANILARAK KOMPLEKS MATRİKSLERDE BAZI İLAÇLARIN ANALİZİ

## ÖZ

Tez çalışmasında iki ayrı ilaç grubu için zenginleştirme yöntemleri geliştirilmiştir. İlk çalışmada sulfonamid ve penisilin antibiyotik ilaçlarının ekstraksiyonu için metal organik kafes bazlı kil malzemeleri sentezlendi. Bu malzemeler adsorbent olarak kullanılarak, antibiyotiklerin yüksek performanslı sıvı kromatografisi ile analizi öncesi dispersive mikro katı faz ekstraksiyonu ile ekstraksiyonları sağlandı. Bakır nitrat ve benzen-1,3,5-trikarboksilik asit kullanılarak metal organik kafes ve montmorillonit kili kullanılarak hazırlanan sorbent malzemeleri karakterize edildi. Seçilen oniki adet antibiyotiğin kromatografik tayini öncesi dispersive mikro katı faz ekstraksiyonu yönteminin adsorbent miktarı, pH, ekstraksiyon süresi ve iyonik şiddet parametreleri optimize edildi. Her iki antibiyotik grubu için analitik parametreler belirlendi. Geliştirilen yöntemin doğruluğu ve uygulanabilirliği gerçek süt örneklerine ve sentetik idrar çözeltilerinde çalışılarak incelendi.

Diğer çalışmada steroid olmayan anti-inflamatuvar ilaçların yüksek performanslı sıvı kromatografisi ve gaz kromatografisi ile tayinleri öncesi katı faz mikroekstraksiyonu yöntemi geliştirildi. Bu amaçla fiber için bakır nitrat ve benzen-1,4-dikarboksilik asit içeren metal organik kafes ve montmorillonit bazlı kaplama malzemesi hazırlandı ve karakterize edildi. Gaz kromatgorafisi ile tayin için seçilen analitler polar oldukları için türevlendirildi. Ekstraksiyon yöntemi (ekstraksiyon süresi, ekstraksiyon sıcaklığı, pH, iyonik şiddet) ve desorpsiyon (elüsyon çözücüsü türü/hacmi ve elüsyon süresi, desorpsiyon süresi ve desorpsiyon sıcaklığı) için her iki kromatografik yöntem ayrı ayrı optimize edildi. Geliştirilen yöntemlerin analitik performansları incelendi. Musluk suyu, atıksu, ilaç ve sentetik idrar örnekleri ile uygulanabilirlikleri ve çalışılan ilaçların gerçek

örneklere eklenmesi ile yöntemin doğruluğu geri kazanım ile incelendi. Her iki çalışmada da yüksek geri kazanımlar elde edildi.

**Anahtar kelimeler:** Dispersif-mikro-katı faz ekstraksiyonu, metal organik kafesler, ilaç, katı faz mikroekstraksiyonu, GC, HPLC

**CONTENTS**

**Page**

THESIS EXAMINATION RESULT FORM ..... ii
ACKNOWLEDGMENTS ..... iii
ABSTRACT ..... iv
ÖZ ..... vi
LIST OF FIGURES ..... xi
LIST OF TABLES ..... xiv
LIST OF SYMBOLS ..... xv
ABBREVIATIONS ..... xvi

**CHAPTER ONE - INTRODUCTION ..... 1**

1.1 Antibiotics ..... 1
1.1.1 Sulfonamides (SAs) ..... 3
1.1.2 Penicillins (PENs) ..... 7
1.2 Non-Steroidal Anti-Inflammatory Drugs (NSAIDs) ..... 11
1.3 Metal Organic Frameworks (MOFs) ..... 14
1.4 Montmorillonite (MMT) ..... 15
1.5 Microextraction ..... 16
1.5.1 Dispersive Micro-Solid Phase Extraction (DMSPE) ..... 17
1.5.2 Solid-Phase Microextraction (SPME) ..... 18
1.6 Literature Review of the Detection of SAs and PENs using DMSPE ..... 19
1.7 Literature Review of the Detection of NSAIDs using SPME ..... 23
1.8 Aim of Study ..... 27

**CHAPTER TWO - EXPERIMENTAL STUDIES ..... 28**

2.1 Reagents, Solvents, and Preparation of Standard Solutions ..... 28
2.2 Material Characterization Instruments ..... 28

2.3 Experimental Studies of SAs and PENs using DMSPE Method ..... 29
2.3.1 Preparation of Cu-BTC ..... 29
2.3.2 Preparation of Cu-BTC/MMT Composites ..... 29
2.3.3 Determination of Point of Zero Charge (PZC) ..... 30
2.3.4 Sample Preparation ..... 30
2.3.5 DMSPE Method ..... 31
2.3.6 HPLC/DAD method for SAs and PENs Analysis ..... 31
2.3.7 Optimization of DMSPE Method ..... 32
2.3.8 Validation of DMSPE Method ..... 32
2.4 Experimental Studies of NSAIDs using SPME Method ..... 33
2.4.1 Synthesis of Cu-BDC ..... 33
2.4.2 Preparation of Cu-BDC/MMT Composites ..... 33
2.4.3 Preparation of SPME Fiber ..... 34
2.4.4 Sample Preparation ..... 35
2.4.5 Direct-Immersion-SPME (DI-SPME) Method for NSAIDs in HPLC/DAD…. 36
2.4.6 Analysis of NSAIDs by HPLC/DAD ..... 36
2.4.7 DI-SPME Method for NSAIDs by GC/MS After Derivatization ..... 36
2.4.8 Analysis of NSAIDs by GC/MS ..... 37
2.4.9 Optimization of DI-SPME Method for HPLC/DAD and GC/MS Determination of NSAIDs ..... 38
2.4.10 Optimization of Derivatization Parameters by GC/MS Determination ..... 38
2.4.11 Validation of SPME Method ..... 39

**CHAPTER THREE - RESULTS AND DISCUSSION ..... 40**

3.1 DMSPE Method ..... 40
3.1.1 Characterization of Cu-BTC and Cu-BTC/MMT composites ..... 40
3.1.1.1 FTIR Spectroscopy Results ..... 40
3.1.1.2 TGA Results ..... 42
3.1.1.3 XRD Results ..... 43

3.1.1.4 BET Results ..... 45
3.1.1.5 SEM Results ..... 46
3.1.2 Chromatographic Separation of SAs and PENs ..... 47
3.1.3 Optimization Conditions of DMSPE Method ..... 47
3.1.3.1 Choosing a Cu-BTC/MMT Composite ..... 48
3.1.3.2 pH Effect ..... 49
3.1.3.3 Effects of Sorbent Mass and Extraction Time ..... 51
3.1.3.4 Salt Effect ..... 52
3.1.3.5 Parameters of Desorption Solvent ..... 53
3.1.4 Reusability of Cu-BTC/MMT ..... 55
3.1.5 Method Validation ..... 56
3.1.6 Application to Milk Samples ..... 63
3.2 DI-SPME Method ..... 64
3.2.1 Characterization of Cu-BDC and Cu-BDC/MMT Composites ..... 64
3.2.2 Optimization of the DI-SPME Method for NSAIDs ..... 67
3.2.3 Optimization of Desorption Conditions for Determination of NSAIDs by Chromatographic Methods ..... 69
3.2.3.1 GC/MS ..... 69
3.2.3.2 HPLC/DAD ..... 71
3.2.4 Comparison of Fibers ..... 72
3.2.5 Method Validation ..... 73
3.2.6 Application to Real Samples ..... 74

**CHAPTER FOUR - CONCLUSIONS ..... 79**

**REFERENCES ..... 81**

## LIST OF FIGURES

**Page**

Figure 1.1 General chemical structure of SAs ..... 3
Figure 1.2 General chemical structure of PENs ..... 8
Figure 1.3 Structure of Cu-BTC (pink is Cu, grey is C, red is O, and white is H) ..... 15
Figure 1.4 The structure of MMT ..... 16
Figure 1.5 Representation of the main steps of the DMSPE method ..... 17
Figure 1.6 Illustration of the main steps of the SPME procedure ..... 19
Figure 3.1 FTIR spectra of Cu-BTC/MMT composites ..... 41
Figure 3.2 FTIR spectra of MMT, Cu-BTC, and Cu-BTC/MMT%2 ..... 41
Figure 3.3 TGA curves of MMT, Cu-BTC, and Cu-BTC/MMT%2 ..... 42
Figure 3.4 TGA curves of Cu-BTC/MMT composites ..... 43
Figure 3.5 XRD patterns of Cu-BTC and Cu-BTC/MMT%2 ..... 44
Figure 3.6 XRD patterns of MMT and Cu-BTC/MMT composites ..... 44
Figure 3.7 $N_2$ adsorption/desorption isotherms of Cu-BTC and Cu-BTC/MMT%2 ..... 45
Figure 3.8 SEM images of Cu-BTC (right) and Cu-BTC/MMT%2 composite (left) ..... 46
Figure 3.9 MMT mass effect in a composite of Cu-BTC/MMT on ER% of PENs and SAs ..... 49
Figure 3.10 Comparison of MMT, Cu-BTC, and Cu-BTC/MMT's extraction effectiveness ..... 49
Figure 3.11 pH effect on ER% of PENs and SAs ..... 50
Figure 3.12 PZC determination of Cu-BTC/MMT composite ..... 51
Figure 3.13 Effect of sorbent mass on ER% of PENs and SA ..... 51
Figure 3.14 Extraction time effect on ER% of PENs and SAs ..... 52
Figure 3.15 Effect of NaCl on ER% of PENs and SAs ..... 53
Figure 3.16 Effect of $Na_2SO_4$ on ER% of PENs and SAs ..... 53
Figure 3.17 Effect of elution solvent type on ER% of PENs and SAs ..... 54
Figure 3.18 Effect of elution volume on ER% of PENs and SAs ..... 54
Figure 3.19 Effect of elution time on ER% of PENs and SAs ..... 55
Figure 3.20 Reusability of Cu-BTC/MMT on adsorption of SAs and PENs ..... 56

Figure 3.21 Chromatograms of unfortified and fortified pasteurized milk in a glass bottle for PENs and SAs at 230 nm..... 62
Figure 3.22 Chromatograms of unfortified and fortified pasteurized milk in a glass bottle for PENs and SAs at 270 nm..... 63
Figure 3.23 FTIR spectrum of Cu-BDC and Cu-BDC/MMT composites..... 64
Figure 3.24 Thermal curves of Cu-BDC/MMT composites and Cu-BDC compound ... 65
Figure 3.25 XRD powder patterns of Cu-BDC/MMT composites and Cu-BDC compound ..... 66
Figure 3.26 SEM images of Cu-BDC and Cu-BDC/MMT%Y composites ..... 67
Figure 3.27 Optimizaiton of DI-SPME method using prepared Cu-BDC/MMT fiber, (A) pH, (B) salt effect, (C) extraction temperature and (D) extraction time ..... 69
Figure 3.28 Optimization of derivative conditions after DI-SPME method using prepared Cu-BDC/MMT fiber, (A) drying time, (B) derivative time, (C) derivative temperature and (D) reagent volume..... 70
Figure 3.29 Type of elution solvent (A), elution solvent volume (B), and elution solvent time (C) for analysis of HPLC/DAD method after DI-SPME using prepared Cu-BDC/MMT fiber ..... 71
Figure 3.30 Comparison of extraction efficiencies of Cu-BDC/MMT composites, Cu-BDC and MMT by DI-SPME method..... 72
Figure 3.31 HPLC chromatograms of blank (A) and 5 µg/L (B) and 50 µg/L (C) NSAIDs added tap water and wastewater samples (1: KET, 2: NAP, 3: DIC, 4: IBU)..... 77
Figure 3.32 HPLC chromatograms of diluted drug sample at 10 µg/L (A) and (20 µg/L (B) and 100 µg/L (C) NSAIDs added drug samples) (1: KET, 2: NAP, 3: DIC, 4: IBU)..... 77
Figure 3.33 GC chromatograms of blank (A) and 5 µg/L (B) and 50 µg/L (C) NSAIDs added tap water and wastewater samples (1: IBU, 2: NAP, 3: KET, 4: DIC)..... 78

Figure 3.34 GC chromatograms of diluted drug sample at 10 µg/L (A) and (20 µg/L (B) and 100 µg/L (C) NSAIDs added drug samples) (1: IBU, 2: NAP, 3: KET, 4: DIC)..... 78

**LIST OF TABLES**

**Page**

Table 1.1 Characteristics of SAs ..... 6
Table 1.2 Characteristics of PENs ..... 11
Table 1.3 Characteristics of NSAIDs ..... 14
Table 2.1 MS conditions for GC/MS analysis of NSAIDs (retention time, characteristic ions and time segment in SIM mode) ..... 37
Table 3.1 Results of $N_2$ adsorption-desorption isotherms ..... 46
Table 3.2 Retention times of Sulfonamides and Penicillins ..... 47
Table 3.3 Analytical performance of SAs and PENs using Cu-BTC/MMT in DMSPE method ..... 57
Table 3.4 Regression line parameters of DMSPE method for SAs ..... 58
Table 3.5 Regression line parameters of DMSPE method for PENs ..... 59
Table 3.6 RSD results of PENs and SAs ..... 60
Table 3.7 RRs and RSDs of PENs and SAs in milk samples ..... 61
Table 3.8 RRs and RSDs of PENs and SAs in synthetic urine ..... 62
Table 3.9 Analytical performance of Cu-BDC/MMT for NSAIDs by DI-SPME-HPLC/DAD ..... 73
Table 3.10 Analytical performance of Cu-BDC/MMT for NSAIDs by DI-SPME-GC/MS. ..... 74
Table 3.11 RRs and RSDs % of NSAIDs in synthetic urine solution and water and drug samples by DI-SPME-HPLC/DAD method ..... 75
Table 3.12 RRs and RSDs % of NSAIDs in synthetic urine solution and water and drug samples by DI-SPME-GC/MS method ..... 76

## LIST OF SYMBOLS

| | |
|---|---|
| β | : Beta |
| h | : Hour |
| °C | : Celsius degree |
| µg/L | : Micrograms per liter |
| pKa | : Acid dissociation constant |
| mg/L | : Milligrams per liter |
| % | : Percentage |
| µg/kg | : Micrograms per kilogram |
| pH | : Power of Hydrogen (acidity scale) |
| g, mg | : Gram, Milligram |
| min | : Minute |
| µL, mL | : Microliter, Milliliter |
| s | : Second |
| v/v | : Percent by volume |
| ng/g | : Nanograms per gram |
| M | : Molar concentration |
| º | : Degree sign |
| °C/min | : Celsius degrees per minute |
| wt% | : Weight percent |
| rpm | : Rotations per minute |
| nm, µm, mm | : Nanometer, Micrometer, Millimeter |
| Å | : Angstrom |
| mL/min | : Milliliters per minute |
| mg/mL, µg/mL | : Milligrams per milliliter, Micrograms per milliliter |
| eV | : Electron volte |
| m/z | : Mass to charge ratio |
| w/v | : Weight to volume percent |
| $R^2$ | : Correlation coefficient |

**ABBREVIATIONS**

| | |
|---|---|
| EU | : European Union |
| MRL | : Maximum Residue Limit |
| EC | : European Union |
| HPLC | : High Performance Liquid Chromatography |
| GC/MS | : Gas Chromatography/Mass Spectrometry |
| SAs | : Sulfonamides |
| SMT | : Sulfamethizole |
| DHPS | : Dihydropteroate Synthetase |
| SMX | : Sulfamethoxazole |
| SSX | : Sulfisoxazole |
| SDA | : Sulfadiazine |
| SDMX | : Sulfadimethoxine |
| SCP | : Sulfachloropyridazine |
| PENs | : Penicillins |
| AMX | : Amoxicillin |
| AMP | : Ampicillin |
| DICLO | : Dicloxacillin |
| CLO | : Cloxacillin |
| NAF | : Nafcillin |
| PEN G | : Penicillin G |
| NSAIDs | : Non-Steroidal Anti-Inflammatory Drugs |
| COX | : Cyclooxygenase |
| SPME | : Solid-Phase Microextraction |
| LPME | : Liquid-Phase Microextraction |
| SPE | : Solid-Phase Microextraction |
| DLLME | : Dispersive Liquid-Liquid Microextraction |
| IBU | : Ibuprofen |
| DIC | : Diclofenac |

| | |
|---|---|
| KET | : Ketoprofen |
| NAP | : Naproxen |
| MOFs | : Metal Organic Frameworks |
| Cu-BTC | : Copper Benzene-1,3,5-tricarboxylate |
| MMT | : Montmorillonite |
| DMSPE | : Dispersive Micro-Solid Phase Extraction |
| Cu-BDC | : Copper Benzene-1,4-dicarboxylate |
| UHPLC-MS/MS | : Ultrahigh Performance Liquid Chromatography-tandem Mass Spectroscopy |
| RSD | : Relative Standard Deviation |
| d-SPE | : Dispersive Solid-Phase Extraction |
| HPLC/DAD | : High Performance Liquid Chromatography/Diode-Array Detection |
| COU-2 | : mesoporous carbon |
| HPLC/UV | : High Performance Liquid Chromatography/ Ultraviolet Detection |
| MDSPE | : Magnetic Dispersive Solid-Phase Extraction |
| GC/FID | : Gas Chromatography/Flame Ionization Detector |
| LDH-ACA | : Layered Double Hydroxide Acid-Calix[4]Arene |
| LR | : Linear Range |
| LOD | : Limit of Detection |
| LOQ | : Limit of Quantitation |
| ACN | : Acetonitrile |
| MeOH | : Methanol |
| FTIR | : Fourier Transform Infrared Spectroscopy |
| DMF | : Dimethylformamide |
| TFA | : Trifluoroacetic Acid |
| MSTFA | : N-Methyl-N-(trimethylsilyl)trifluoroacetamide |
| MDEU | : Modified Dihydroxy Ethylene Urea |
| TGA | : Thermal Gravimetric Analysis |
| BET | : Brunauer-Emmett-Teller |
| PZC | : Point of Zero Charge |

| | |
|---|---|
| XRD | : X-Ray Diffraction |
| SEM | : Scanning Electron Microscopy |
| PTFE | : Polytetrafluoroethylene |
| SSW | : Stainless Steel Wire |
| DI-SPME | : Direct-Immersion- Solid-Phase Microextraction |
| SIM | : Selected Ion Monitoring |
| ER | : Extraction Recovery |
| SD | : Standard Deviation |
| RR | : Relative Recovery |

# CHAPTER ONE
# INTRODUCTION

## 1.1 Antibiotics

Antibiotics are a class of very effective antimicrobial substances used in treating and preventing infectious diseases in both human and veterinary medicine. They either destroy bacteria or inhibit their reproduction (Majdinasab, Mishra, Tang, & Marty, 2020; Ben et al., 2019). Approximately 220 types of antibiotics are found in world, although more than 250 semi-synthetic or modified natural product-based medications are produced (Bérdy, 2012). According to various functional chemical structures, antibiotics can be categorized into ten major categories: quinolones, macrolides, polypeptides, β-lactams, lincosamides, sulfonamides, tetracyclines, aminoglycoside, chloramphenicol, and others (Wang et al., 2015).

Veterinary antibiotics were initially preferred for preventing and treating animal infections, however now they are mostly used as feed components, prophylactics, and growth boosters, vastly outweighing their initial intended purpose for treating animals (Gelband et al., 2015). Aquaculture and cattle sectors utilize large amounts of antibiotics each year, but their improper usage has long-term negative impacts on both human health and the environment (Kolpin et al., 2002). Antibiotics can be carried in water and land environment by means of several different paths, including the release of sewage water from public facilities, the manufacturing sector, livestock farming, and garbage leachates of antibiotic disposal (Ashbolt et al., 2013). The use of treated wastewater for watering and animal dung for fertilizer are two of the most likely routes for the spread of antibiotics into the agricultural system (Ji et al., 2010). Antibiotic residues that take place in the environment are considered stable organic pollutants due to their regular and broad use as well as continuous emissions (Ben et al., 2019).

When animals are given antibiotics, they may leave antibiotic residues in foods, including fish, milk, eggs, beef, poultry meat, and honey (Majdinasab et al., 2017). In humans, these medications' residues can cause allergic reactions, immune effects, liver toxicity, nephropathy, carcinogenic effects, bone marrow poisoning, and pregnancy complications (Bacanlı & Başaran, 2019). Antibiotic residues in food are regarded as undesirable results because of the occurrence of antimicrobial resistance which has been a big problem in the world. Through the food chain, bacterial disease pathogens that are resistant to treatment can reach people, which might contribute to antibiotic therapy's ineffectiveness (Leibovici et al., 2016). Some antimicrobial growth has been forbidden by the European Union (EU) due to the undesirable effects of veterinary drugs like antibiotics. Maximum Residue Limit (MRL) for not prohibited ones has been established by the United States and EU to the protection of consumers from exposure to antibiotic residue in animal-derived foods (Majdinasab et al., 2017). There is no risk to the consumer's health below this level (Ngangom, Tamunjoh, & Boyom, 2019). It is an important necessity of screening methods with high sensitivity and selective monitoring of veterinary residues to ensure the amounts of antibiotic residues in food below the MRL. The screening method includes extracting, identifying, and isolating a chemical or a class of substances from a sample at the interested level. Results obtained from screening methods are typically qualitative or semi-quantitative (European Commission [EC], 2002).

These techniques can be divided into traditional and modern ways. Traditional methods have been applied for a long time, including microbiological and immunological techniques. The sensitivity and specificity of microbiological procedures are low despite their ease of use, speed, and low cost (Chen et al., 2017). Modern methods rely on new technologies and recognition items (Gaudin, 2017). Analytical techniques based on chromatography such as high-performance liquid chromatography (HPLC), liquid chromatography-mass spectroscopy, and gas chromatography-mass spectrometry (GC/MS) are used for confirmation of the accuracy of the screening methods (Chiesa, Nobile, Panseri, & Arioli, 2017; Hlabangana & Memeza, 2018).

### *1.1.1 Sulfonamides (SAs)*

One group of synthetic antimicrobials known as sulfonamides are typically referred to human and veterinary clinical medicine to diagnose and treat contagious diseases caused by microorganisms (Dai et al., 2016; Jia et al., 2017). Under the trade name Prontosil, the Bayer firm first created SAs as antibacterial drugs, which are structurally related to amino and sulfonyl groups, in the 1930s. Over ten SAs and their derived products have been recently utilized in animals that are used for food production for the aim of medicinal, protective, and encouraging growth (Shih, Wang, Singco, Lin, & Huang, 2016). Nevertheless, misuse and unnecessary dosage of SAs can lead to chemical residue buildup in livestock, which can subsequently lead to veterinary products that have negative effects on humans like extreme allergic reactions, drug resistance disorders, and even cancer-causing effects (Di Corcia & Nazzari, 2002; Koesukwiwat, Jayanta, & Leepipatpiboon, 2007). Additionally, SAs are biologically poisonous and challenging to remove using traditional biochemical sewage treatment methods. As a result, wastewater treatment facilities release frequently these substances and their metabolites into environmental water domains, causing spreading around and allowing substantial risks to the environment and hygiene (Pu et al., 2020). Several studies on the detection of SAs in environmental water, foods such as eggs, milk, and honey have been published (Dai et al., 2016). The chemical structure of SAs are given in Figure 1.1.

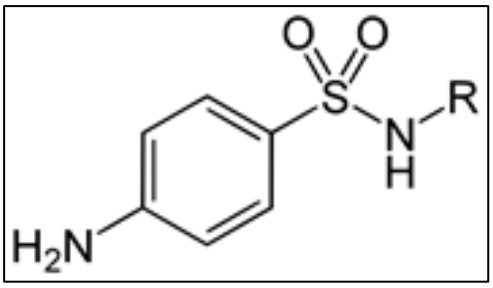



Figure 1.1 General chemical structure of SAs (Raich-Montiu, Beltrán, Prat, & Granados, 2010)

Sulfamethizole (SMT), one of the sulfonamides, is used to treat infections caused by bacteria in humans and animals. SMT adopted by the food and drug administration in 1953 is strongly linked to the inactivation of dihydropteroate synthetase (Yuan et al., 2019). It is generally preferred to cure urinary tract infections and interpreting stomach emptying in people with functional dyspepsia (Alalawy et al., 2022). Because of its quick metabolism and methodical removal, SMT has a short half-life of 2.1 h (Suresh et al., 2015).

Sulfamethoxazole (SMX) is a widely used antibiotic. It is utilized to treat prostatitis, intestinal infections, extreme urinary tract infections, and respiratory infections. The task of SMX is ending the dihydrofolic acid synthesis which is important for alive of bacteria. It is also utilized as a herbicide and for preventive care in aquaculture as well as for the treatment of diseases in animals. The solubility of SMX in water is low (0.61 g/L at 37 °C) and a half-life is about 10 h (Habila et al., 2021; Mestre & Carvalho, 2019). SMX commonly takes place in soil, wastewater and feces at high concentrations as mg/L. SMX has been categorized as a third-degree carcinogen by the world health organization. The residues of SMX passing to drinking water and food chains are harmful to human beings, animals, and other living things. These residues could cause growing bacteria that are persistent in medication, which causes a significant risk to humans and the environment (Wang et al., 2020).

Sulfisoxazole (SSX) is a popular SA antibiotic that is utilized to prevent or cure bacterial infections such as ear infections, respiratory infections, and bladder infections. SSX exhibits an antibiotic effect on gram-negative and gram-positive bacteria (Bavandpour, Rajabi, & Karimi-Maleh, 2020), by working as a selective inhibitor of p-amino benzoic acid, a source for the DHPS, and therefore preventing the production of dihydrofolic acid, which is essential for bacteria to stay alive (Sabry et al., 2022). The use of SSX in veterinary medicine has regrettably led to the emergence of Escherichia coli which is resistant to SSX. Additionally, SSX has been listed as a Group 3 carcinogen as of 2017. The harmful effects of SSX can include hypersensitivity and

endocrine disturbances (El-Azazy, Ahsan, & Bensalah, 2022). Furthermore, SSX at high doses has a long list of undesirable side effects, including breathlessness, diarrhea, appetite loss, joint pain, and stomach aches (Bavandpour et al., 2020).

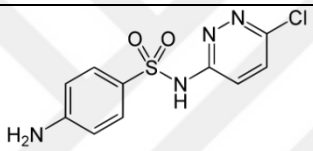
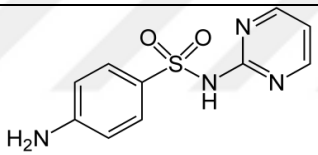
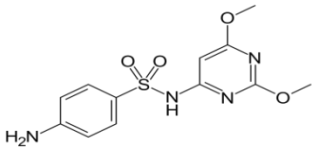
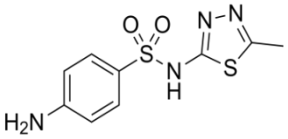
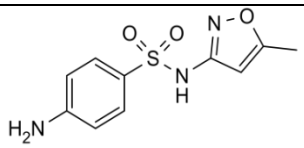
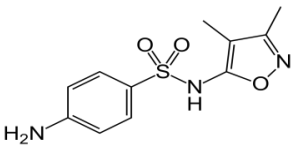
Sulfadiazine (SDA) is a common antibiotic that is frequently employed in daily life. Due to the inability of human and animal bodies to completely disintegrate the p-aminophenamide of SDA, the remaining amounts of SDA are excreted into the environment. Because of the chronic toxicity of SDA, this process provides a significant health danger to the environment (Zhu, Shi, Deng, & Duan, 2021). In its free form, SDA is often employed as a sodium salt. It is used to treat toxoplasmosis, wound sepsis, chancroid, and nocardiosis. It can be identified as a common therapy antibiotic used in veterinary and human medicine with stabilized curative effects (Sriram et al., 2021). Excessive exposure to SDA can lead to unfavorable physiological and biochemical circumstances, including liver failure, antibiotic-resistant, gene harm, and toxicity in all living things (Kokulnathan, Ashok Kumar, & Wang, 2020).

Sulfadimethoxine (SDMX) is an SA antibiotic that is frequently utilized for treating bacterial infections in cattle and aquatic organisms. However, SDMX has reached the ecosystem through animal metabolism and the food chain due to its improper and immoderate use. The toxic effects of SDMX, which have grown to be a critical challenge for both human health and the environment, can be seen even at low concentrations of SDMX. The EU and China have imposed an MRL value of 100 µg/L for SDMX in food products (Dang et al., 2018). Additionally, studies have demonstrated that even at low concentrations, SDMX is poisonous to the organs it targets, including the liver and kidney (Zuo, He, Wang, & Wei, 2022).

Sulfachloropyridazine (SCP) is an antibacterial drug in the sulfanilamide category. It typically works against chlamydia and is used as an inhibitor of aerobic bacteria. SCP and its derivatives are being extensively utilized in veterinary medicine. SCP has been found in the environment all around the world, including in surface water and

groundwater due to its widespread use in the livestock sector (Xinbao, Yating, Ali, Nan, & Hongkun, 2019). There are possible dangers to ecosystems and human health from bioaccumulation of SCP, which even at low concentrations of SCP can result in alterations in resistance genes for long-term exposure to aquatic creatures in the environment (Tao et al., 2020). Table 1.1 represents some properties of SAs.

Table 1.1 Characteristics of SAs (Babić, Horvat, Pavlovic, & Kaštelan-Macan, 2007; Zhou, Yang, Ji, & Wei, 2019; He, Jain, & Yalkowsky, 2010)

| **SAs** | **Chemical structure** | **Chemical formula** | **Molecular weight (g/mol)** | **$pKa_1$, $pKa_2$** | **Water solubility (mg/L)** |
|---|---|---|---|---|---|
| SCP |  | $C_{10}H_9ClN_4O_2S$ | 284.7 | 1.9, 5.4 | 321 |
| SDA |  | $C_{10}H_{10}N_4O_2S$ | 250.3 | 2.1, 6.28 | 77 |
| SDMX |  | $C_{12}H_{14}N_4O_4S$ | 310.3 | 1.87, 5.86 | 343 |
| SMT |  | $C_9H_{10}N_4O_2S_2$ | 270.3 | 2.1, 5.3 | 1050 |
| SMX |  | $C_{10}H_{11}N_3O_3S$ | 253.3 | 1.6, 5.7 | 610 |
| SSX |  | $C_{11}H_{13}N_3O_3S$ | 267.3 | 1.5, 5 | 300 |

### *1.1.2 Penicillins (PENs)*

PENs belong to the class of bicyclic chemical compounds distinguished by the presence of a thiazoline ring linked to a β-lactam ring. Since Alexander Fleming's discovery of the antibiotic PEN in 1928, a variety of microbial illnesses have been successfully treated with it. These medications prohibit the enzymes necessary for the cell wall's peptidoglycan to be produced. PENs are categorized depending on their effectiveness, or their ability to inhibit bacterial β-lactamases, allowing them to be employed as narrow-spectrum antibiotics. Third-generation broad-spectrum PENs, which are semi-synthetic adaptations of natural PEN, were first released in the 1960s. They are more powerful against gram-negative and gram-positive bacteria (Alampanos, Samanidou, & Papadoyannis, 2019; Hrioua et al., 2021).

Due to its potent pharmacological effects, PEN is used as a drug to treat bacterial diseases such as strep throat, diphtheria, leptospirosis, pneumonia, and gas gangrene. Various biotechnology, pharmaceutical, and cosmetic firms have manufactured this medication due to its broad range of therapeutic applications in both people and livestock. The wide use of penicillins in treatment directly and limitless consuming causes unwanted results such as the spreading of drug-resistant bacteria and drug-induced hypersensitization (Salihu, Yusof, Mohammad, Abdullah, & Al-Lohedam, 2019). MRL values were determined in European countries and Taiwan for observing the current antibiotic drugs. For instance, the MRL value for milk is ranged from 4 to 300 μg/L based on the available β-lactam antibiotic drugs (Lirio, Liu, Lin, Lin, & Huang, 2016). The PENs chemical structrures are given in Figure 1.2.

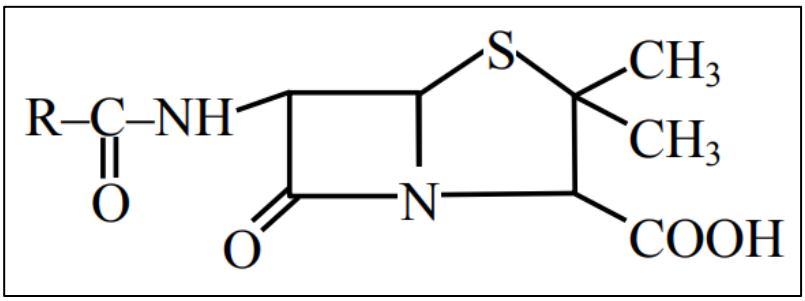



Figure 1.2 General chemical structure of PENs (Vardanyan & Hruby, 2006)

Amoxicillin (AMX) belongs to the group of PENs known as β-lactam antibiotics. It is a semi-synthetic antibiotic. In addition, bacteria cell wall production is prevented by a beta-lactam ring and this causes the bacteria to disappear (Fallahzadeh et al., 2019). Beecham Research Laboratory discovered AMX at the beginning of the 1970s as "amoxil" brand name and later it was marketed as "amoxicillin" brand name (Aryee, Han, & Qu, 2022). AMX has shown to be efficient against a variety of illnesses brought on by both gram-positive and gram-negative bacteria. It has been preferred in the treatment of many bacterial infections that are effective in the urinary system, lungs, skin, throat, ear, and nose. These infections include tonsillitis, pharyngitis, respiratory infections, gastrointestinal disorders, duodenal ulcer diseases, skin bacterial infections, and urinary tract infections (Hrioua et al., 2021; Trucillo, Ferrari, Campardelli, Reverchon, & Perego, 2020). The MRL value for AMX in food derived from animals was set at 50 µg/kg by the EU in 2010. Humans excrete around 60% of the AMX they ingest through urine, without having it decomposed (Fallahzadeh et al., 2019).

Ampicillin (AMP) is a popular β-lactam antibiotic. It has been extensively employed in medicine to cure a variety of bacterial diseases, including meningitis, salmonellosis, endocarditis, urinary infection, respiratory infection, and sepsis (Gawrońska, Kowalik, & Makowski, 2022). Humans excrete more than 30% of the whole dosage of AMP as partly metabolized or derivatives of AMP. The existence of AMP or its derivatives in the environment can cause it to enter food chains and aquatic life, as well as increase the number of bacteria that are resistant to antibiotics. This poses a serious risk to human

and animal health and complicates efforts to control bacterial infections (Al-Musawi, Rajiv, Mengelizadeh, Arghavan, & Balarak, 2021).

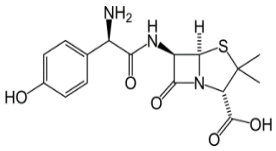
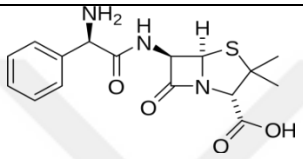
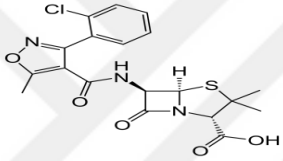
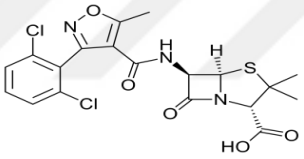
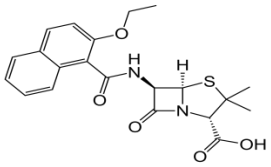
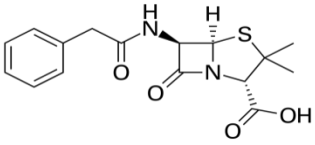
Dicloxacillin (DICLO) is a β-lactam antibiotic and is a member of the penicillin family. It is employed to cure gram-positive bacterial infections. DICLO effectively destroys the bacteria by preventing the manufacture of the cell wall. People eliminate around 65% of the DICLO they eat through urine without being decomposed, which has severe effects on aquatic systems and perhaps enhances the growth of antibiotic-resistant bacteria and genes that result in having their way into the environment (Sunsandee, Ramakul, Phatanasri, & Pancharoen, 2020; Alvarez-García & Ramírez-García, 2021). The EU set MRL values for DICLO as 50 µg/kg in the liver and 300 µg/kg in muscle and milk (Pang, 2018). DICLO is now widely used to cure pneumonia and other bacterial infections of the urinary tract, skin, bone, and ear (Alshamsan et al., 2019).

Cloxacillin (CLO) is a beta-lactam antibiotic from the penicillin family. It prevents the formation of the bacterial wall. CLO is exceptionally efficient at controlling and curing staphylococcal bacterial infections. CLO can cure a variety of illnesses, including cellulitis, impetigo, pneumonia, urinary tract infections, skin infections, and wound infections. The half-life of CLO ranges from 1 to 5 h. It can be extended to 2.5 h in cases with impaired kidney function. The kidney typically excretes between (30-60 %) of the CLO through urine without being decomposed (Jafari, Dehghani, Nasirizadeh, Baghersad, & Azimzadeh, 2019; Malafatti et al., 2021). The use of CLO in animals incorrectly or for an extended time can lead to the buildup of CLO in animals raised for food production. These residues might cause a potential risk to human health and be also harmful to the environment by being permanent as drugs in soil and water. The determined MRL value of CLO is 300 µg/kg in muscle and 30 µg/kg in milk by EU (Zhang, Zhang, Zhao, Chen, & He, 2020).

Nafcillin (NAF) is a beta-lactam antibiotic. Due to its effectiveness, NAF has been widely employed to cure infections caused by penicillinase-producing staphylococci, including soft tissue infections, catheter-related infections, and endocarditis. NAF has been documented to be associated with the possibility of hepatotoxicity and acute interstitial nephritis, even though NAF is well tolerated and has few adverse effects. NAF misuse in livestock can result in residue troubles in cattle, which poses a significant health risk. The MRL value of NAF is evaluated as 30 µg/kg in milk and 300 µg/kg in fat, liver, and muscle (Guardia, Badia, Granda-Valdes, & Diaz-Garcia, 2020).

Penicillin G (PEN G) is a narrow-spectrum antibiotic and is known as benzylpenicillin. PEN G is commonly employed to cure certain bacterial infections. PEN G is effective against anthrax bacillus, diphtheria's causative agent, and gram-positive bacteria such as staphylococcus, streptococcus, and pneumococci. Stomach acid decomposes PEN G. It is found in pharmaceutical preparations as potassium or sodium salts that are water-soluble. Using biotechnology, the fungus Penicillium chrysogenum works as the source of PEN G. PEN G is employed for skin infections, soft tissue and mucous membrane infections, urinary tract infections, syphilis, diphtheria, and other infectious disorders (Baezzat, Pourghobadi, & Pourghobadi, 2021; Vardanyan & Hruby, 2006). Table 1.2 represents some properties of PENs.

Table 1.2 Characteristics of PENs (He et al., 2010; Bylund & Enna, 2008)

| PENs | Chemical structure | Chemical formula | Molecular weight (g/mol) | $pKa_1$, $pKa_2$ | Water solubility (mg/L) |
|---|---|---|---|---|---|
| AMX |  | $C_{16}H_{19}N_3O_5S$ | 365.4 | 2.4, 9.6 | 4000 |
| AMP |  | $C_{16}H_{19}N_3O_4S$ | 349.4 | 2.5, 7.2 | 2306 |
| CLO |  | $C_{19}H_{18}ClN_3O_5S$ | 435.9 | 2.8, - | 53.2 |
| DICLO |  | $C_{19}H_{17}Cl_2N_3O_5S$ | 470.3 | 2.5, - | 30 |
| NAF |  | $C_{21}H_{22}N_2O_5S$ | 414.5 | 2.7, - | 17.2 |
| PEN G |  | $C_{16}H_{18}N_2O_4S$ | 334.4 | 2.8, - | 2675 |

## 1.2 Non-Steroidal Anti-Inflammatory Drugs (NSAIDs)

The most widely used analgesics in the world are NSAIDs. They are primarily used for treating fever, inflammation, and pain in humans and animals. NSAIDs can lengthen human life, lower the risk of Alzheimer's disease, and enhance the qualitative attributes of milk products (Mirzajani, Kardani, & Ramezani, 2019). The pharmacological effects

of NSAIDs are associated with their ability to treat inflammation by inhibiting cyclooxygenase (COX), a vital enzyme in prostaglandin formation, at the inflammation site (Barfi et al., 2015).

In cases of chronic use or overdose, NSAIDs can cause several toxic side effects, such as the risk of cardiovascular disease, platelet dysfunction, an increased risk of renal injury, risk of hepatic tumors, gastrointestinal mucosal injury, and the extension of pregnancy or spontaneous delivery. Consequently, it is crucial for human health to monitor and assess the risks associated with NSAIDs in the environment. Specialized and sensitive analytical techniques such as solid-phase extraction (SPE), and dispersive liquid-liquid microextraction (DLLME), liquid-phase microextraction (LPME), and solid-phase microextraction (SPME) has been applied for detection of NSAIDs at low concentrations in biological materials (Liu et al., 2019; Mirzajani et al., 2019). Depending upon their chemical structure, NSAIDs are categorized into five groups; propionic acid derivatives (ibuprofen, naproxen), salicylates (aspirin, diflunisal), acetic acid derivatives (indomethacin, diclofenac), enolic acid derivatives (piroxicam, meloxicam), and anthranilates (mefenamic acid) (Ghlichloo & Gerriets, 2019; Bindu, Mazumder, & Bandyopadhyyay, 2020).

Ibuprofen (IBU) is among the most used anti-inflammatory, analgesic, and antipyretic medications nowadays. In 1969, IBU which is the first member of the propionic acid derivative family was marketed as an excellent aspirin substitute. It is COX-1 and COX-2's non-selective inhibitor. A serum half-life of 1.8 to 2 h indicates that IBU undergoes fast biotransformation. After the final dose, the medication is metabolized away within 24 h. IBU is primarily employed therapeutically to treat spondylitis, osteoarthritis, and soft tissue disorders, as well as the treatment of severe orthostatic hypotension, tooth pain, rheumatoid osteoarthritis, dysmenorrhea, fever, and headache. Also, IBU is used as a preventative for diseases like Alzheimer's, Cystic fibrosis, Parkinson's, and breast cancer (Bushra & Aslam, 2010; Rainsford, 2009).

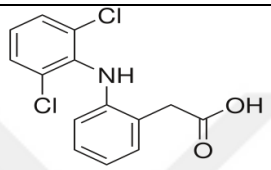
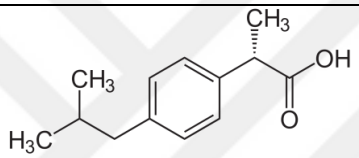
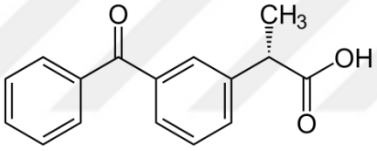
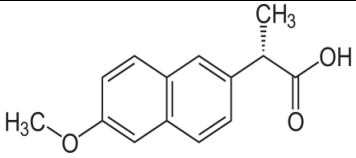
Diclofenac (DIC) is a member of the phenylacetic acid family and has analgesic, antipyretic, and anti-inflammatory effects. DIC has an inhibitory effect on the COX-2 enzyme more potently than it does on the COX-1 enzyme, which is the opposite of the way most conventional NSAIDs behave. To increase effectiveness, tolerability, and patient comfort, various alternative DIC-containing medicinal formulations have been produced since the compound was first introduced in 1973. DIC's biological half-life is approximately 2 h, and its removal rate is quick. The amount of DIC dosage eliminated in the urine and biliary is around 65% and 35%, respectively. DIC has the highest toxic effect among all NSAIDs and has been found in surface water and sewage treatment facilities due to its widespread usage and impedance to the biological degradation process in the water environment (Altman, Bosch, Brune, Patrignani, & Young, 2015; Rosset, Sfreddo, Hidalgo, Perez-Lopez, & Feris, 2019).

Ketoprofen (KET) is a propionic acid derivative that possesses anti-inflammatory, analgesic, and antipyretic characteristics. It was created in 1968. KET is frequently employed because of its quick absorption, straightforward metabolism, and effectiveness. Nevertheless, the main reasons impacting this drug's publicity are the numerous negative effects that KET produces. KET is employed to treat rheumatoid arthritis, ankylosing spondylitis, and lower backache. KET is also used to treat pains after a surgical operation and trauma. Its biological half-life is about 1.5 to 4 h. The amount of KET dosage eliminated in the urine is approximately 80% (Miles, 2007; Kuczyńska & Nieradko-Iwanicka, 2021).

Naproxen (NAP) is a well-known medication from the class of non-selective NSAIDs. It is a propionic acid derivative. NAP first became available on the market in 1976. NAP inhibits COX-1 and COX-2, which are necessary to produce prostacyclin, thromboxane, and prostaglandins from arachidonic acid. The benefits of NAP include its quick absorption, prolonged duration of effect due to its biological half-life of about 13 h, and its ability to firmly bind to plasma proteins. Its diffusion into the synovial fluid is another benefit. NAP is the recommended medication when treating osteoarthritis in

people with a high cardiovascular risk (Wojcieszyńska & Guzik, 2020). Table 1.3 reprepsents some properties of NSAIDs.

Table 1.3 Characteristics of NSAIDs (He et al., 2010; Bylund & Enna, 2008; Mestre & Carvalho, 2019)

| NSAIDs | Chemical structure | Chemical formula | Molecular weight (g/mol) | pKa | Water solubility (mg/L) |
|---|---|---|---|---|---|
| DIC |  | $C_{14}H_{11}Cl_2NO_2$ | 296.16 | 4.15 | 2.37 |
| IBU |  | $C_{13}H_{18}O_2$ | 206.29 | 5.2 | 21 |
| KET |  | $C_{16}H_{14}O_3$ | 254.29 | 5.94 | 51 |
| NAP |  | $C_{14}H_{14}O_3$ | 230.27 | 4.15 | 15.9 |

## 1.3 Metal Organic Frameworks (MOFs)

MOFs are well-coordinated, cavity-filled, and porous crystalline structures. MOFs consist of organic linkers and inorganic metal ions bonded by strong bonds to create a complicated bi-dimensional or three-dimensional net. In the middle of the 1990s, MOFs have been interested due to their intriguing architectures and distinctive qualities (Gutiérrez-Serpa, Pacheco-Fernández, Pasán, & Pino, 2019; Li, Chen, Yang, Wang, & Liu, 2020). One of the most well-known examples of MOFs is copper bound to benzene-1,3,5-tricarboxylate (Cu-BTC). It is also known as MOF-199 or HKUST-1

(Marx, Kleist, & Baiker, 2011; Phuong et al., 2016). Figure 1.3 represents the Cu-BTC MOF structure.

Some incredible characteristics of MOFs in comparison to other materials include wide surface area, clear pore architecture, great chemical, and thermal stability, facile tunability, and uncomplicated preparation. MOFs are used in an astonishing variety of scientific domains, including gas storage systems, photovoltaic materials, and gas purifying and separating. Concerning their application in analytical chemistry, MOFs are principally preferred as sorbents in sample preparation methods, and stationary phases in separation techniques, profiting from tunability, their high surface area, and chemical and thermal stability. Apart from this, they take advantage of being sensors in electrochemical techniques (Rocío-Bautista, Taima-Mancera, Pasán, & Pino, 2019; Gutiérrez-Serpa et al., 2019; Li et al, 2020).

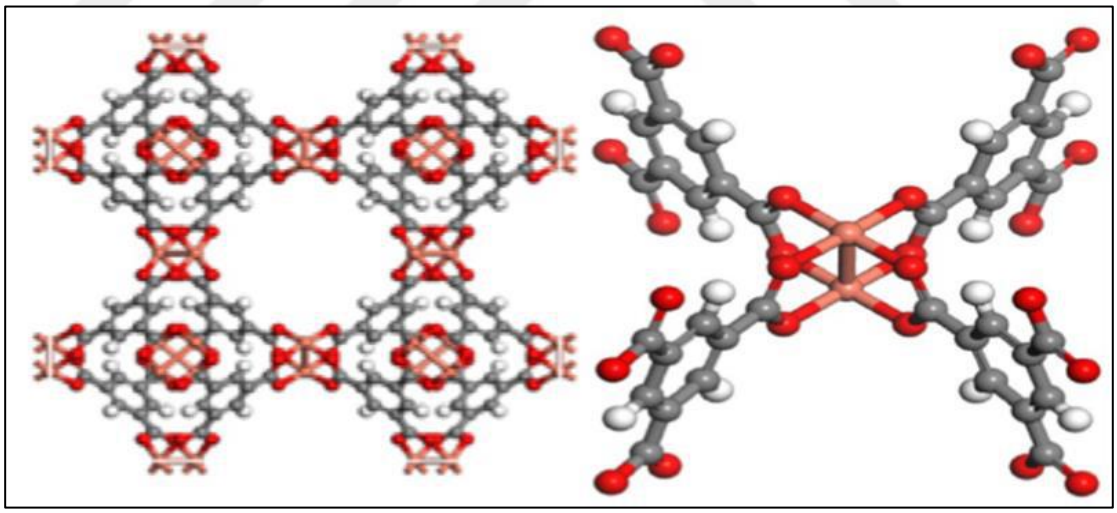


Figure 1.3 Structure of Cu-BTC (pink is Cu, grey is C, red is O, and white is H) (Zhang et al., 2018)

### 1.4 Montmorillonite (MMT)

MMT is a special kind of smectitic clay and is common in the natural environment. MMT is a fairly soft phyllosilicate. The term MMT derives from Montmorillon, France, where it was first discovered. Three layers contribute to MMT: one octahedral layer of

aluminum in the middle flanked by two tetrahedral layers of silica. MMT has Na, Ca, A, Mg, and Si besides water in its chemical structure and its formula is given as (Na, $Ca)_{0.33}$(Al, Mg)$2Si_4O_{10}(OH)_2.nH_2O$ (Gu, Kang, Wang, Lichtfouse, & Wang, 2019). Figure 1.4 shows the structure of MMT. For many years, a variety of applications have made use of MMT clay. MMT clay is commonly employed in the field of treating tropical illnesses due to its substantial bioactivities. In the food sector, acid-activated MMT clay is frequently used as a bleach. Modified MMT has a great adsorption capacity for removing heavy metals from aqueous environments with the help of its wide surface area and extendable layered structure (De Paiva, Morales, & Diaz, 2008; Wang, Yang, Zhang, Wang, & Li, 2014).

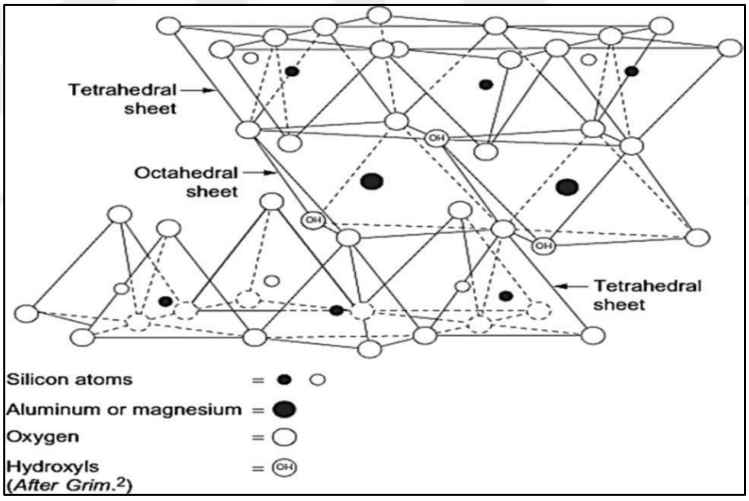



Figure 1.4 The structure of MMT (Gu et al., 2019)

## 1.5 Microextraction

In the microextraction method, some of the analytes are extracted and a small volume of extracting phase is sufficient. This volume is very small compared to the total volume of the sample (Lord & Pawliszyn, 2000). Analytical procedures generally include four steps, these are in turn, collection of samples, preparation of samples, separation of analytes from the matrix, and the analysis of analytes in the sample. The most significant step is the sample preparation due to analyte loss from selecting

inappropriate sample preparation techniques. The analyte is lost throughout the time-consuming, laborious, multi-stage activities involved in current solvent-based sample preparation techniques. Nowadays, a variety of cutting-edge techniques offer benefits like improved extraction efficiency, speedy analysis, automation compatibility, lower chemical solvent consumption, and being environmentally friendly (Jalili, Barkhordari, & Ghiasvand, 2020). Examples of these microextraction techniques include SPME, DLLME, LPME, and dispersive micro-solid phase extraction (DMSPE) (Gutiérrez-Serpa et al., 2019).

### *1.5.1 Dispersive Micro-Solid Phase Extraction (DMSPE)*

In the DMSPE method, a small amount of sorbent is first distributed in the sample solution and analytes are sorbed on the surface of adsorbent particles. The obtained suspension is then centrifuged. After that, the analytes are ultimately eluted using a suitable organic solvent. It can be described as an easy and quick microextraction method that is very suitable for HPLC (Alampanos et al., 2019). The main steps of the DMSPE method are demonstrated in Figure 1.5.

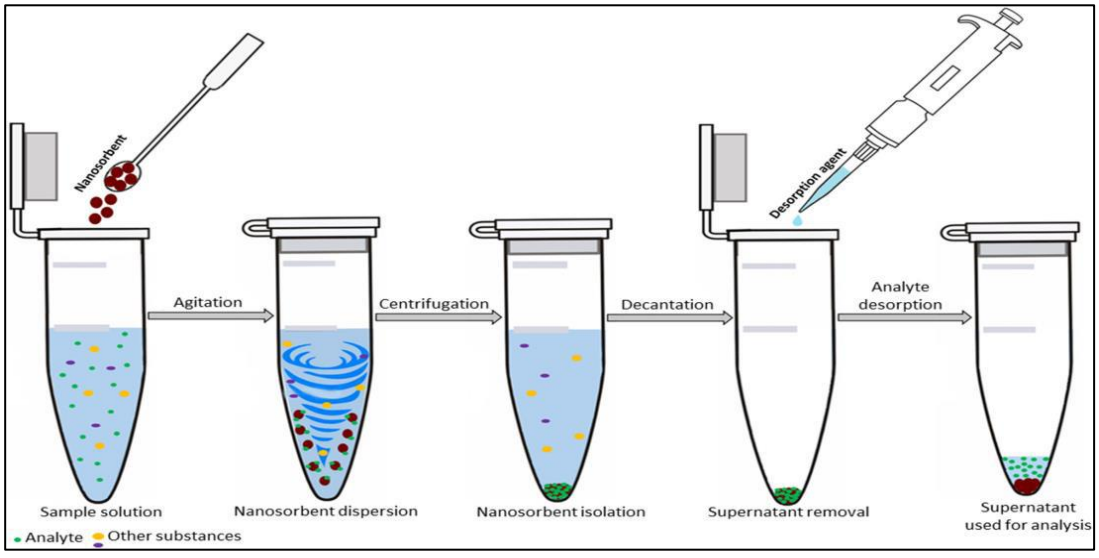



Figure 1.5 Representation of the main steps of the DMSPE method (Hagarová & Nemček, 2021)

Only a minimal quantity of sorbent and organic solvents are required for the entire DMSPE process. Additionally, it provides a simple and quick technique together with great extraction performance. This technique prevents the blocking that can happen in a traditional SPE column. All DMSPE-compliant materials ought to have a wide surface area that can ensure quick, precise sorption and elution. These substances should also be very capable of dispersing in liquid samples. Examples of these substances are carbon nanotubes, graphene, MOFs, and magnetic nanoparticles. By employing various sorbents, the DMSPE technique has been effectively used to separate and preconcentrate pharmaceuticals, water pollutants, and pesticides from various matrices, including samples of blood, urine, serum, water, and food (Alampanos et al., 2019; Jia et al., 2017).

### *1.5.2 Solid-Phase Microextraction (SPME)*

One of the most popular sample-preparation techniques is named SPME which is a sorptive-based extraction technique for gaseous or aqueous samples. The initial SPME device was created in the early 1990s. In the SPME technique, the sample is contacted with the surface of the fiber for extraction of analyte from aqueous or gaseous samples to coating material on the surface of the fiber. Following extraction, the sorbed analytes are desorbed into an analytical instrument such as gas chromatography or liquid chromatography for the detection of analytes. Figure 1.6 represents the main steps of the SPME procedure. In the preparation of fiber, sorbent material can be coated on silica or some kinds of metal wire like stainless steel wire or nickel wire. Selecting a sorbent that has a high affinity for the targeted analytes is crucial. In selecting of sorbent for SPME fiber, some physical properties of analytes like polarity, molecular weight, vapor pressure, boiling point and functional groups availability are considered. For interaction of analyte and sorbent, the polarity of analyte and the sorbent coating polarity should be in harmony. High temperatures, extreme pH, salts, and other additions should not affect the sorbent's coating (Mitra, 2003; Ansari & Karimi, 2017; Zhang, Zeng, Wang, & Chen, 2013).

In contrast to other separation methods, SPME allows for the fusion of numerous procedural phases into a single step, including sampling, pre-concentration, extraction, and sample introduction. The SPME method has several additional benefits, including being solvent-free, cheap, quick, automated, simple, and dependable. Two modes of SPME, namely headspace and direct immersion, can be used with good selectivity and sensitivity in aqueous samples (Mitra, 2003). The improvement of the SPME technique is directly based on the progressing new sorbents for different kinds of analytes such as functionalized multiwalled carbon nanotube composite, mesoporous materials, and molecularly imprinted polymers (Mirzajani et al., 2019).

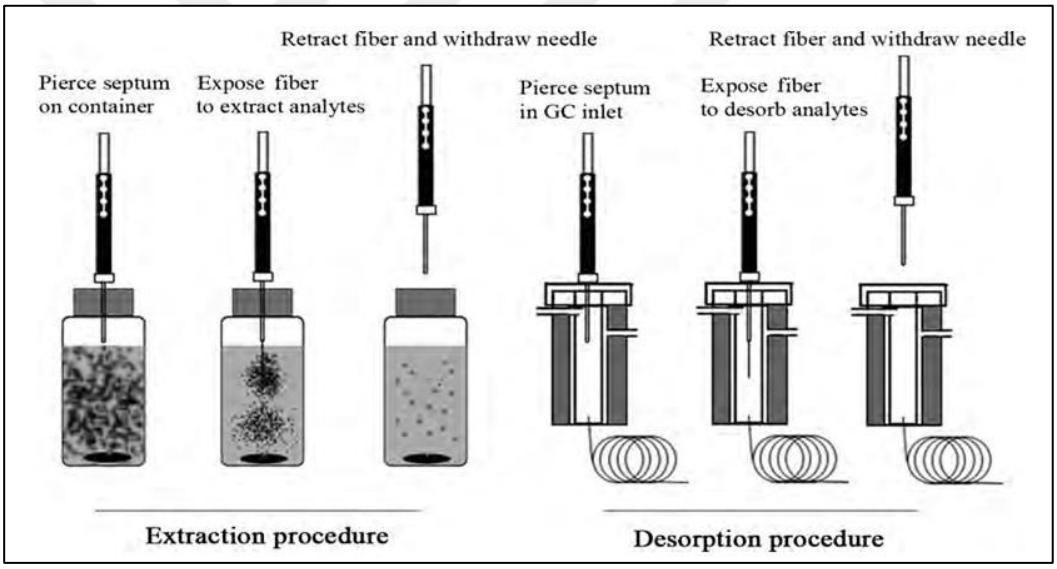



Figure 1.6 Illustration of the main steps of the SPME procedure (Zhang et al., 2013)

## 1.6 Literature Review of the Detection of SAs and PENs using DMSPE

Cr-BDC@GO (chromium-benzene dicarboxylate@ graphite oxide) material was prepared and presented as a sorbent for the dispersive micro solid phase extraction method for extraction sulfonamides (sulfamerazine, sulfapyridine, sulfamethoxypyridazine, sulfaquinoxaline, sulfadoxine, sulfamethazine, sulfamonomethoxine, SDA, SCP, SMT, SMX, SDMX) in milk samples. Determination

of the sulfonamides studied were achieved using ultrahigh performance liquid chromatography /tandem mass spectroscopy. Several parameters such as mass of sorbent, extraction time, elution solvent types, volume of elution solvent and time of elution were optimized. The determined values were 5 mg of sorbent, 20 min as extraction time, 500 μL of 5% ammonia-methanol as elution solvent and 15 min as elution time. By applying the optimum experimental parameters, the linearity in the range of 0.1 to 50 μg/L, the limit of detections in the range of 0.012 to 0.145 μg/L, precision less than 10 RSD%, and the recoveries in the range of 79.83 to 103.8% were obtained (Jia et al., 2017).

Magnetic zinc ferrite was prepared as a sorbent for DMSPE method for extraction and determination of sulfonamides (sulfapyridine, sulfacetamide, sulfamethoxypyridazine, sulfathiazole, sulfamerazine, sulfamethazine, sulfaquinoxaline, SDA, SCP, SSX, SMX, SDMX) by HPLC/diode-array detection (HPLC/DAD). The developed method was performed to lake water and egg samples. The sorbent amount was 20 mg, the extraction time was 30 min, the elution solvent was ACN with 2% formic acid, the elution volume was 2 mL and elution time as 30 s were optimized. In these conditions, linearity was between 0.06 and 250 μg/L, limit of quantifications ranged from 0.06 to 0.11 μg/L, repeatabilities as RSD ranged from 3.4 to 7.2%, and recoveries were found between 88 and 101% (Chatzimitakos & Stalikas, 2020).

COU-2 (mesoporous carbon) was prepared and used as a sorbent in DMSPE method for extraction of three drugs of PENs (oxacillin, CLO, DICLO) and determination of milk samples by HPLC/ultraviolet detection (HPLC/UV). Some experimental parameters were optimized, those were 75 mg of adsorbent mass, 1.5 min of extraction time, methanol as elution solvent, 100 μL as elution solvent volume, and 3 min as elution time. The analytical performance of this method was studied, given parameters were linearity (10-5000 μg/L), precision as RSD (6.2-8.8%), recovery (80.3-99.5%), the limit of quantitations (6-10 μg/L) and the limit of detections (2-3.3 μg/L) (Yahaya et al., 2015).

The material of a new ionic liquid-modified magnetic nanoparticle named as (DABCO-$C_3$OH)Cl/MNPs was prepared. Five drugs of PENs (oxacillin, AMX, AMP, PENG, CLO) were analyzed by UHPLC-MS/MS after DMSPE method using the prepared magnetic nanoparticle as a sorbent in milk samples. Some parameters such as extraction time mass of adsorbent, type of elution solvent, elution solvent volume and elution time were optimized. These parameters were found as 6 min, 22 mg, methanol with 3% formic acid, 500 µL and 2.5 min, respectively. The validated analytical performances were linear range from 0.1 to 300 µg/L, the limit of detections from 0.03 to 0.20 µg/L, limit of quantitations within 0.1 to 0.68 µg/L, recoveries from 87 to 107%, and repeatabilities as RSD from 1.9 to 5.8% (Sahebi, Konoz, Ezabadi, Niazi, & Ahmadi, 2020).

The synthesized sorbent of magnetic molecularly imprinted polymers having hydrophilic character was used in dispersive solid-phase extraction (d-SPE) for extraction of sulfonamides (sulfathiazole, sulfamethoxydiazine, sulfamethazine, sulfamethoxypyridazine, sulfameter, sulfamerazine, SDA, SCP, SMX, SSX). The determination of sulfonamides was carried out by HPLC/DAD in chicken and milk samples. After optimization of the sorption and desorption parameters of d-SPE method, the extraction was carried out within 25 min using 50 mg of the prepared sorbent and then the desorption was achieved with 2 mL of methanol using 5 min. The analytical bias was summarized as a working range from 5 to 10 mg/L, recoveries from 85.09 to 110.93%, limit of detections from 0.57 to 1.5 µg/L and precision as RSD less than 7.23%, and (Zhao et al., 2021).

The synthesized magnetic chitosan nanoparticles were presented as sorbent to determine AMX by DMSPE combined with HPLC/DAD in hair and human urine. After optimization of the sorption and desorption parameters of DMSPE method, the extraction was carried out within 20 min using 65 mg of the prepared sorbent and then the desorption was achieved with 0.8 mL of methanol using 12 min. After optimization, linearity within the range of 3.5-1000 µg/L, precision within the range of 4.78-5.01%,

recoveries within the range of 97.02-104.9%, and limit of detection as 1.1 μg/L were determined (Soleimanirad, Badameh, Raoufi, & Ebrahimi, 2022).

Magnetic mesoporous core-shell structure nanocomposite was synthesized. By using this material as a sorbent, sulfonamides (sulfathiazole, sulfamethazine, sulfamerazine, sulfamethoxypyridazine, sulfadiazine) were extracted with magnetic dispersive solid phase extraction method and determined by HPLC/DAD in food samples such as meat. In the optimization of the MDSPE method, the mass of adsorbent was 25 mg, the extraction time was 8 min, the elution solvent was acetic acid in methanol, the desorption solvent volume was 800 μL, and the desorption time was 10 min. The analytical parameters were linear range from 3.97 to 1000 μg/L, repeatabilities from 2.1 to 6.4%, recoveries from 76.1 to 102.6%, limit of detections from 1.73 to 5.23 μg/L, and limit of quantitations from 3.97 to 15.89 μg/L (Xia et al., 2017).

Magnetic MGO-TSD/PANI (graphene oxide-N-[3-(trimethoxysilyl)propyl]ethylene diamine/polyaniline) was synthesized and used as adsorbent for ultrasound-assisted MDSPE for extraction of three PENs (AMX, AMP, PENG) and their determinations HPLC/DAD in food samples like milk samples. After optimization of the sorption and desorption parameters of MDSPE method, the extraction was carried out within 2 min using 12 mg of the prepared sorbent and then the desorption was achieved with 75 μL of methanol using 2.5 min. By applying optimum parameters, working range in the range of 2.5-1000 μg/L, the limit of detections within 0.5-0.9 μg/L, the limit of quantitations in the range of 2.1-3.1 μg/L, recoveries within 90-99%, and the repeatabilities as RSD in the range of 2.5-3.1% were performed (Shirani, Akbari-Adergani, Rashidi Nodeh, & Shahabuddin, 2020).

YS-$Fe_3O_4$@GC (yolk-shell $Fe_3O_4$@graphitic carbon) material was prepared and used in the MDSPE method as a sorbent for extraction of four SAs (sulfamerazine, Sulfamethazine, SDA, SMX), and their analysis by HPLC/DAD in food samples such as milk samples. The studied optimization parameters were adsorbent mass (6 mg),

extraction time (15 min), the elution solvent (methanol: 1M NaOH) and the elution time (5 min), and the elution volume (0.6 mL). After optimization, the analytical method performance parameters were determined. The linear working ranges from 1 to 250 μg/L, the limit of detections within 0.11 - 0.25 μg/L, the limit of quantitations within 0.37 - 0.83 μg/L, recoveries within 77.2 to 118%, and precision as RSD from 4.5 to 7.2% were found (Liu, Tong, & Zhang, 2020).

$CoFe_2O_4$-graphene was prepared and used in the SPE method as a magnetic sorbent for the determination of five SAs (sulfamerazine, sulfadoxine, SMT, SMX, SSX) by HPLC/UV in food samples like milk. The SPE method was optimized: the mass of sorbent was 15 mg, the extraction time was 20 min, the elution solvent was methanol with 5% acetic acid, the elution volume was 0.5 mL, and the elution time was 2 min. The working range was found within 0.02-50 mg/L. The limit of detections and the limit of quantitations of the studied SAs were within 1.16-1.59 μg/L and 3.52-4.81 μg/L, respectively. The recoveries from 62 to 104% and the precisions as RSD from 1.6 to 14% were determined (Li et al., 2015).

COU-2 material was used in the DMSPE method as a sorbent to extract and determine CLO by HPLC with ultraviolet detection in drinking water. Some parameters were optimized. These parameters were the adsorbent mass (100 mg), the extraction time (1 min), the desorption solvent (methanol), the desorption solvent volume (0.3 mL), and the desorption time (5 min). The working range was found between 0.1 and 100 mg/L. The limit of detection of CLO was found as 0.06 μg/L and the limit of quantitation of CLO was determined as 0.17 μg/L. The recoveries within 89.7 - 113.6% and the precisions as RSD from 4.6 to 7.1% were determined (Yahaya et al., 2013).

### 1.7 Literature Review of the Detection of NSAIDs using SPME

$Fe_3O_4$/Cu-BTC nanocomposite was synthesized and used as a coating material in the preparation of SPME fiber. The applied coating process was sol gel method using a

capillary glass tube with methyltrimethoxysilane. Using the prepared SPME fiber, four NSAIDs (nalidixic acid, IBU, DIC, NAP) from plasma, serum, urine, and tablet samples were extracted and determined by HPLC. The optimized SPME method conditions were summarized as 30 min the extraction time, and acetonitrile: water (60:40 v/v) the elution solvent. Under the experimental conditions, the analytical performance of the method was given as a working range from 0.1 to 400 μg/L, limit of detection within 0.03-0.05 μg/L, limit of quantitation within 0.12-0.18 μg/L, precision within 1.1 and 4.7 RSD%, and recovery from 94 to 102% (Mirzajani et al., 2019).

Cotton@PDA@UiO-66 (cotton@polydopamine@Zr-BDC) was synthesized and packed into a pipette tip and used as SPME fiber for extraction of three NSAIDs (flurbiprofen, KET, NAP) from swine muscle samples and determination by HPLC/UV. The given analytical performances of the proposed method were summarized as the linear range between 0.1 and 500 μg/L, limit of detection as 0.01-0.03 μg/L, limit of quantitation as 0.03-0.1 μg/L, precision as RSD% between 0.15 and 3.77%, and recovery from 88.54 to 95.7% (Li, Wang, & Chen, 2018).

Multi-walled carbon nanotubes functionalized with polyethyleneglycol was synthesized and used for coating on silica for preparation of SPME fiber by applying sol-gel method. Determination of three NSAIDs (DIC, IBU, NAP) in different real water samples were accompolished by a gas chromatography/flame ionization detector (GC/FID) after extraction using the prepared SPME fiber. Some sorption and desorption experimental conditions such as extraction time and extraction temperature, desorption temperature, and desorption time were optimized and determined as 60 min at 50 °C and 280 °C for 5 min, respectively. Under optimized SPME and desorption conditions, linearity from 0.05 to 200 μg/L, the limit of detections as 0.007-0.03 μg/L, the limit of quantitation as 0.05-0.07 μg/L, precision as 5.9-8.1%, and recovery as 84-107% were found (Sarafraz-Yazdi, Amiri, Rounaghi, & Eshtiagh-Hosseini, 2012).

Zr-BDC@graphene oxide was prepared and used in the preparation of SPME fiber by applying hydrothermal method on a stainless-steel wire. The ibuprofen and diclofenac were determined using GC/FID method after SPME in water samples. The extraction temperature and extraction time for optimization of sorption conditions for SPME method and desorption time and injection temperature for optimization of desorption conditions were examined and determined as at 60 °C for 40 min and 7 min at 260 °C, respectively. The analytical data were linearity as 0.01-500 μg/L, limit of detections as 0.001-0.03 μg/L, limit of quantitations as 0.01-0.1 μg/L, repeatability as RSD% between 5.1 and 5.4%, and recovery as 97-99% (Liu, Fan, Dang, Li, & Yu, 2020).

Polytetrahydrofuran was used as an adsorbent and capsuled by applying the sol-gel method. After extraction of ibuprofen, it was determined by UHPLC in urine samples. The optimized value of extraction time and type of desorption solvent, volume of desorption solvent and desorption time were 40 min, and 0.5 mL of methanol for 1 min, respectively. By applying optimized experimental parameters, linearity, limit of detection, limit of quantitation, precision, and recovery of the method were assigned as 50-5000 μg/L, 14 μg/L, 50 μg/L, 1.5-4.6%, and 90-91.3% (Manousi, Kabir, Furton, Samadiou, & Zacharis, 2022).

The synthesized $Fe_3O_4/SiO_2/TiO_2$ nanocomposite was used as a sorbent material in hollow fiber solid-phase microextraction method. Sol-gel method was used in the preparation fiber. The six NSAIDs (acetylsalicylic acid, piroxicam, indomethacin, mefenamic acid, DIC, NAP) were extracted by SPME method and then determined by HPLC in human hair samples. The optimized parameters were extraction time as 60 min, sorbent amount as 300 mg, elution solvent as methanol: formic acid: acetonitrile, and elution time as 40 min. By applying experimental parameters, linearity within 100-10000 μg/L, limit of detections between 10 and 100 μg/L, limit of quantitation between 40 and 300 μg/L, repeatability as RSD within the range of 3.09 to 6.61%, and recovery as % from 79.72 to 86.77% were determined (Es'haghi & Esmaeili-Shahri, 2014).

Carboxylic Mg/Al layered double hydroxide acid-calix[4]arene was synthesized by intercalation of carboxylic acid-calix[4]arene between Mg/Al layered double hydroxide. The prepared adsorbent material was used to prepare a solid phase extraction cartridge. The three NSAIDs (aspirin, IBU, NAP) were extracted and determined by HPLC/UV after solid phase extraction in water and urine samples. By applying experimental parameters, sorbent mass as 15 mg, extraction time as 10 min, and elution solvent as methanol were determined. The linearity of method within 0.5 to 500 μg/L, limit of detections and limit of quantitation within 0.005-0.386 μg/L, and 0.015-1.287 μg/L, respectively were found. The repeatability of method is from 0.5 to 3.5%, and recovery from 90.4 to 98.5% (Shafiei-Navid, Hosseinzadeh, & Ghani, 2022).

Four NSAIDs (KET, NAP, IBU, DIC) were extracted by applying ultrasound -assisted extraction combined with SPME method and determined in river sediment samples using GC/MS. The optimized SPME method conditions were extraction time (45 min) and extraction temperature (40 °C). Before GC/MS analysis, derivatization was required using N-methyl-N-(tertbutyldimethylsilyl) trifluoroacetamide as a derivatization reagent. The derivatization time was determined as 30 min. The desorption time, and desorption temperature were optimized as 10 min and 250 °C, respectively. Linearity, recovery, repeatability, and limit of detection were studied and determined as 1-10 ng/g, 56.2-108%, 3.5-7.5%, 0.1-0.3 ng/g, and 0.04-0.11 ng/g (Díaz & Peña -Alvarez, 2017).

Three NSAIDs (IBU, NAP, DIC) were extracted by solid phase extraction and determined with HPLC in different water samples such as wastewater and river. The molecularly imprinted polymer synthesized was used as a sorbent for SPE. The sorbent amount as 50 mg and the elution solvent as acetic acid: acetonitrile were optimized. The analytical data were summarized as the limit of detections within 0.15-1 μg/L, limit of quantitations within 0.49-3.33 μg/L, and recovery above 82% (Madikizela & Chimuka, 2016).

Magnetic $Fe_3O_4$/carbon nanodots/graphene oxide was synthesized and used as an adsorbent. Ibuprofen was determined in human blood samples by HPLC after extraction with magnetic solid phase extraction. The optimized conditions were summarized as 60 mg sorbent amount, 2 min extraction time, 2 mL of ethanol for 2 min. The analytical performances were as linearity (50-2000 μg/L), recovery range (91-95%), precision (3.5%,) limit of detection (8 μg/L) and limit of quantitation (25.4 μg/L) (Yuvali, Narin, Soylak, & Yilmaz, 2020).

Three NSAIDs (DIC, IBU, KET) were determined by HPLC after the solid bar microextraction method using a sorbent of multi-walled carbon nanotubes in urine samples. The optimized parameters were summarized as 10 mg amount of adsorbent, 40 min extraction time, and 250 μL of methanol for 5 min. Under optimization conditions, LR from (5-100 μg/L), LOD from (0.36-0.52 μg/L), LOQ from (1.2-1.7 μg/L), RSD% was less than 5.7%, and R% from (48.8-53.5%) (AL-Hashimi, Aleih, Fasfous, & AlKhatib, 2018).

### 1.8 Aim of Study

1. Synthesis and characterization of copper-benzene tricarboxylate (Cu-BTC) and Cu-BTC/montmorillonite (Cu-BTC/MMT) composites and analytical study of Cu-BTC/MMT as a sorbent for DMSPE to determine six SAs (SDA, SDMX, SCP, SMX, SMT, SSX) and six PENs (PEN G, NAF, AMX, CLO, AMP, DICLO) from milk and synthetic hydrolyzed urine samples followed by HPLC/DAD.

2. Synthesis and characterization of copper-benzene dicarboxylate (Cu-BDC) and Cu-BDC/montmorillonite (Cu-BDC/MMT) composites and analytical study of Cu-BDC/MMT as an adsorbent for SPME fiber to determine four NSAIDs (KET, NAP, DIC, IBU) from tap water, wastewater, synthetic hydrolyzed urine, and drug samples followed by GC/MS and/or HPLC/DAD.

# CHAPTER TWO
# EXPERIMENTAL STUDIES

## 2.1 Reagents, Solvents, and Preparation of Standard Solutions

Copper(II) nitrate. trihydrate, terephthalic acid ($H_2$BDC, benzene-1,4-dicarboxylic acid), trimesic acid ($H_3$BTC, benzene-1,3,5-tricarboxylic acid), dimethylformamide (DMF), acetonitrile (ACN), trifluoroacetic acid (TFA), N-Methyl-N-(trimethylsilyl) trifluoroacetamide (MSTFA), ethanol, methanol (MeOH), PENs (PENG, CLO, AMX, DICLO, AMP, and NAF), NSAIDs (KET, NAP, DIC, and IBU), and SAs (SSX, SMT, SDMX, SCP, SMX, and SDA) were purchased from Merck and Sigma-Aldrich. Modified dihydroxy ethylene urea (MDEU) and MMT were supplied from Fluka. All chemicals used were of analytical grade or above. Deionized water was used in all experiments.

Stock standard solutions of SAs, PENs, and NSAIDs were prepared as 1000 mg/L using MeOH, ACN, or deionized water. The prepared intermediate stock solutions and working test solutions of antibiotics and NSAIDs were kept in a refrigerator at 4 °C. The pH 4 buffer solution was prepared with sodium dihydrogen phosphate and citric acid by adjusting its ionic strength to 0.01 M.

## 2.2 Material Characterization Instruments

The instruments that were utilized to describe the structure and/or morphology of the prepared Cu-BDC/MMT and Cu-BTC/MMT materials include scanning electron microscopy (SEM), thermal gravimetric analysis (TGA), X-ray diffraction analysis (XRD) and Brunauer-Emmett-Teller (BET) analysis. FTIR spectrometer (Perkin Elmer Spectrum 100) was used to obtain FTIR spectra using a KBr pellet from 4000-400 $cm^{-1}$. X-ray diffractometer with copper-Kα radiation from 3º to 25º at 2θ/s was used to conduct the XRD powder patterns. Thermal analysis was acquired (Perkin Elmer

Diamond thermogravimetry/differential thermal analyzer) under $N_2$ atmosphere using a Pt pan. The heating rate was 5 °C/min and the samples were heated up to 700 °C. SEM images were obtained by applying an acceleration voltage of 5 kV. The surface area and pore volume of BET were measured through nitrogen adsorption/desorption isotherms.

## 2.3 Experimental Studies of SAs and PENs using DMSPE Method

### *2.3.1 Preparation of Cu-BTC*

By slight modification of the procedures given in the literature, Cu-BTC was synthesized (Habimana, Shi, & Ji, 2018; Schlesinger, Schulze, Hietschold, & Mehring, 2010). For this purpose, $Cu(NO_3)_2.3H_2O$ as 0.5 g was dissolved in deionized water (2.5 mL), and $H_3BTC$ as 0.25 g was dissolved in DMF (12.5 mL). After a combination of these solutions, the resulting mixture is sonicated for 30 min using an ultrasonic bath. In the next step, the final solution was heated at 100 °C and stirred for 24 h. Finally, the mixture was kept at room temperature for cooling. After separation of the solid, it was first washed using methanol and dried at 80 °C for 12 h by applying a vacuum.

### *2.3.2 Preparation of Cu-BTC/MMT Composites*

The composites of Cu-BTC/MMT having different MMT were synthesized by small modifications of previously given methods in literature (Habimana et al., 2018). Dispersion of different amout of MMT as 0.015, 0.0375, 0.075, 0.15, 0.3, and 0.45 g was ensured using deionized water as 10 mL, then $Cu(NO_3)_2.3H_2O$ as 0.5 g was added to deionized water (2.5 mL). After addition of $Cu(NO_3)_2.3H_2O$ solution into the dispersion of MMT, the final mixture was stirred at room temperature overnight. Trimesic acid of 0.25 g was dissolved in 12.5 mL of DMF and added to the other mixture to get Cu-BTC/MMT composites. According to the different percentages of MMT (2-5-10-20-40-60 wt%), Cu-BTC/MMT composites with various MMT were designated as Cu-BTC/MMT%Y (Y = 2, 5, 10, 20, 40, and 60). After the sonication of

the final mixture using the ultrasonic bath for 30 min, it was heated at 100 °C, and stirred for 24 h. The obtained solid part was cooled up to room temperature, washed with MeOH, then dried at 80 °C for 12 h by applying a vacuum.

### *2.3.3 Determination of Point of Zero Charge (PZC)*

The salt addition method as described by Mahmood et al. (2011) was applied for the determination of PZC. A Cu-BTC/MMT composite (0.05 g) was put into 0.1 M NaCl solution (5 mL) using a plastic test tube. The adjustment of solution pH to 3, 4, 5, and 6 was done using NaOH or HCl (0.1 M) solutions. Solutions waited for 4 h, and then their pHs were measured. For determination of PZC, graph first plotted the initial pH versus the final pH. Then, the intersection point of the initial pH and final pH lines was evaluated as the PZC value.

### *2.3.4 Sample Preparation*

Three different kinds of milk samples (raw and pasteurized bottled in glass bottle and tetra pack) were supplied from local producers and the local market in Izmir. They were stored at 4 °C for 1-2 days. The pasteurized milk sample in glass bottle was first analyzed and the studied SAs and PENs were not detected. Then, it was used as a blank milk sample in the validation of the DMSPE method and also in the recovery studies. For accuracy control, three different concentrations of SAs and PENs standard solutions (10-100-300 µg/L) were added to real milk samples and then were stirred for homogenization of the resulting sample solution for 10 min. To two mililiters of milk samples whether blank or fortified, ethyl acetate as 5 mL was first added, then homogenized for 30 s, and finally ultrasonicated for 2 min. The addition of ethyl acetate was repeated two times. After centrifugation at 10000 rpm for 8 min, the supernatant was separated and it was evaporated under $N_2$ atmosphere. The pH 4 solution as 5 mL was added to the residue and vortexed for 30 s. It was used for further DMSPE method (Lirio et al., 2016; Jia et al., 2017).

Synthetic human urine in hydrolyzed forms was prepared in previously given studies (Zhang, Sun, Boyer, Zhao, & Huang, 2015). The prepared synthetic urine solution includes NaCl at 0.06 M, $Na_2SO_4$ at 0.015 M, KCl at 0.04 M, ammonia at 0.25 M, $NaH_2PO_4$ at 0.0136 M, and $NH_4HCO_3$ at 0.25 M. It was diluted (1:4 (v/v)) using deionized water in the study of the validation of the proposed DMSPE method. For recovery studies, different concentrations of SAs and PENs (10-100-300 µg/L) were fortified to synthetic urine solution. Also, the working solutions of synthetic urine solutions ranging from 0.5 to 400 µg/L were used for the linearity study. The solution pH was set to 4 for the DMSPE method (Safari, Shahlaei, Yamini, Shakorian, & Arkan, 2018).

### *2.3.5 DMSPE Method*

Cu-BTC/MMT%2 as 10 mg were taken and put into a synthetic solution for optimization of the method or a real blank milk sample or synthetic urine solution for validation of the method and recovery studies. The pH of these solutions was pH 4. For adsorption, first ultrasonication for 30 s and then vortex for 10 min were applied. Later, the separation of two phases succeeded after centrifugation for 5 min. After removing the upper aqueous phase, the analytes were desorbed from the adsorbent by adding 1 mL of MeOH:ACN (50:50). This mixture was sonicated for 5 min. The supernatant was removed after applying centrifuge to the mixture for 5 min. The eluate was filtered using a PTFE filter (0.22 µm) and then dried under nitrogen flow. For analysis in HPLC/DAD, the residue was dissolved by ACN: 0.1% TFA (50:50) (100 µL).

### *2.3.6 HPLC/DAD method for SAs and PENs Analysis*

Chromatographic separation and determination of analytes were achieved by using HPLC/DAD (Thermo Scientific Dionex Ultimate 3000). For this purpose, the chromatographic column used was a C18 column with dimensions of 15 cm x 4.6 mm, 5 µm particle size, and 100 Å pore size. The flow rate of the mobile phase was 1 mL/min.

A 0.1% TFA in water (A) and ACN (B) were used as mobile phase solvents. The applied gradient program was given: 10% of B for 2 min, an increase of B to 70% from 2 to 26 min, a decrease of B to 10% from 26 min to 27 min, and 1 min more at 10% B. A 20 µL of the sample was injected using an autosampler. The SAs were monitored at 270 nm and the PENs were monitored at 230 nm.

### *2.3.7 Optimization of DMSPE Method*

In the DMSPE method, some sorption and elution parameters were optimized. The studied sorption parameters were sample pH, sorbent mass, extraction time, and ionic strength. The elution parameters were solvent types, elution time and solvent volume were investigated. The sample pH was from 3 to 8, sorbent mass from 2 to 10 mg, extraction time from 0 to 20 min, and sodium chloride and sodium sulfate concentrations from 0 to 0.1 M were tested. In the elution part, types of solvents such as MeOH, ACN, and ACN: MeOH at different ratios, solvent volume from 0.25 to 1.25 mL, and elution time from 1 to 15 min were studied. Synthetic solutions having 100 µg/L of analytes were synthesized at pH 4 and all experiments were repeated three times.

### *2.3.8 Validation of DMSPE Method*

Regarding the European Commission, the DMSPE method was validated using a synthetic aqueous solution, blank milk sample and synthetic urine solution for the studied antibiotics (EC, 2002). The analytical performance was studied as working range, sensitivity, specificity, the limit of quantitation, the limit of detection, repeatability, and recovery. The working range (0.5 - 400 µg/L of SAs and PENs) was performed using 8 or 10 calibration solutions. The calibration line for each analyte was plotted as concentration versus peak area. The slopes and the intercepts with their standard deviations and the coefficient of determinations were found for each analysis by using the least linear regression analysis method.

The signal-to-noise ratio of 3 for calculation of the limit of detection and the signal-to-noise ratio of 10 for calculation of the limit of quantitations were used. The blank milk sample was studied at 230 nm for PENs and at 270 nm for SAs to demonstrate the specificity of the proposed method.

The within-day and between-day repeatabilities of the proposed method were presented as RSD (%). Synthetic solutions, synthetic urine solutions, and milk solutions were fortified by the studied antibiotics (100 µg/L). These experiments were repeated five times. The recovery studies have performed the evaluation of the accuracy of the proposed method. The synthetic urine solution and the blank milk sample were fortified with 10, 100, and 300 µg/L of the studied analytes. These experiments were repeated as five parallel.

## 2.4 Experimental Studies of NSAIDs using SPME Method

### *2.4.1 Synthesis of Cu-BDC*

By slight modification of the procedures given in the literature, Cu-BDC was synthesized (Sun, Xia, Zhao, Li, & Li, 2014; Habimana et al., 2018). A 0.24 g of $Cu(NO_3)_2.3H_2O$ was dissolved in deionized water (2.5 mL), and 0.166 g of terephthalic acid was dissolved in 12.5 mL of DMF. After mixing of these solutions, it sonicated for 30 min. Later, the final solution was heated at 100 °C by stirring for 24 h. Finally, the mixture was kept at room temperature for cooling. After removing supernatants, the solid was washed using methanol and dried at 80 °C for 8 h by applying vacuum.

### *2.4.2 Preparation of Cu-BDC/MMT Composites*

The Cu-BDC/MMT composites having different MMT were prepared by small modifications of previously given methods in literature (Sun et al., 2014; Habimana et al., 2018). After dispersion of different amount of MMT as 0.00812, 0.0203, 0.0406, and

0.0609 g in deionized water (100 mL) for 2 h, $Cu(NO_3)_2.3H_2O$ as 0.24 g was added to deionized water (2.5 mL). After addition of $Cu(NO_3)_2.3H_2O$ solution into the dispersion of MMT, the mixture was stirred for 24 h at room temperature. After dissolving of 0.166 g of terephthalic acid DMF (12.5 mL), it was added to the mixture of MMT and copper salt solution to get Cu-BDC/MMT composites. According to the percentage of MMT (2 -5-10-15 wt%), the Cu-BDC/MMT composites with various MMT were designated as Cu-BDC/MMT%Y (Y = 2, 5, 10, and 15). After sonication of the final mixture for 30 min, it was heated at 100 °C by stirring for 24 h. The obtained solid part was kept on hold at room temperature, washed using methanol, and then dried at 80 °C by applying a vacuum for 8 h.

### *2.4.3 Preparation of SPME Fiber*

To prepare SPME fiber, stainless steel wire (SSW) was (about 10-15 cm in length and a diameter of 0.3 mm) used. The sol-gel procedure was used for coating MOF/clay composite on SSW as described procedures in literature (Attari, Bahrami, Shahna, & Heidari, 2015; Es-haghi, Hosseininasab, & Bagheri, 2014; Amiri & Ghaemi, 2017). The steps are given below:

1. For cleaning, acetone and metanol were used for cleaning of one end of SSW (2 cm). After cleaning, it was dried for 5 min at room temperature. Then, it was washed with distilled water and dried for 5 min at room temperature.

2. For etching, SSW was first put into water: aqua regia (50:50) solution for 30 min and then into distilled water for 1 min. Later, it was immersed in 2 M NaOH solution at room temperature for at least 2 h. For hydroxylation of the surface SSW.

3. For coating SSW, hydroxylated SSW has immersed into MDEU crosslinker for 60 min by stirring at room temperature. Later, it was dried at 80 ºC for 1 h. Then, it was dipped into Cu-BDC/MMT%Y dispersed solution (10 mg/2 mL distilled

water). The last two steps were iterated at least three times to increase coating thickness.

4. The coated SPME fiber was dried in the atmosphere, and stored in a desiccator overnight. Finally, at different temperatures such as 150, 200, and 250 °C, it was conditioned using GC injection port for 30 min at each temperature, respectively.

### *2.4.4 Sample Preparation*

Synthetic human urine in hydrolyzed forms was prepared according to the same procedure given in Section 2.3.4. Before applying the SPME method, pH of synthetic urine solution was adjusted to 4.

For removing the possible suspended materials, 0.22 µm PTFE filter was used for tap water and wastewater samples and the pH was set to 4. After that, the studied NSAID analytes were spiked into these water samples for recovery studies. The proposed SPME method was applied to the target NSAID analytes spiked and unspiked water samples.

5 mL of Pedifen syrup (100 mg IBU/5 mL) was diluted to 100 mL with distilled water (1st soln, 1000 µg/mL IBU). Then,1 mL of 1st soln was diluted to 100 mL with distilled water (2nd soln, 10 µg/mL IBU). For the SPME experiment, 2 mL of 2nd soln was taken, adjusted to pH 4, and diluted to 100 mL (200 µg/L IBU). Depending on the given SPME experiment method, determination of IBU in the drug was performed in three parallels. For recovery studies, 20 and 100 µg/L of NSAIDs standard solution was spiked to 10 µg/L of drug solution and determination of NSAIDs in the drug was performed in three parallels.

1 g of Naprosyn plus gel (100 mg NAP/1 g) was diluted to 100 mL with distilled water (1st soln, 1000 µg/mL NAP). Then,1 mL of 1st soln was diluted to 100 mL with distilled water (2nd soln, 10 µg/mL NAP). For the SPME experiment, 2 mL of 2nd soln

was taken, adjusted to pH 4, and diluted to 100 mL. (200 µg/L NAP). Depending on the given SPME experiment method, the determination of NAP in the drug was performed in three parallels. For recovery studies, 20 and 100 µg/L of NSAIDs standard solution was spiked to 10 µg/L of drug solution and determination of NSAIDs in the drug was performed in three parallels.

### *2.4.5 Direct-Immersion-SPME (DI-SPME) Method for NSAIDs in HPLC/DAD*

18 mL of a 15% NaCl aqueous test solution containing NSAIDs at 100 µg/L (pH 4) was put into a 20 mL SPME vial. The prepared SPME fiber was put into the test solution and extraction was taken place for 40 min at 60 °C by stirring at 600 rpm. Then, the fiber was inserted into 1.2 mL of 0.1% TFA in MeOH: ACN (40:60) and stirred at 500 rpm for 20 min at room temperature for elution of NSAIDs. The eluate was transferred into another vial, then dried under nitrogen flow. For analysis in HPLC/DAD, the residue was dissolved by 200 µL of deionized water:ACN (50:50).

### *2.4.6 Analysis of NSAIDs by HPLC/DAD*

Chromatographic separation and determination of NSAIDs were achieved by using HPLC/DAD (Thermo Scientific Dionex Ultimate 3000). The isocratic separation of NSAIDs was performed using a C18 column, 100 Å pore size with 15cm x 4.6 mm, 5 µm particle size at a flow rate of 0.5 mL/min. The studied column temperature was 30 °C. The mobile phase was deionized water: ACN (55:45). A 20 µL of the sample was injected using an autosampler. The NSAIDs were monitored at 230 nm.

### *2.4.7 DI-SPME Method for NSAIDs by GC/MS After Derivatization*

18 mL of a 15% NaCl aqueous test solution containing NSAIDs at 100 µg/L (pH 4) was put into a 20 mL SPME vial. The prepared SPME fiber was put into the test solution and extraction was taken place for 40 min at 60 °C by stirring at 600 rpm. Then,

the fiber was dried under nitrogen flow for 5 min. Then 60 µL of MSTFA reagent was added to 10 mL of the SPME vial. The fiber was placed into the vial with heating at 60 °C for 30 min. Later, it was pulled back from the vial and immediately inserted into the GC injection port at 280 ºC for 5 min for desorption.

### *2.4.8 Analysis of NSAIDs by GC/MS*

Gas chromatography equipped with single quadrupole mass analyzer mass spectrometry (GC/MS) was used for chromatographic analysis of NSAIDs (Thermo Fisher Scientific QP2010). The column used was TG-5MS capillary column with dimensions of 30 m × 0.25 mm, 0.25µm particle size. The carried gas was He gas and its constant flow rate was 1 mL/min. The gradient temperature program was used. The applied program includes these steps: beginning temperature 70 ºC and waiting 2 min, rising temperature to 280 ºC with a heating rate of 25 ºC/min and waiting 9 min. The solvent delay time was 7 min. The MS transfer line temperature was 250 °C, the ion source temperature was 200 °C, and the injection port temperature was 280 °C. The injection was studied in splitless mode. The MS was operated in electron ionization mode with an electron energy of 70 eV. The selected ion monitoring (SIM) mode of NSAIDs was studied (Ghambarian et al., 2020). Table 2.1 shows the conditions for NSAIDs.

Table 2.1 MS conditions for GC/MS analysis of NSAIDs (retention time, characteristic ions and time segment in SIM mode)

| **NSAIDs** | **Retention time (min)** | **Segment (min)** | **Characteristic ions (m/z)** |
|---|---|---|---|
| IBU | 8.28 | 7.00 | 161, 234, 263, 278 |
| NAP | 10.29 | 10.00 | 185, 243, 287, 302 |
| KET | 10.78 | 10.40 | 105, 282, 311, 326 |
| DIC | 11.21 | 10.80 | 214, 242, 277, 367 |

### *2.4.9 Optimization of DI-SPME Method for HPLC/DAD and GC/MS Determination of NSAIDs*

Extraction temperature, pH, salt effect, and extraction time as optimization parameters were optimized for the DI-SPME method. For desorption of NSAIDs and determination by GC/MS, optimization of desorption time and desorption temperature were required. For determination by HPLC/DAD, elution solvent type, elution volume and elution time were optimized. For this purpose, Synthetic solutions having 100 µg/L of NSAIDs were synthesized, and all experiments were conducted three times. Test solutions at different pH (3, 4, 5, 6, 7, 8), using different salt solutions (0, 5, 10, 15, 20, 25 % (w/v) NaCl), extraction temperature (25, 40, 50, 60, 80 ºC), and extraction time (15, 30, 40, 60 min) were investigated. In HPLC/DAD analysis, elution solvents (MeOH, ACN, MeOH: ACN (50:50), 0.1%TFA in MeOH: ACN (50:50), 0.1%TFA in MeOH: ACN (40:60)), elution volume (0.6, 0.8, 1.2, 1.4 mL), and elution time (5, 10, 15, 20, 30 min) were investigated for NSAID retention efficiencies.

### *2.4.10 Optimization of Derivatization Parameters by GC/MS Determination*

Since the studied NSAID analytes are polar, the analytes were derivatized with MSTFA, one of the trimethyl silane compounds, after the SPME method in order to increase the sensitivity in GC analysis (Wang et al., 2013). Since trimethyl silane compounds are hydrolyzed in aqueous media, the fiber must be dried after SPME extraction. In derivatization, the drying time of the fiber after SPME (5, 10, 15 min), the volume of derivatizing reagent (40, 50, 60, 75 µL), derivatization temperature (40, 50, 60, 70 ºC) and derivatization time (20, 30, 40 min) were studied. Synthetic solutions having 100 µg/L of NSAIDs were synthesized, and all experiments were conducted three times.

### *2.4.11 Validation of SPME Method*

Regarding the European Commission, the DI-SPME method was validated using the synthetic aqueous solution for the studied antibiotics (EC, 2002). Analytical performance, working range, detection limit, sensitivity, and reproducibility were examined. In addition, recovery was studied for accuracy. The working range was achieved using 6 or 8 calibration solutions between 0.1 and 200 µg/L NSAIDs. The calibration line for each analyte was plotted as concentration versus peak area. The signal-to-noise ratio of 3 was used for calculation of the limit of detection.

The precision of the proposed method was examined by RSD (%) synthetic solutions (100 µg/L). Recovery studies were enforced to evaluate the accuracy of the proposed method. In this maner, synthetic urine solution, wastewater samples and tap water samples spiked with 5 and 50 µg NSAID/L concentrations and drug spiked with 20 and 100 µg NSAID/L concentrations of target analyte were prepared. All these experiments were repeated five times.

# CHAPTER THREE
# RESULTS AND DISCUSSION

## 3.1 DMSPE Method

### *3.1.1 Characterization of Cu-BTC and Cu-BTC/MMT composites*

The characterization of the structure and morphology of the prepared Cu-BTC and Cu-BTC/MMT composites were evaluated by the results of FTIR spectroscopy, TGA, XRD, BET, and SEM.

#### *3.1.1.1 FTIR Spectroscopy Results*

The spectra of Cu-BTC and Cu-BTC/MMT composites were largely comparable. The single bond OH vibrations of water molecules in Cu-BTC and MMT were seen at 3406 $cm^{-1}$ and 3398 $cm^{-1}$, respectively. This peak was detected in the composites around 3414-3409 $cm^{-1}$. The ligand BTC's $COO^-$ asymmetric vibrations were located at 1643 and 1372 $cm^{-1}$. C-O-Cu vibration was identified at 1106 $cm^{-1}$. Additionally, the peak at 729 $cm^{-1}$ is known as specific absorption band of Cu-BTC (Dai et al., 2019; Hao & Liu, 2022). The peaks at 3605 $cm^{-1}$ and 1655 $cm^{-1}$ belong to stretching and bending vibrations of -OH bonded to Al or Mg ions in MMT. The broad peak at 3398 $cm^{-1}$ belongs to water stretching vibration in MMT. The strong peak at 1037 $cm^{-1}$seen in MMT belongs to the Si-O stretching vibration and it was shifted to 1040-1060 $cm^{-1}$ in the studied composites. The peaks at 795, 522, and 420 $cm^{-1}$ represents the presence of amorphous silica, Si-O-Al, and Si-O-Si bending vibrations, respectively (Zeynizadeh, Rahmani, & Tizhoush, 2020). In composites, the presence of the basic peaks of Cu-BTC and MMT and Cu-BTC, demonstrate the successfulness of the prepared composites. Figures 3.1 and 3.2 represents the FTIR spectra of MMT, Cu-BTC, and Cu-BTC/MMT composites.

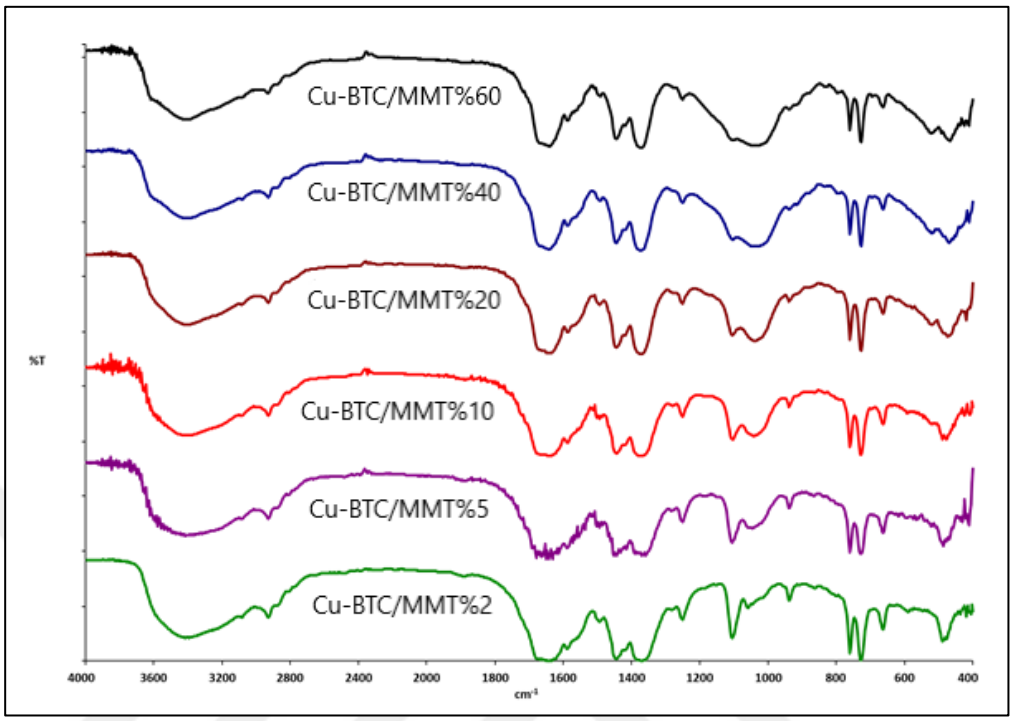



Figure 3.1 FTIR spectra of Cu-BTC/MMT composites

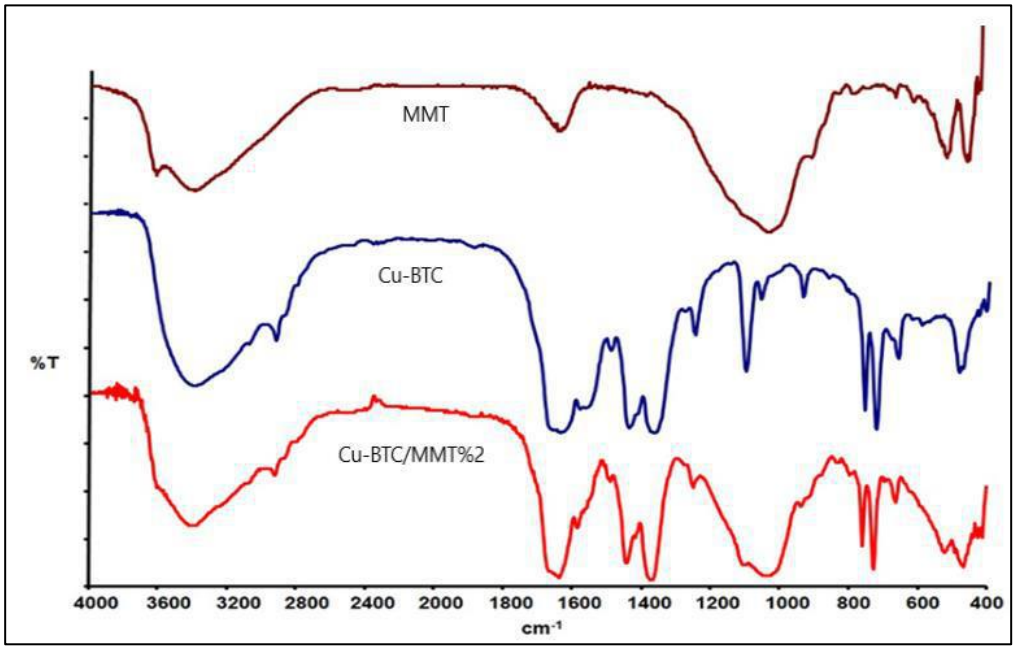



Figure 3.2 FTIR spectra of MMT, Cu-BTC, and Cu-BTC/MMT%2

*3.1.1.2 TGA Results*

The presence of MMT in increasing amounts caused to rise in the humidity exit temperature and contents due to the MMT's significant humidity-holding capacity. Cu-BTC had a moisture exit temperature of 50 °C, whereas the composite had one of about 100 °C. Cu-BTC and its composite both experienced a second mass loss at 220 and 280 °C, respectively, as a result of DMF being removed from the pores and coordinated water molecules being lost (Sun et al., 2014; Sule & Mishra, 2019). When MMT was added, there was no discernible difference in the end disintegration temperature, which matched with the material's thermal stability at 280-300 °C (Li & Wu, 2021). Figures 3.3 and 3.4 illustrate the thermal responses of Cu-BTC, MMT, and the Cu-BTC/MMT composites. The thermal behavior's agreement with earlier studies proved that Cu-BTC and the composite had been successfully created. Furthermore, it was discovered that an increase in the remaining amount of decomposition occurred along with an increase in MMT amount levels (Figure 3.4).

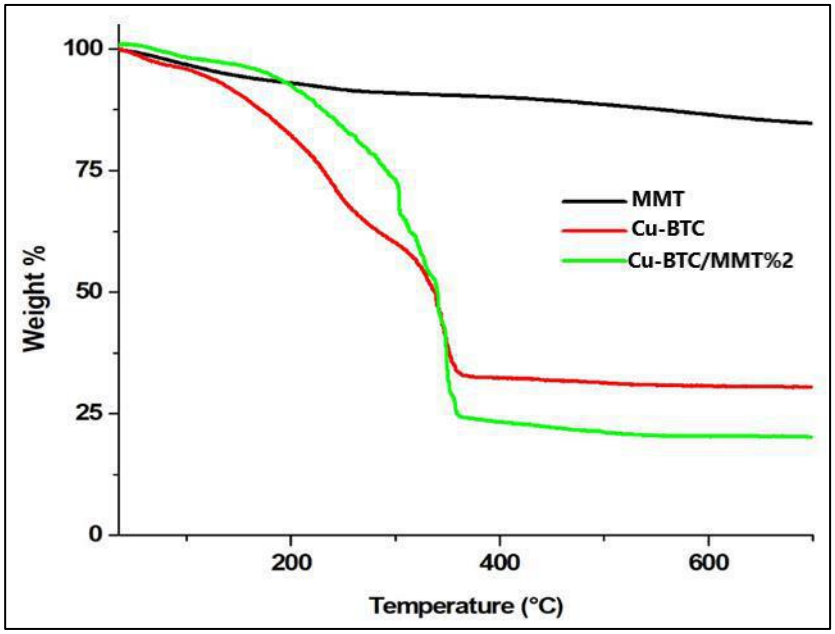



Figure 3.3 TGA curves of MMT, Cu-BTC, and Cu-BTC/MMT%2

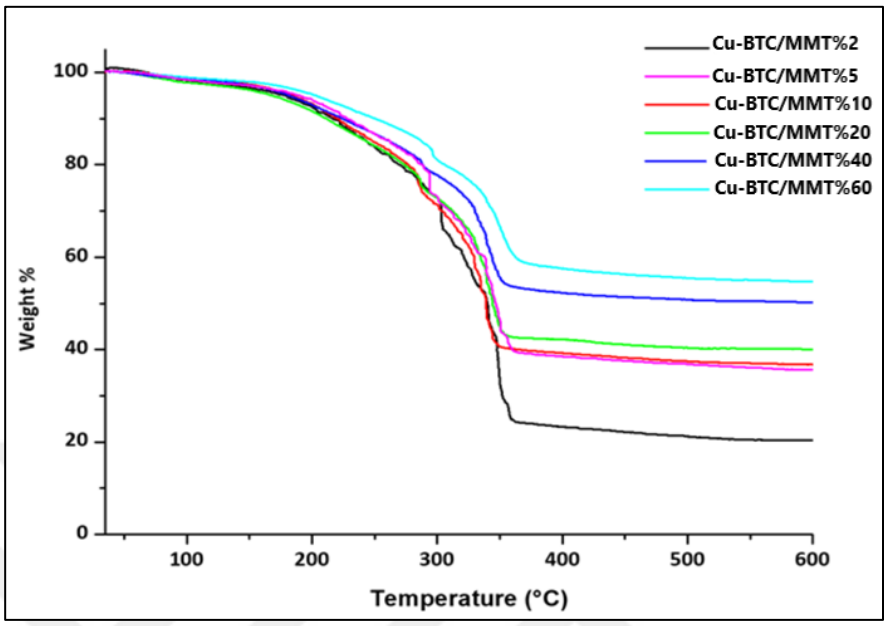



Figure 3.4 TGA curves of Cu-BTC/MMT composites

*3.1.1.3 XRD Results*

Figures 3.5 and 3.6 show the XRD patterns of MMT, Cu-BTC, and Cu-BTC/MMT composites. The distinctive Cu-BTC peaks at 6.7º, 9.4º, 11.6º, 13.4º, 16.5º, 17.5º, 19.1º, 20.2º were consistent with those reported in earlier studies (Hao & Liu, 2022; Li & Wu, 2021). The Cu-BTC crystal structure was substantially preserved following MMT loading, according to the similar powder diffractions of Cu-BTC and Cu-BTC/MMT composites (Habimana et al., 2018). Additionally, the interaction of MMT with Cu-BTC indicates a decrease in peak intensity. Also, Cu-BTC/MMT composites with varying MMT amounts have exhibited XRD patterns that are very similar (Figure 3.6). The Cu-BTC/MMT composites have preserved the Cu-BTC's microstructure as evidenced by the similar characteristic peaks of all composites to the Cu-BTC. Another indication of the composite's smooth crystalline structure was the sharp and distinct XRD pattern (Hao & Liu, 2022; Li et al., 2019).

As demonstrated in Cu-BTC-based graphene oxide composites, The change in the Cu-BTC/MMT composites' peaks intensity with the addition of MMT references the interactivity of MMT with Cu-BTC (Dai et al., 2019).

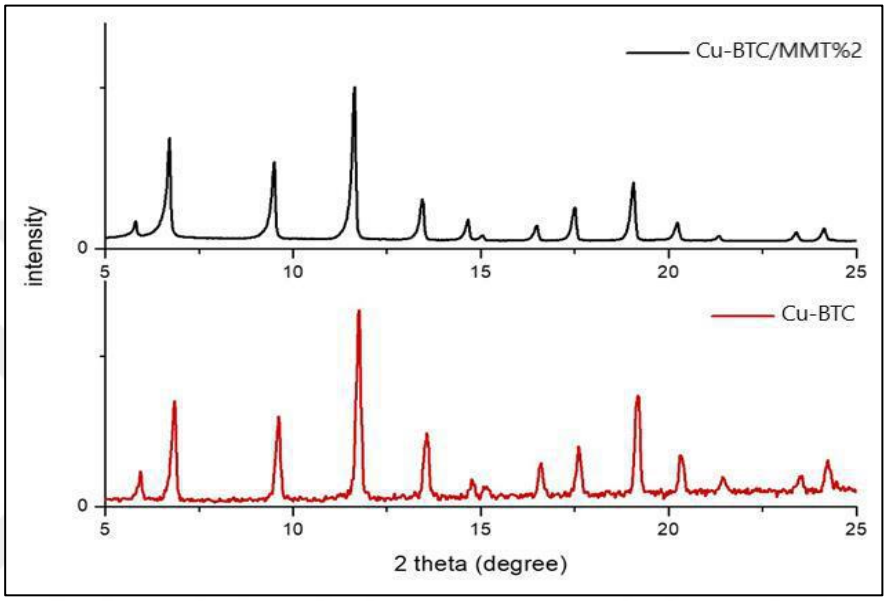



Figure 3.5 XRD patterns of Cu-BTC and Cu-BTC/MMT%2

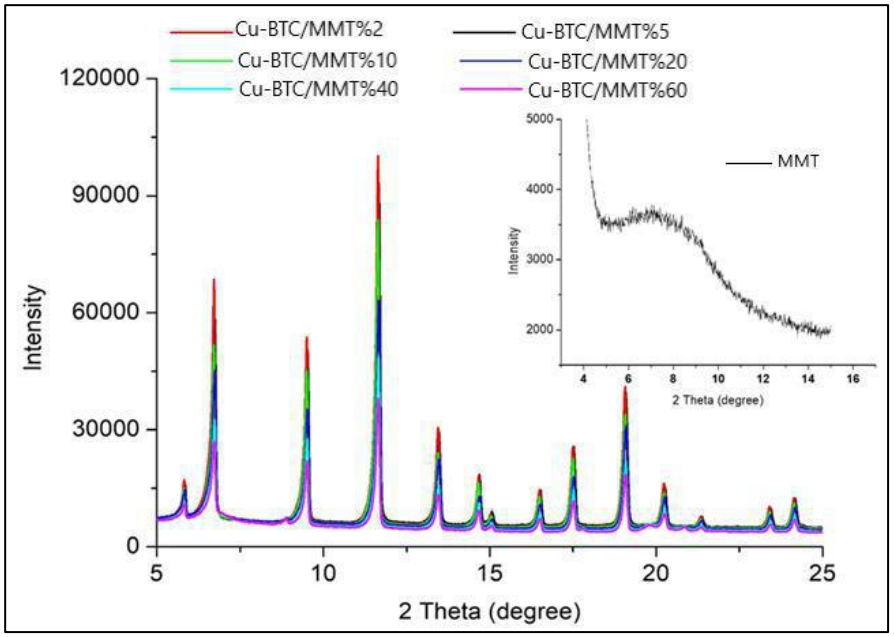



Figure 3.6 XRD patterns of MMT and Cu-BTC/MMT composites

*3.1.1.4 BET Results*

Figure 3.7 represents the $N_2$ adsorption/desorption isotherms of Cu-BTC and Cu-BTC/MMT%2. Table 3.1 also includes a summary of the BET results. Cu-BTC, Cu-BTC/MMT%2, and MMT had surface areas that were 985, 826, and 46 $m^2/g$, respectively, and these values were similar to the previous researches (Sule & Mishra, 2019; Liu, Fan et al., 2020; Li et al., 2019). Regarding the results, the composite had a specific surface area that was somewhat less than Cu-BTC and significantly larger than MMT. This might be explained by how MOF and MMT interacted, as well as by how well the composite was made. It was discovered that the composite's surface area was marginally less than Cu-BTC's. This can be explained by the setting of particles of MMT into the pores of Cu-BTC surface. Cu-BTC has a total pore volume higher than Cu-BTC/MMT%2 composite. Due to MMT particles obstructing Cu-BTC's pores, the composite had a smaller pore volume. Furthermore, a reduction in pore size added support to this circumstance (Liu, Fan et al., 2020).

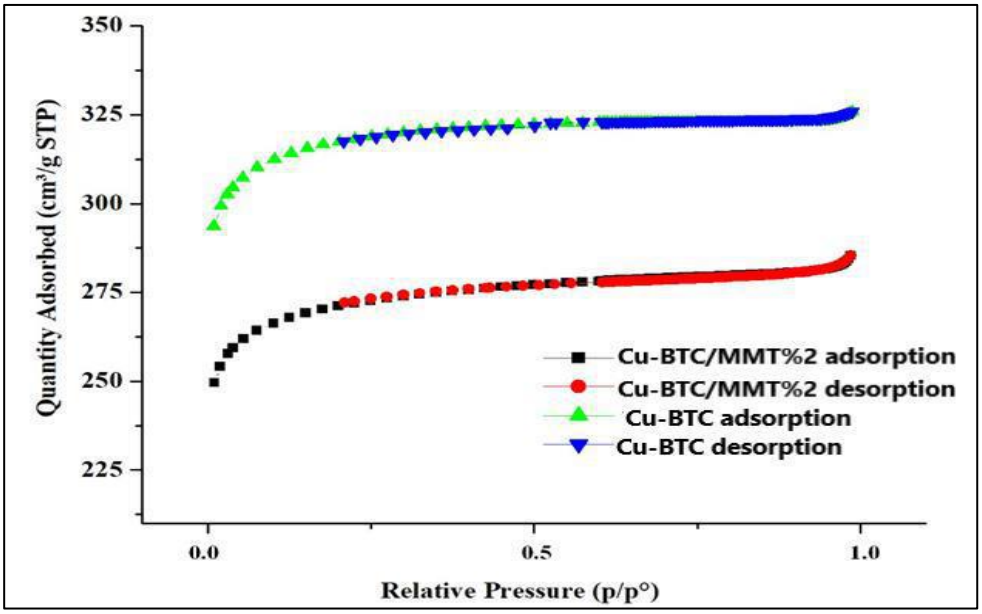



Figure 3.7 $N_2$ adsorption/desorption isotherms of Cu-BTC and Cu-BTC/MMT%2

Table 3.1 Results of $N_2$ adsorption-desorption isotherms

| Compound | Surface area ($m^2/g$) | Total pore volume ($cm^3/g$) | Micropore volume ($cm^3/g$) | Pore size (nm) |
|---|---|---|---|---|
| Cu-BTC | 985 | 0.5 | 0.45 | 20.46 |
| MMT | 46 | 0.13 | 0.52 | 14.98 |
| Cu-BTC/MMT%2 | 826 | 0.31 | 0.27 | 19.84 |

*3.1.1.5 SEM Results*

Figure 3.8 shows SEM images of Cu-BTC and Cu-BTC/MMT%2 composite. In the SEM images, it is clearly seen that Cu-BTC has a smooth surface and the composite is in the form of a polyhedron that has a sharp. Additionally, it could be demonstrated that the particles of MMT are surrounded by the particles of Cu-BTC. Cu-BTC and Cu-BTC/MMT%2 had similar dimensions and forms. The crystal size was decreased from 5 μm to 1.5 μm due to composite creation. Due to the centrifugation and washing processes, some fractured polyhedron particles may also be seen.

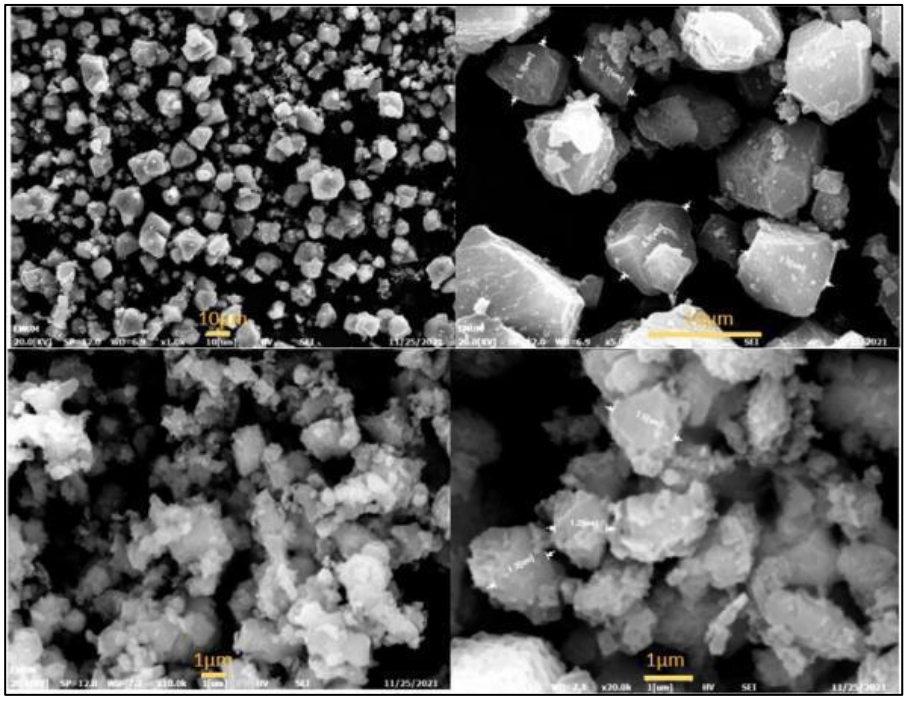



Figure 3.8 SEM images of Cu-BTC (right) and Cu-BTC/MMT%2 composite (left)

### 3.1.2 Chromatographic Separation of SAs and PENs

Several mobile phases were tested in gradient elution mode to create an HPLC approach for the separation of PENs and SAs at the same time depending on the earlier studies (Jia et al., 2017; Injac, Kočevar, & Štrukelj, 2009; Samanidou, Michaelidou, Kabir, & Furton, 2017). The chromatographic column used was a C18 column. The mobile phase flow rate is 1 mL/min. A 20 µL of the sample was injected. Following were the mobile phases used in gradient elution: 0.2% TFA in water:acetonitrile (50:50), and 0.1% TFA in water:acetonitrile (50:50). With the last studied mobile phase, separation and a sufficient peak resolution were attained in just 28 min. Afterwards, to achieve optimal sensitivity, the absorption of all studied antibiotics were investigated at their maximum absorption wavelengths (220 nm, 230 nm and 270 nm). Maximum absorption was achieved at a detection wavelength of 230 nm for PENs and 270 nm for SAs. The retention times of antibiotics are given in Table 3.2.

Table 3.2 Retention times of Sulfonamides and Penicillins

| **SAs** | **Retention time, min** | **PENs** | **Retention time, min** |
|---|---|---|---|
| SDA | 4.96 ± 0.03 | AMX | 6.03 ± 0.06 |
| SMT | 8.42 ± 0.05 | AMP | 9.18 ± 0.05 |
| SCP | 10.28 ± 0.06 | PENG | 9.88 ± 0.06 |
| SMX | 11.42 ± 0.04 | CLO | 19.41 ± 0.06 |
| SSX | 12.26 ± 0.05 | NAF | 19.92 ± 0.05 |
| SDMX | 13.70 ± 0.03 | DICLO | 21.02 ± 0.03 |

### *3.1.3 Optimization Conditions of DMSPE Method*

In order to get the best extraction conditions, many variables were examined, including the type of sorbent, pH, adsorbent mass, the extraction time, ionic strength, desorption solvent, desorption time and the volume of desorption solvent in the DMSPE method by mixing 100 µg/L of each SA and PEN drugs in 5 mL aqueous test solution.

All experiments were done three times.The extraction parameters were evaluated as extraction recovery (ER%).

$$\text{ER (\%)} = \frac{n_f}{n_{int}} = \frac{C_f \, x V_f}{C_{int} \, x \, V_{int}} x \, 100 \qquad (3.1)$$

where $C_{int}$ - initial concentration of antibiotics, and $C_f$ - final concentration of antibiotics in the test solution (100 µL). $V_{int}$ is initial volume of a test or sample solution. $V_f$ is the final volume (100 µL) of the test solution. The calibration equations and the peak areas of antibotics are used to determine $C_f$.

*3.1.3.1 Choosing a Cu-BTC/MMT Composite*

For the separating and enriching of the studied PENs and SAs, the extraction abilities of the synthesized materials containing various amounts of MMT were examined. Under the same experimental conditions, the extraction performance of Cu-BTC, MMT and Cu-BTC/MMT%Y materials (Y= 2, 5, 10, 20, 40, and 60) were studied (Figure 3.9). For all analyzed antibiotics, Cu-BTC/MMT%2 composite exhibited better ERs between 84.4 and 98.0%. It is evident that the Cu-BTC/MMT composites' extraction recoveries decreased as the amount of MMT increased. The big dispersion of Cu sites in the clay surface could be a possible explanation for this (Habimana et al., 2018). As a result, Cu-BTC/MMT%2 was selected as the best option for further DMSPE process parameter optimization since it was better suited for the separating and preconcentration of analytes. Thereafter, the composite was referred to simply as Cu-BTC/MMT in further experiments.

Cu-BTC and Cu-BTC/MMT composites had greater ERs of PENs and SAs than MMT, as shown in Figure 3.10. It is concluded that electrostatic interactions between antibiotic groups and clay is likely to be minimal, resulting in ER of under 70%. In comparison to Cu-BTC, the extraction recovery of the examined analytes increased by 1 to 14% in the Cu-BTC/MMT%2 composite due to the inclusion of MMT. Despite the

composite having a somewhat smaller surface area than the MOF compound, it is obvious that the composite has a larger holding capacity than both MOF and MMT when the amount of material that has been adsorbed is considered.

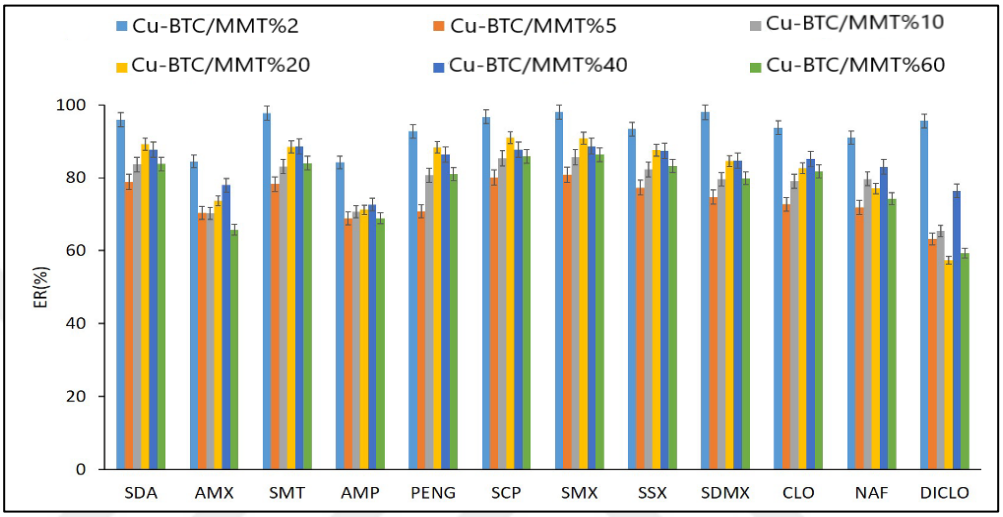



Figure 3.9 MMT mass effect in a composite of Cu-BTC/MMT on ER% of PENs and SAs

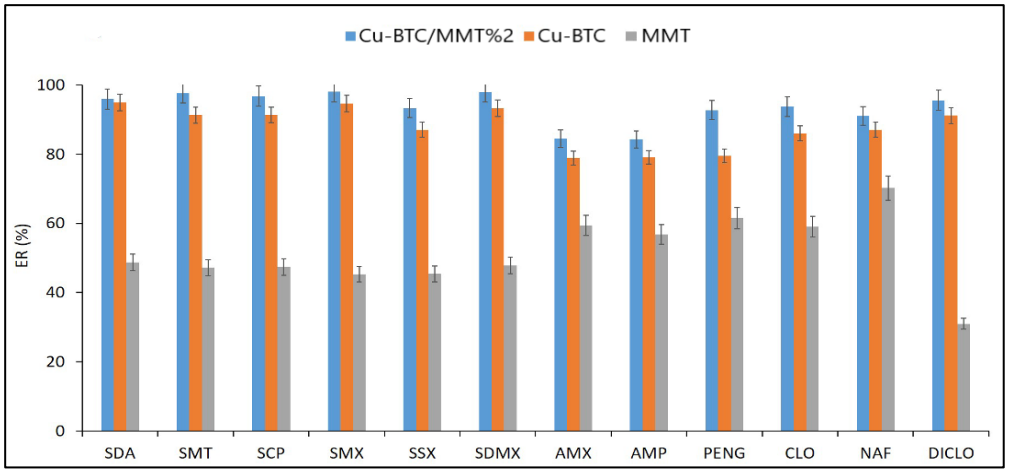



Figure 3.10 Comparison of MMT, Cu-BTC, and Cu-BTC/MMT's extraction effectiveness

### *3.1.3.2 pH Effect*

One of the most important variable is pH of sample solution in the extraction of analytes. The analyte recovery is affected from the pH medium. The studied antibiotic

groups are ionizable and have one or more pKa values. pKa1 and pKa2 values of SAs are ranged from 1.6 to 2.13 and 4.7 to 6.5, respectively. pKa1 value of PENs is ~ 2.6 and pKa2 of some PENs (AMX and AMP) is 7.4. Therefore, pH effect was investigated from 3 to 8 for the extraction of antibiotic groups. The analytes' functional groups can be in anionic forms or mono-charged depending on the pH of the sample solution. As seen in Figure 3.11, the extraction efficiencies of the antibiotic groups were highest at pH 4. This sorption at this pH can be explained by the begining of deprotonation of the carboxylic acid group in PENs and amino group in SAs. This deprotonation causes H-bonding and electrostatic interacitons between the antibiotics and the surface of Cu-BTC/MMT adsorbent. At higher pH values, anionic forms of antbiotics could not be interact with the composite because its surface is negative at pH 5.6 that is point of zero charge (Figure 3.12). Furthermore, the increase in pH could cause degradation in penicillins (Brouwers et al., 2020). So, sample solutions were adjusted to pH 4 for further studies.

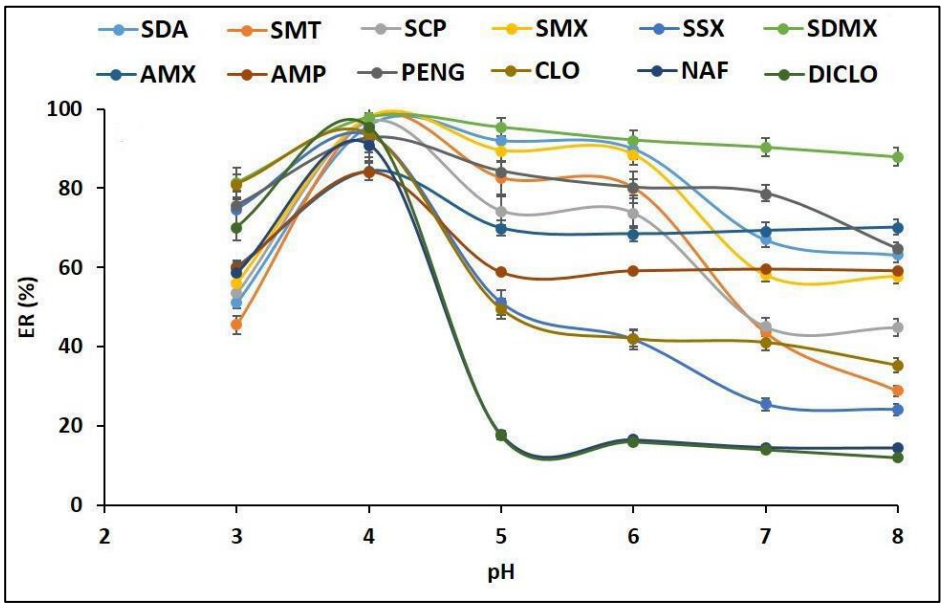



Figure 3.11 pH effect on ER% of PENs and SAs

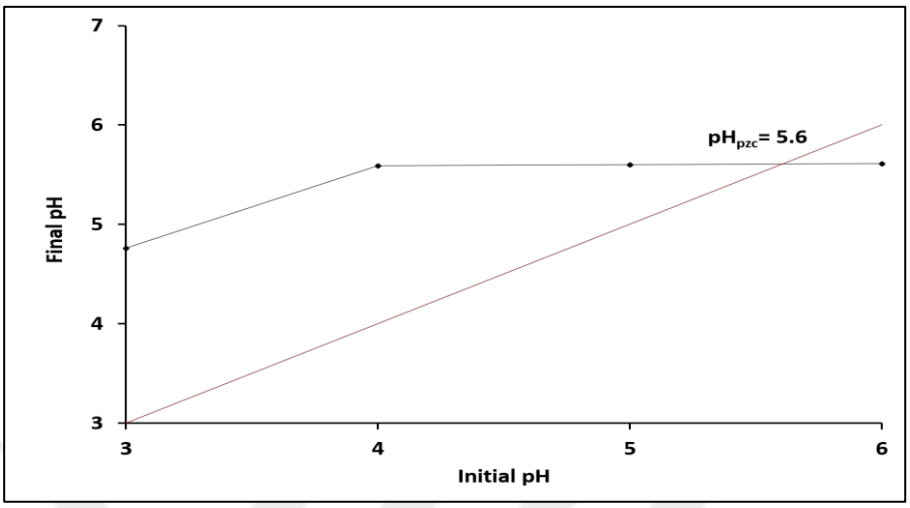



Figure 3.12 PZC determination of Cu-BTC/MMT composite

*3.1.3.3 Effects of Sorbent Mass and Extraction Time*

The amount of sorbent was examined in the range of 2-10 mg to investigate the best extraction recovery. The results were given in Figure 3.13. The extraction ability of the composite reached to the plateau of 8 mg and over for antibiotic groups. For further studies, the amount of sorbent was chosen as 10 mg.

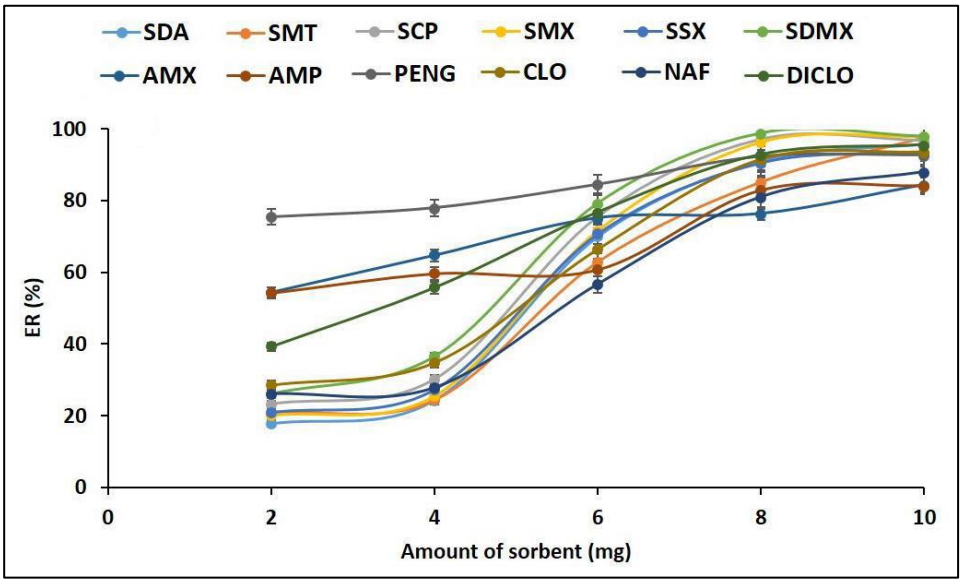



Figure 3.13 Effect of sorbent mass on ER% of PENs and SA

To reach equilibrium in the DMSPE method, the vortex was used for the adsorption of the analyte on the sorbent. The equilibrium reached its maximum after 10 min, as seen in Figure 3.14, and altered slightly for more than 10 min. H-bonding and electrostatic interactions could be responsible for the interactions between antibiotics and the Cu-BTC/MMT composite. It can be said that these interactions encourage adsorption. So, the extraction time was applied as 10 min for the later studies.

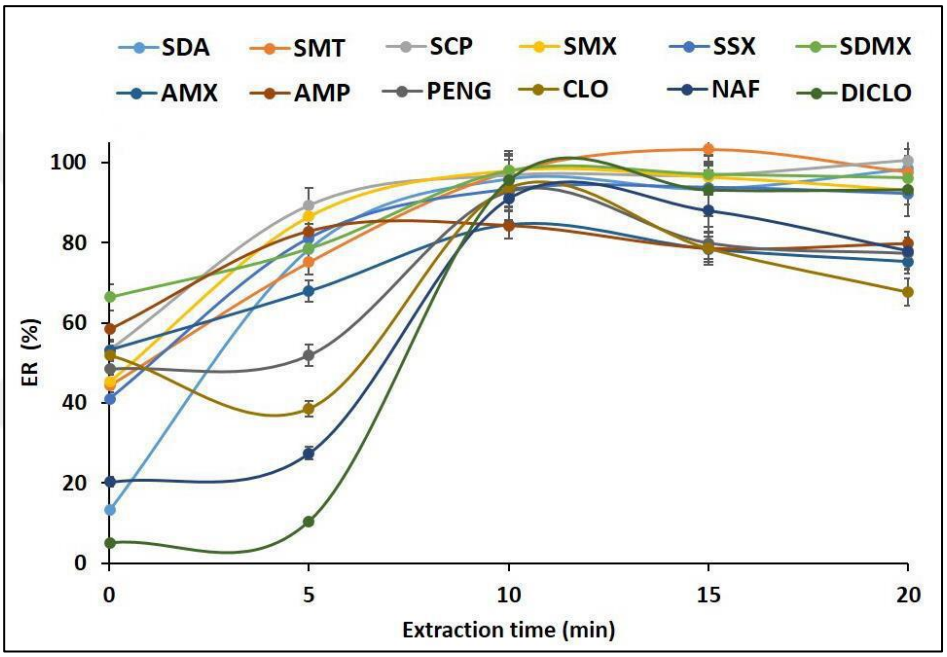



Figure 3.14 Extraction time effect on ER% of PENs and SAs

*3.1.3.4 Salt Effect*

NaCl and $Na_2SO_4$ were used to measure the impact of salt concentration in the range of 0 M to 0.1 M with increments of 0.02. The extraction efficiencies of all analytes were decreased by the addition of both salts. All analytes' extraction recoveries changed by less than 30%, as shown in Figure 3.15 and 3.16. This alteration can result from the sample solution's increased density and viscosity, which make it more difficult to interact between the analyte and the adsorbent. Because of this, salt was not added to test solutions for increasing extraction ability.

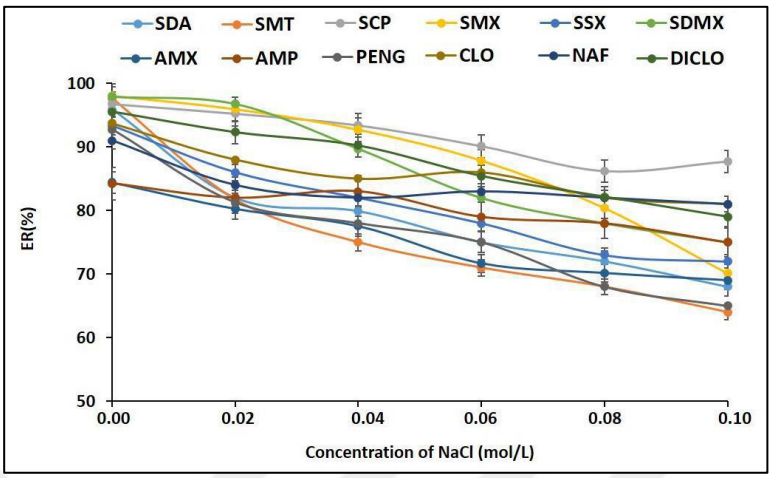



Figure 3.15 Effect of NaCl on ER% of PENs and SAs

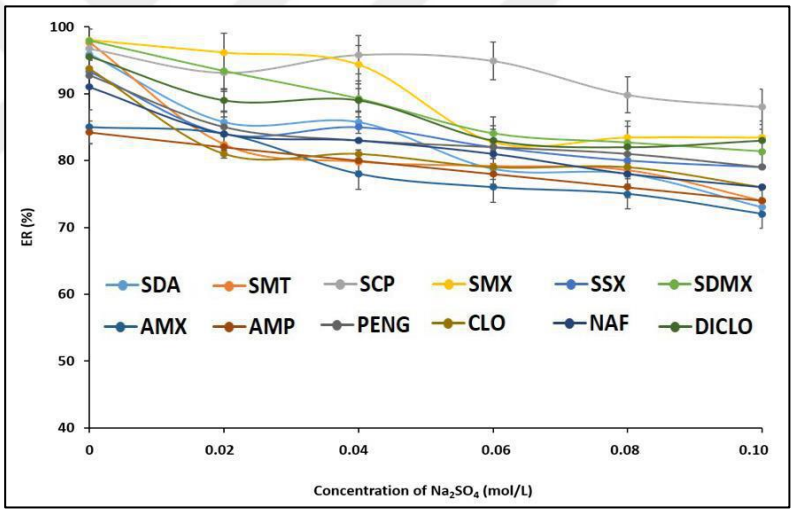



Figure 3.16 Effect of $Na_2SO_4$ on ER% of PENs and SAs

*3.1.3.5 Parameters of Desorption Solvent*

To completely recover the analytes from the sorbent, the solvents and their amounts are crucial. As a result, the different desorption solvents, the volume of desorption solvent, and the time of desorption were investigated. Previously, the following substances were subject to extraction methods: dimethylformamide, ethanol, acetonitrile, methanol, trifluoroacetic acid as 0.1%, ACN: 0.1%TFA (50:50), acetic acid:ethanol (1:9), and acetic acid:methanol (1:9). Acetonitrile for PENs and methanol

for SAs were found as best elution solvents. To use one desorption solvent, different ratios of methanol and acetonitrile were studied and the highest desorption was achieved for each group with a 50:50 ratio of acetonitrile and methanol mixture. As seen in Figure 3.17, the acetonitrile and methanol mixture as 50:50 caused the raise in the extraction efficiency of the studied antibiotic groups. As a result, the elution solvent was chosen to be ACN: MeOH (1:1).

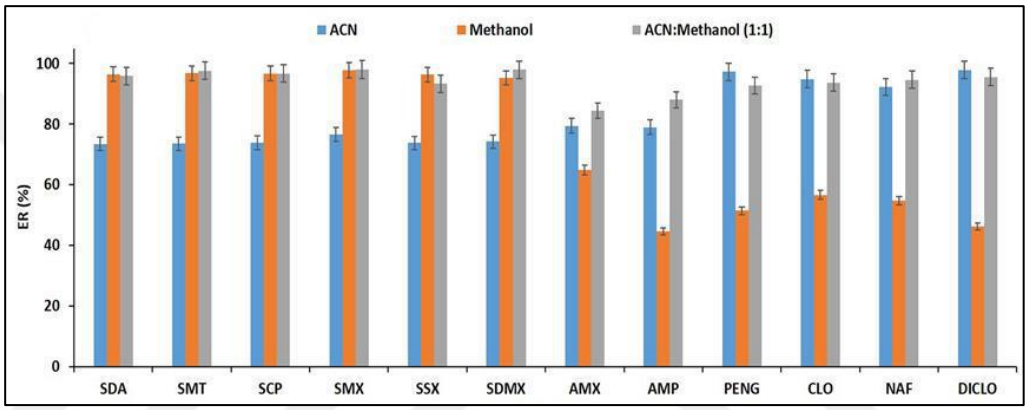



Figure 3.17 Effect of elution solvent type on ER% of PENs and SAs

The desortion solvent volume was studied for up to 1.25 mL. Regarding the outcomes, ER for SAs with 0.75 mL reached more than 90%, whilst ER for PENs reached more than 72%. In samples of 1 mL and greater, PENs recovery ranged from 85 to 96%, and SAs recovery was enhanced to more than 93% (Figure 3.18).

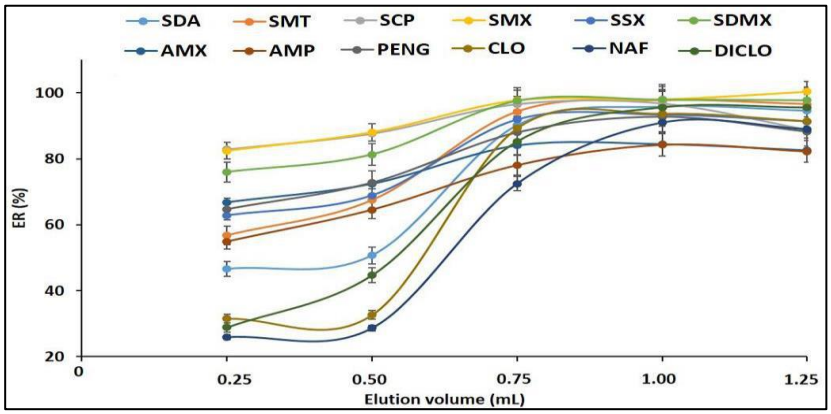



Figure 3.18 Effect of elution volume on ER% of PENs and SAs

The desorption time was also investigated for up to 15 min, and the maximum analyte recovery was attained at 5 min and then stabilized after that (Figure 3.19). 5 min was chosen to be the ideal elution time to ensure successful extraction and prevent a long analysis duration.

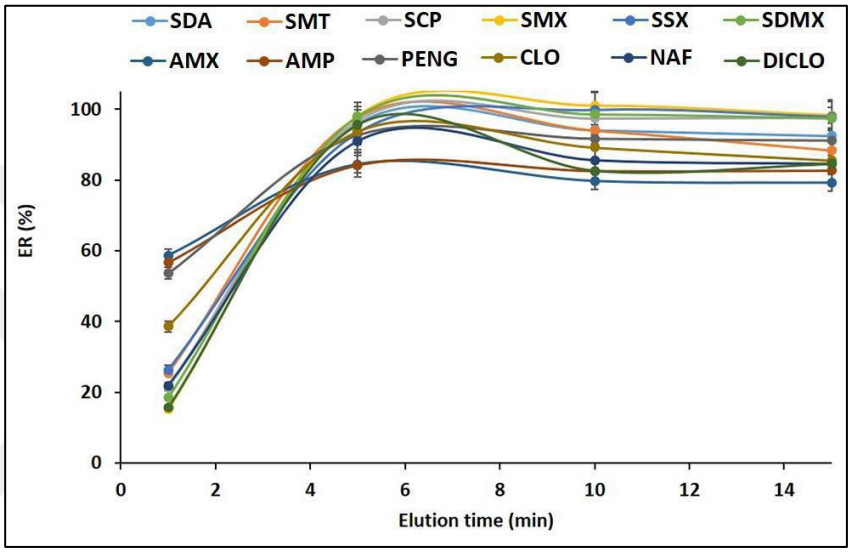



Figure 3.19 Effect of elution time on ER% of PENs and SAs

### *3.1.4 Reusability of Cu-BTC/MMT*

The reusability of an adsorbent can be used to evaluate its effectiveness. The sorption/elution process was repeated to determine the reusability of the prepared adsorbent for 100 µg/L of PENs and SAs under optimized working parameters. The used adsorbent before reusing was washed with first ACN: MeOH (1:1) solution and then deionized water after each sorption and elution procedure and dried. The extraction recovery fell by about 5-7% after five cycles, as shown in Figure 3.20, showing a slight reduction in the adsorption of each analyte. For SAs and PENs, the repeatability of extraction efficiency was between 2.4 and 4.0 RSD%. The reusability of proposed adsorbent was similar was with some materials given in earlier studies (graphene oxide including MOF and hydrophilic molecular imprinted polymers (Jia et al., 2017; Zhao et al., 2021).

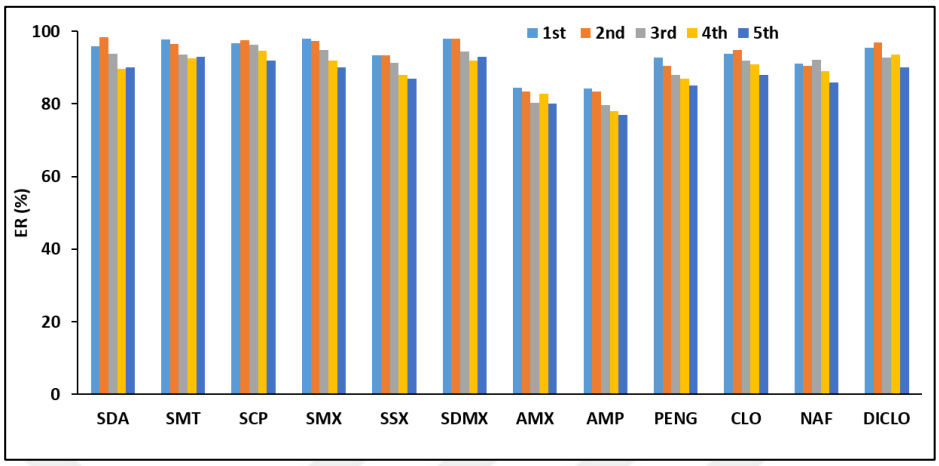



Figure 3.20 Reusability of Cu-BTC/MMT on adsorption of SAs and PENs

### *3.1.5 Method Validation*

Under optimal conditions, the developed DMSPE-HPLC/DAD technique was assessed for linearity, limit of detection, limit of quantitation, precision, specificity, accuracy and sensitivity (Table 3.3) for synthetic urine, milk and deionized water. The suggested approach was used to analyze a pasteurized milk sample (glass bottle) before the method's validation and no SAs or PENs were found. With $R^2$ ≥0.9947 in all examined solutions, working range from 1 to 400 µg/L for PENs and 0.5 to 400 µg/L for SAs was obtained.

Three various milk samples were employed to test the method's specificity, and no potential interferences were found close to the PENs and SAs retention times at 230 nm and 270 nm, respectively.

Standard deviations (SDs) were shown in Tables 3.4 and 3.5 for the slope and intercept of the regression equations for each sample. The slope values ranged from 0.0122 to 0.0629, and the SDs were between 0.0007 and 0.000722. The limit of detections of PENs and SAs were in the range of 0.30 to 1.50 µg/L and 0.10 to 0.15 µg/L, respectively. Limit of quantitaitons of PENs and SAs were in the range of 1.00 to 5.00 µg/L and 0.33 to 0.50 µg/L, respectively.

Table 3.3 Analytical performance of SAs and PENs using Cu-BTC/MMT in DMSPE method

| Analytes | Deionized water | | | | Pasteurized milk (glass bottle) | | | | Synthetic urine | | | |
|---|---|---|---|---|---|---|---|---|---|---|---|---|
| | **Working range (µg/L)** | **$R^2$** | **LOD (µg/L)** | **LOQ (µg/L)** | **Working range (µg/L)** | **$R^2$** | **LOD (µg/L)** | **LOQ (µg/L)** | **Working range (µg/L)** | **$R^2$** | **LOD (µg/L)** | **LOQ (µg/L)** |
| AMP | 5-400 | 0.9959 | 1.50 | 5.00 | 5-400 | 0.9947 | 1.46 | 4.87 | 5-400 | 0.9895 | 1.45 | 4.83 |
| CLO | 2.5-400 | 0.9993 | 0.68 | 2.27 | 2.5-400 | 0.9994 | 0.74 | 2.47 | 2.5-400 | 0.9998 | 0.73 | 2.43 |
| AMX | 2.5-400 | 0.9995 | 0.72 | 2.40 | 2.5-400 | 0.9986 | 0.66 | 2.20 | 2.5-400 | 0.9966 | 0.75 | 2.50 |
| PENG | 5-400 | 0.9991 | 1.38 | 4.60 | 5-400 | 0.9992 | 1.39 | 4.63 | 5-400 | 0.9972 | 1.25 | 4.17 |
| DICLO | 1-400 | 0.9952 | 0.30 | 1.00 | 1-400 | 0.9966 | 0.30 | 1.00 | 1-400 | 0.9991 | 0.30 | 1.00 |
| NAF | 5-400 | 0.9992 | 1.24 | 4.13 | 5-400 | 0.9992 | 1.31 | 4.37 | 5-400 | 0.9993 | 1.12 | 3.73 |
| SMT | 0.5-400 | 0.9994 | 0.13 | 0.43 | 0.5-400 | 0.9990 | 0.12 | 0.40 | 0.5-400 | 0.9999 | 0.14 | 0.47 |
| SSX | 0.5-400 | 0.9996 | 0.10 | 0.33 | 0.5-400 | 0.9996 | 0.13 | 0.43 | 0.5-400 | 0.9997 | 0.14 | 0.47 |
| SCP | 0.5-400 | 0.9979 | 0.14 | 0.47 | 0.5-400 | 0.9995 | 0.15 | 0.50 | 0.5-400 | 0.9997 | 0.13 | 0.43 |
| SDMX | 0.5-400 | 0.9990 | 0.12 | 0.40 | 0.5-400 | 0.9993 | 0.14 | 0.47 | 0.5-400 | 0.9998 | 0.14 | 0.47 |
| SDA | 0.5-400 | 0.9985 | 0.14 | 0.47 | 0.5-400 | 0.9995 | 0.15 | 0.50 | 0.5-400 | 0.9998 | 0.14 | 0.47 |
| SMX | 0.5-400 | 0.9984 | 0.12 | 0.40 | 0.5-400 | 0.9986 | 0.13 | 0.43 | 0.5-400 | 0.9995 | 0.14 | 0.47 |

Table 3.4 Regression line parameters of DMSPE method for SAs

| SAs | Deionized water | | Pasteurized milk (glass bottle) | | Synthetic urine | |
|---|---|---|---|---|---|---|
| | **Slope ± SD** | **Intercept ± SD** | **Slope ± SD** | **Intercept ± SD** | **Slope ± SD** | **Intercept ± SD** |
| SDA | $4.71 \times 10^{-2} \pm 6.50 \times 10^{-4}$ | $1.08 \times 10^{-1} \pm 1.11 \times 10^{-1}$ | $4.79 \times 10^{-2} \pm 3.78 \times 10^{-4}$ | $2.22 \times 10^{-2} \pm 6.58 \times 10^{-2}$ | $4.83 \times 10^{-2} \pm 2.61 \times 10^{-4}$ | $-1.47 \times 10^{-2} \pm 4.55 \times 10^{-2}$ |
| SMT | $5.96 \times 10^{-2} \pm 5.05 \times 10^{-4}$ | $4.54 \times 10^{-2} \pm 8.79 \times 10^{-2}$ | $5.82 \times 10^{-2} \pm 6.49 \times 10^{-4}$ | $4.75 \times 10^{-2} \pm 1.13 \times 10^{-1}$ | $5.96 \times 10^{-2} \pm 1.90 \times 10^{-4}$ | $-4.47 \times 10^{-2} \pm 3.31 \times 10^{-2}$ |
| SCP | $5.71 \times 10^{-2} \pm 9.17 \times 10^{-4}$ | $8.35 \times 10^{-2} \pm 1.60 \times 10^{-1}$ | $5.85 \times 10^{-2} \pm 4.66 \times 10^{-4}$ | $2.44 \times 10^{-2} \pm 8.11 \times 10^{-2}$ | $5.78 \times 10^{-2} \pm 3.63 \times 10^{-4}$ | $-1.24 \times 10^{-2} \pm 6.32 \times 10^{-2}$ |
| SMX | $6.20 \times 10^{-2} \pm 8.74 \times 10^{-4}$ | $1.07 \times 10^{-1} \pm 1.52 \times 10^{-1}$ | $1.25 \times 10^{-1} \pm 1.19 \times 10^{-3}$ | $1.34 \times 10^{-1} \pm 2.07 \times 10^{-1}$ | $6.25 \times 10^{-2} \pm 4.84 \times 10^{-4}$ | $1.07 \times 10^{-2} \pm 8.43 \times 10^{-2}$ |
| SSX | $6.02 \times 10^{-2} \pm 4.47 \times 10^{-4}$ | $7.15 \times 10^{-2} \pm 7.78 \times 10^{-2}$ | $6.01 \times 10^{-2} \pm 4.46 \times 10^{-4}$ | $3.05 \times 10^{-2} \pm 7.78 \times 10^{-2}$ | $6.03 \times 10^{-2} \pm 3.80 \times 10^{-4}$ | $-2.79 \times 10^{-3} \pm 6.61 \times 10^{-2}$ |
| SDMX | $6.31 \times 10^{-2} \pm 7.14 \times 10^{-4}$ | $6.74 \times 10^{-2} \pm 1.24 \times 10^{-1}$ | $6.29 \times 10^{-2} \pm 6.01 \times 10^{-4}$ | $2.44 \times 10^{-2} \pm 1.05 \times 10^{-1}$ | $6.38 \times 10^{-2} \pm 3.39 \times 10^{-4}$ | $-6.39 \times 10^{-2} \pm 5.91 \times 10^{-2}$ |

Table 3.5 Regression line parameters of DMSPE method for PENs

| PENs | Deionized water | | Pasteurized milk (glass bottle) | | Synthetic urine | |
|---|---|---|---|---|---|---|
| | **Slope ± SD** | **Intercept ± SD** | **Slope ± SD** | **Intercept ± SD** | **Slope ± SD** | **Intercept ± SD** |
| AMX | $4.38 \times 10^{-3} \pm 3.88 \times 10^{-5}$ | $-1.07 \times 10^{-2} \pm 7.56 \times 10^{-3}$ | $4.54 \times 10^{-3} \pm 7.00 \times 10^{-5}$ | $-2.14 \times 10^{-2} \pm 1.36 \times 10^{-2}$ | $4.34 \times 10^{-3} \pm 1.04 \times 10^{-4}$ | $-2.33 \times 10^{-2} \pm 2.02 \times 10^{-2}$ |
| AMP | $4.04 \times 10^{-3} \pm 1.16 \times 10^{-4}$ | $-2.39 \times 10^{-2} \pm 2.42 \times 10^{-2}$ | $4.17 \times 10^{-3} \pm 1.36 \times 10^{-4}$ | $-2.64 \times 10^{-2} \pm 2.82 \times 10^{-2}$ | $4.28 \times 10^{-3} \pm 1.97 \times 10^{-4}$ | $-5.39 \times 10^{-2} \pm 4.10 \times 10^{-2}$ |
| PENG | $1.21 \times 10^{-2} \pm 1.62 \times 10^{-4}$ | $-1.74 \times 10^{-2} \pm 3.37 \times 10^{-2}$ | $1.22 \times 10^{-2} \pm 1.58 \times 10^{-4}$ | $-1.82 \times 10^{-2} \pm 3.28 \times 10^{-2}$ | $1.23 \times 10^{-2} \pm 2.89 \times 10^{-4}$ | $-8.11 \times 10^{-2} \pm 6.02 \times 10^{-2}$ |
| CLO | $2.79 \times 10^{-2} \pm 3.04 \times 10^{-4}$ | $-3.88 \times 10^{-2} \pm 5.91 \times 10^{-2}$ | $2.84 \times 10^{-2} \pm 2.88 \times 10^{-4}$ | $-2.69 \times 10^{-2} \pm 5.61 \times 10^{-2}$ | $2.81 \times 10^{-2} \pm 1.61 \times 10^{-4}$ | $-9.03 \times 10^{-2} \pm 3.14 \times 10^{-2}$ |
| NAF | $5.89 \times 10^{-2} \pm 7.57 \times 10^{-4}$ | $-8.53 \times 10^{-2} \pm 1.58 \times 10^{-1}$ | $5.96 \times 10^{-2} \pm 7.68 \times 10^{-4}$ | $-1.03 \times 10^{-1} \pm 1.60 \times 10^{-1}$ | $5.94 \times 10^{-2} \pm 7.22 \times 10^{-4}$ | $-2.98 \times 10^{-1} \pm 1.50 \times 10^{-1}$ |
| DICLO | $2.85 \times 10^{-2} \pm 6.97 \times 10^{-4}$ | $2.43 \times 10^{-1} \pm 1.21 \times 10^{-1}$ | $2.96 \times 10^{-2} \pm 6.07 \times 10^{-4}$ | $1.98 \times 10^{-1} \pm 1.06 \times 10^{-1}$ | $2.90 \times 10^{-2} \pm 3.21 \times 10^{-4}$ | $1.84 \times 10^{-1} \pm 5.59 \times 10^{-2}$ |

Table 3.6 lists the relative standard deviations for both within-day and between-day repeatability. Both antibiotic groups had good within-day and between-day precisions which are less than 1.98 RSD% and 3.26 RSD%, respectively in deionized water. All of the examined analytes had within-day and between-day precisions ranging between 1.16-2.32 RSD% and 1.57-3.05 RSD% in other samples, respectively.

Table 3.6 RSD results of PENs and SAs

| Analytes | Deionized water | | Pasteurized milk (glass bottle) | | Synthetic urine | |
|---|---|---|---|---|---|---|
| | Within-day[a] RSD% | Between-day[b] RSD% | Within-day RSD% | Between-day RSD% | Within-day RSD% | Between-day RSD% |
| AMP | 1.64 | 2.16 | 2.32 | 3.05 | 1.77 | 1.97 |
| CLO | 1.55 | 1.82 | 2.03 | 2.11 | 1.74 | 1.91 |
| DICLO | 1.33 | 1.81 | 1.64 | 2.06 | 1.55 | 2.03 |
| AMX | 1.84 | 3.26 | 2.15 | 3.04 | 2.19 | 2.59 |
| PENG | 1.98 | 2.14 | 1.79 | 2.21 | 2.00 | 2.17 |
| NAF | 1.45 | 1.65 | 2.31 | 2.56 | 1.72 | 2.03 |
| SDA | 0.64 | 1.86 | 1.79 | 2.34 | 1.68 | 2.19 |
| SCP | 0.54 | 1.25 | 1.88 | 2.37 | 1.88 | 1.84 |
| SMT | 0.41 | 1.13 | 1.16 | 2.33 | 1.41 | 1.91 |
| SMX | 1.15 | 1.48 | 1.43 | 1.78 | 1.27 | 2.09 |
| SDMX | 0.49 | 0.88 | 1.98 | 2.02 | 1.51 | 1.57 |
| SSX | 1.40 | 1.91 | 1.91 | 2.99 | 1.55 | 1.87 |

[a , b] 100 µg/L, n = 5.

Recovery assays of samples (synthetic urine and milk) fortified with 10, 100, and 300 µg/L of antibiotic standards were studied to demonstrate the validity of the proposed approach. The relative recoveries ranged from 82.3 to 116.4%, as shown in Tables 3.7 and 3.8, with relative standard deviations (< 3.7-3.9%).

Table 3.7 RRs and RSDs of PENs and SAs in milk samples

| Analytes | Milk samples | | | | | | | | |
|---|---|---|---|---|---|---|---|---|---|
| | Pasteurized in glass bottle | | | Pasteurized in tetra pack | | | Raw milk | | |
| | RR, RSD (%) | RR, RSD (%) | RR, RSD (%) | RR, RSD (%) | RR, RSD (%) | RR, RSD (%) | RR, RSD (%) | RR, RSD (%) | RR, RSD (%) |
| | 10 µg/L | 100 µg/L | 300 µg/L | 10 µg/L | 100 µg/L | 300 µg/L | 10 µg/L | 100 µg/L | 300 µg/L |
| AMX | 101.7, 1.9 | 105.4, 2.9 | 100.3, 3.5 | 104.3, 2.6 | 106.5, 2.9 | 101.8, 3.8 | 101.3, 3.9 | 102.1, 2.7 | 94.5, 2.4 |
| PENG | 107.3, 2.7 | 106.4, 2.4 | 102.8, 1.2 | 102.8, 1.2 | 107.0, 2.1 | 101.2, 2.7 | 101.3, 2.4 | 105.6, 1.9 | 96.9, 4.2 |
| AMP | 114.5, 0.5 | 115.0, 2.1 | 102.9, 3.7 | 102.9, 3.7 | 116.4, 2.7 | 100.1, 2.4 | 99.8, 2.8 | 114.5, 2.3 | 96.2, 1.4 |
| CLO | 84.3, 2.8 | 104.3, 2.2 | 100.8, 2.8 | 85.1, 4.7 | 103.1, 2.9 | 100.8, 2.7 | 82.3, 2.4 | 101.9, 3.3 | 98.8, 2.1 |
| DICLO | 98.7, 3.2 | 92.4, 2.2 | 102.6, 1.2 | 99.4, 0.6 | 92.4, 2.4 | 101.6, 1.1 | 97.1, 1.7 | 90.8, 2.9 | 98.3, 2.9 |
| NAF | 107.8, 2.6 | 105.9, 2.2 | 101.5, 1.6 | 101.5, 1.6 | 106.6, 0.3 | 102.1, 2.5 | 94.6, 2.9 | 104.8, 2.4 | 98.7, 0.6 |
| SMT | 105.5, 1.9 | 101.5, 2.1 | 103.2, 1.8 | 104.2, 1.3 | 103.6, 0.6 | 104.4, 2.7 | 103.0, 2.1 | 102.3, 1.7 | 101.6, 2.3 |
| SMX | 108.3, 1.5 | 102.6, 0.4 | 102.5, 1.7 | 107.8, 1.2 | 102.3, 1.1 | 103.6, 1.6 | 105.1, 0.8 | 101.1, 0.8 | 97.9, 1.7 |
| SDMX | 91.3, 3.2 | 104.1, 2.1 | 102.8, 2.1 | 89.8, 3.3 | 103.3, 1.9 | 102.1, 1.5 | 88.7, 1.0 | 102.8, 2.01 | 99.9, 1.8 |
| SCP | 90.4, 2.5 | 102.7, 2.5 | 100.5, 1.6 | 90.4, 0.9 | 100.1, 1.1 | 99.8, 2.2 | 88.9, 1.3 | 98.7, 3.1 | 98.7, 2.9 |
| SDA | 94.6, 0.9 | 103.8, 1.8 | 104.6, 2.6 | 93.2, 3.0 | 103.4, 0.6 | 103.3, 0.8 | 91.2, 2.3 | 101.7, 1.2 | 100.7, 2.1 |
| SSX | 92.9, 2.1 | 103.4, 2.5 | 104.0, 2.7 | 92.4, 0.9 | 103.3, 1.8 | 106.7, 2.2 | 88.3, 0.4 | 101.6, 2.2 | 100.9, 3.2 |

RR: Relative recovery, n = 5

Table 3.8 RRs and RSDs of PENs and SAs in synthetic urine

| Analytes | RR, RSD (%) | RR, RSD (%) | RR, RSD (%) |
|---|---|---|---|
| | 10 µg/L | 100 µg/L | 300 µg/L |
| SDA | 96.2, 1.7 | 100.4, 1.7 | 101.2, 0.8 |
| SMT | 98.7, 1.9 | 100.5, 1.4 | 98.6, 2.6 |
| SCP | 93.2, 2.6 | 100.5, 1.9 | 99.8, 1.6 |
| SMX | 90.7, 1.8 | 100.1, 1.3 | 99.3, 1.7 |
| SSX | 93.0, 3.2 | 100.6, 1.6 | 100.8, 2.2 |
| SDMX | 99.1, 0.8 | 102.1, 1.5 | 99.6, 2.3 |
| AMX | 108.2, 2.1 | 107.1, 2.2 | 98.1, 1.2 |
| AMP | 107.1, 1.3 | 113.3, 1.8 | 95.3, 2.6 |
| PENG | 114.2, 2.6 | 106.8, 2.0 | 98.3, 1.2 |
| CLO | 104.7, 2.7 | 104.3, 1.7 | 100.1, 1.8 |
| NAF | 99.2, 1.3 | 107.8, 1.7 | 99.5, 3.4 |
| DICLO | 102.2, 0.2 | 92.3, 1.6 | 101.8, 1.7 |

n = 5

Figures 3.21 and 3.22 show the typical chromatograms for the proposed method's analysis of the unfortified and fortified pasteurized milk in a glass bottle with SAs and PENs (10 and 100 µg/L).

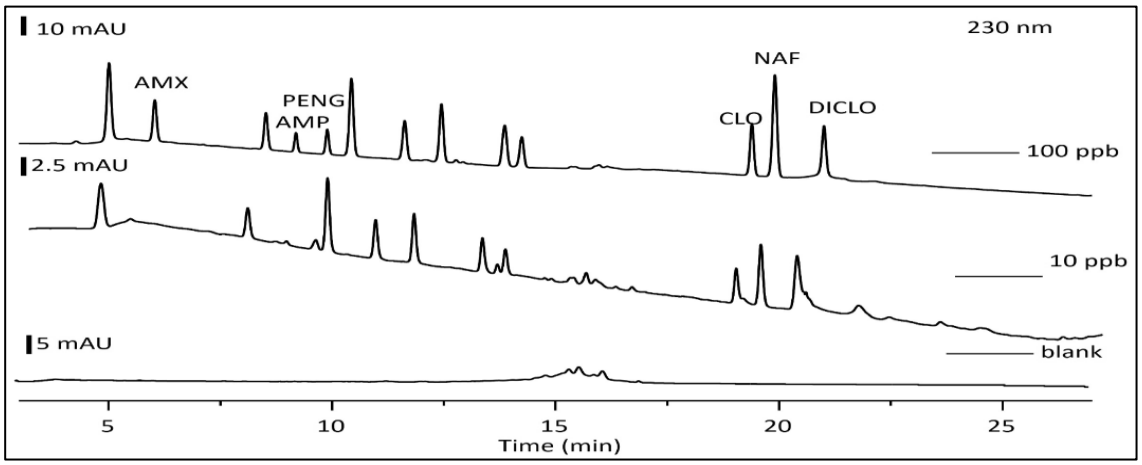



Figure 3.21 Chromatograms of unfortified and fortified pasteurized milk in a glass bottle for PENs and SAs at 230 nm

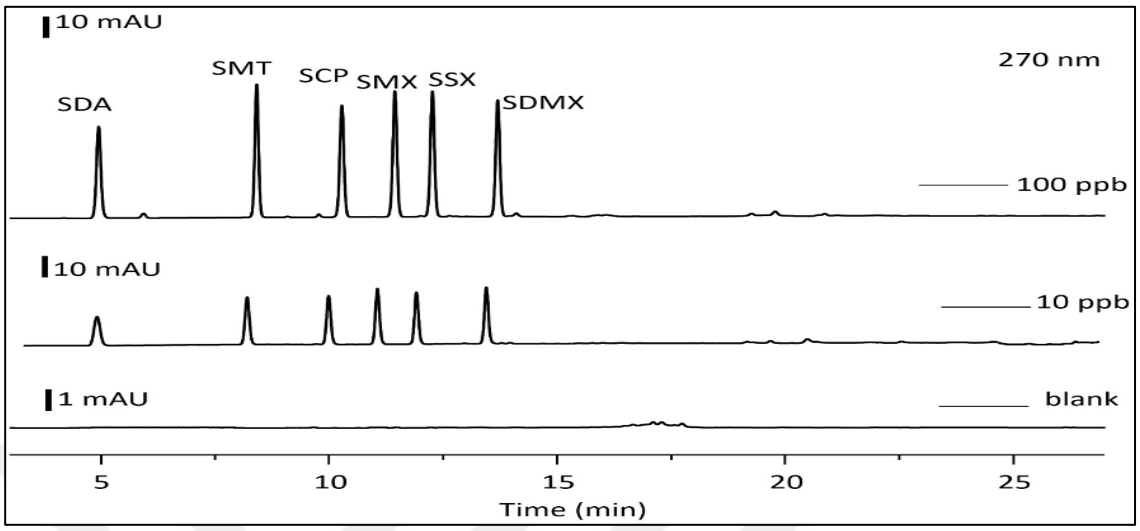



Figure 3.22 Chromatograms of unfortified and fortified pasteurized milk in a glass bottle for PENs and SAs at 270 nm

### *3.1.6 Application to Milk Samples*

The developed method was applied for the determination of SAs and PENs in milk samples. Considering the European Commission, the MRL values for DICLO, CLO, and NAF are 30 µg/kg, or PENG, AMP, and AMX are 4 µg/kg, and for all SAs are 100 µg/kg (EC, 2002). Different real milk samples (one of them is raw, four of them are pasteurized and packaged in tetra pack and the other four of them are also pasteurized and packaged in glass bottles) were analyzed in five replicates. Antibiotics were detected in only two milk samples which are pasteurized in bottles. In one sample, SSX, SMT and DICLO were determined as 14.12 ± 0.15 µg/L, 8.34 ± 0.18 µg/L and 9.87 ± 0.25 µg/L, respectively. In the other sample, SSX and SDA were determined as 5.00 ± 0.12 µg/L and 17.22 ± 0.35 µgL, respectively. In other milk samples, the studied antibiotics could be lower than their LODs. The antibiotic values discovered were within the limits of EU standards.

## 3.2 DI-SPME Method

### *3.2.1 Characterization of Cu-BDC and Cu-BDC/MMT Composites*

FTIR spectra of Cu-BDC and Cu-BDC/MMT composites represented high similarities (Figure 3.23). The main IR bands of 1,4-benzene dicarboxylate are clearly seen through the spectrum. The peak around 3430 $cm^{-1}$ corresponds to O–H stretching vibrations, and the peaks at 2932 and 2879 $cm^{-1}$ correspond to C–H stretching vibrations. The peaks at 1390 and 1680 $cm^{-1}$ represented the presence of carboxylate groups. The peaks around 1577 and 736 $cm^{-1}$ correspond to the stretching vibrations of C=C and C–H in the aromatic rings, respectively. The Cu–O stretching vibrations are seen at 467 and 562 $cm^{-1}$. In addition, the peaks at 795, 522, and 420 $cm^{-1}$ show the Cu-O and aromatic C-H bands and those overlap with bending vibrations of amorphous silica, Si–O–Al, and Si–O–Si (Zeynizadeh, Rahmai, & Tizhoush, 2020). All bands of MMT are embedded in sharp bands of Cu-BDC. A significant decrease in the peak intensities of Cu-BDC with increasing MMT amount is an indicator of the formation of composites.

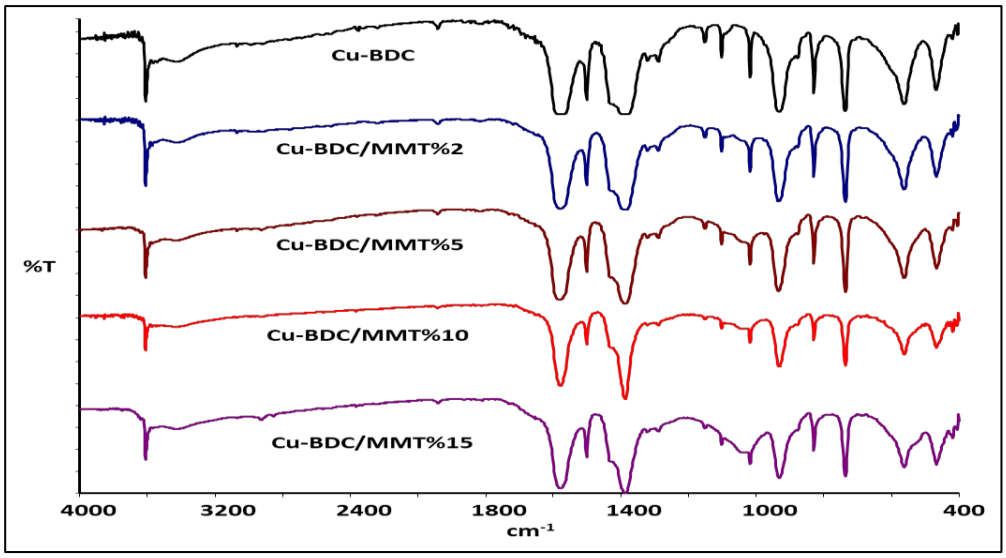



Figure 3.23 FTIR spectrum of Cu-BDC and Cu-BDC/MMT composites

TGA results are shown in Figure 3.24. It can be observed that Cu-BDC and Cu-BDC/MMT composites show similar thermal behavior in the investigated temperature range (30-900 °C). They are stable at temperatures below 280 °C. The thermal stability of Cu-BDC/MMT composites having different amounts of MMT was not changed considerably compared to Cu-BDC. It was observed that mass loss in all structures occurred in two stages. The first mass reduction from 280 to 359 °C corresponds to the loss of DMF and adsorbed water, as given in the literature. The next reduction between 359-500°C in mass corresponds to the organic group's decomposition and the complete decomposition temperature for Cu-BDC and Cu-BDC/MMT is around 426 and 433 °C (Tran, Nguyen, & Doan, 2021).

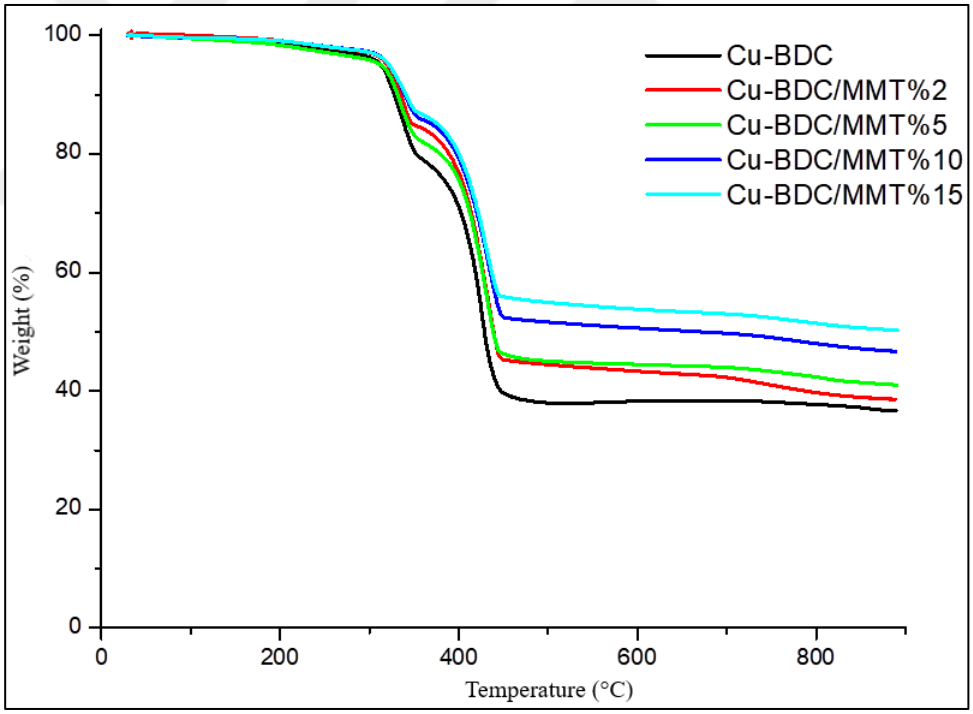



Figure 3.24 Thermal curves of Cu-BDC/MMT composites and Cu-BDC compound

XRD powder diffractions of the synthesized Cu-BDC were obtained in accordance with the literature data. The three diffraction peaks of Cu-BDC at 8.8°, 17.8° and 27.7° at 2θ correspond to reflection planes (110), (201) and (221), respectively (Li, Zhou et al., 2018; Wang et al., 2020). The powder diffractions of Cu-BDC and Cu-BDC/MMT

composites were similar (Figure 3.25), indicating that the Cu-BDC crystal structure did not change with the addition of MMT. The change in the Cu-BDC/MMT composites' peaks intensity with the addition of MMT references the interactivity of Cu-BDC with MMT, while the presence of sharp peaks is a proof that the crystal structure is still preserved (Do, Ho, Doan, Le, & Hoai Thuong, 2019).

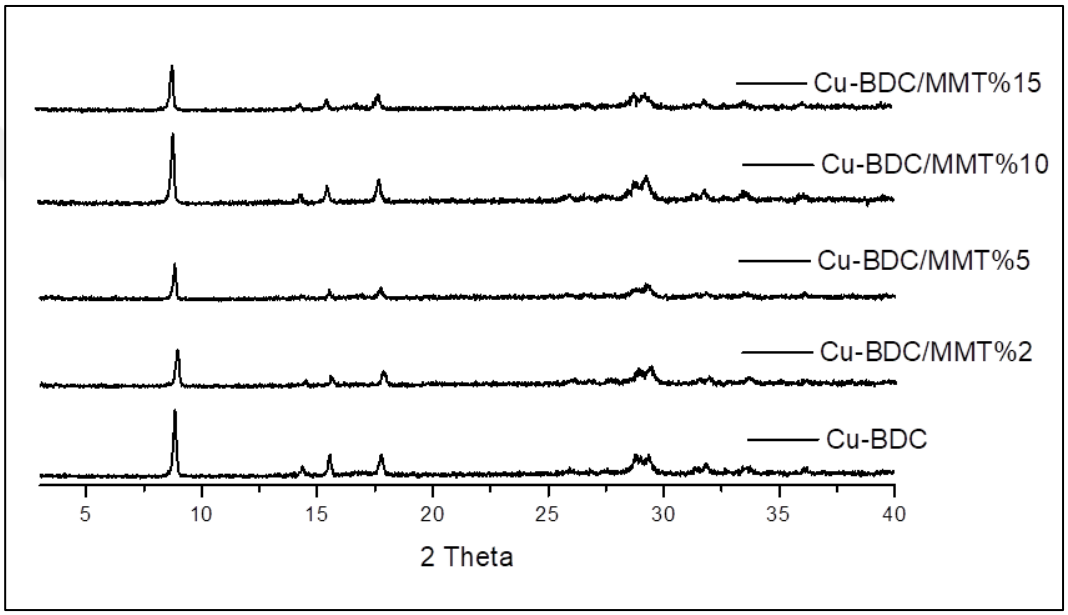



Figure 3.25 XRD powder patterns of Cu-BDC/MMT composites and Cu-BDC compound

The surface morphologies of Cu-BDC and Cu-BDC/MMT composites are clearly seen in SEM images in Figure 3.26 SEM images are compatible with the literature, and it is seen that the particles formed are in the form of nano-leaflets and that these nano-leaflets form spherical structures around the clay layers with the addition of clay. It is clearly seen in the SEM images that the structure formed parallel to the clay amount has a more homogeneous and more regular distribution.

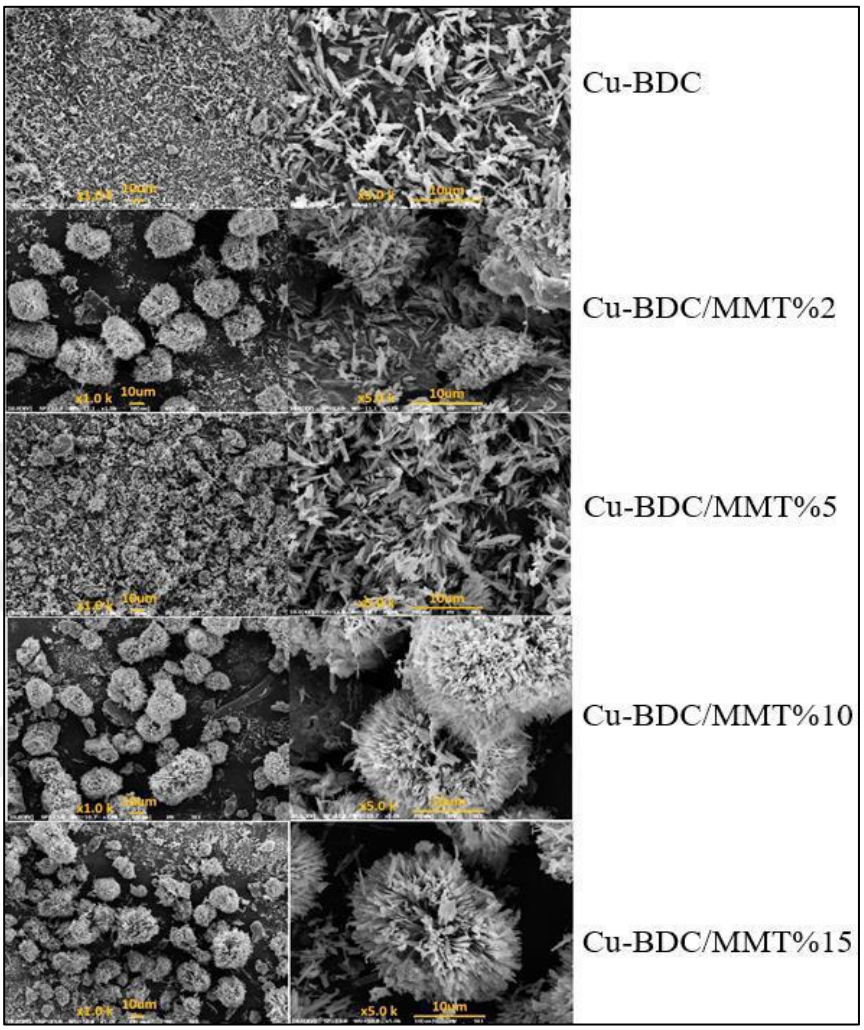



Figure 3.26 SEM images of Cu-BDC and Cu-BDC/MMT%Y composites

### *3.2.2 Optimization of the DI-SPME Method for NSAIDs*

Experimental conditions such as pH, extraction time, extraction temperature and ionic strength in DI-SPME method were optimized by mixing 500 µg/L aqueous test solutions of each NSAID drug at 600 rpm to get the highest extraction efficiency. All analytes were determined by GC/MS method. All experiments were done in three parallels. In the determination of the analytes after the DI-SPME method, the fiber was dried in nitrogen atmosphere for 5 min, derivatized with MSTFA reagent and desorbed in GC/MS at 280 ºC for 5 min.

The adsorption of analytes on the surface of SPME fiber is affected by the pH of the sample solution. The analytes interact with fiber coating with respect to the similarities of their polarities. The pH of the sample solution is adjusted to obtain reproducible extraction efficiency. Considering the pKa values of NSAIDs, the effect of pH was examined between 3 and 8. The extraction efficiencies of the four NSAIDs studied were highest at pH 4 (Figure 3.27A). There is an interaction with the carboxylic acid groups in the composite structure as an H-bond (Liu, Fan et al., 2020). The pKa values of all drugs are in the range of approximately pH 5 or pH 4.5. Therefore, the highest interaction was obtained at pH 4. In addition, electrostatic interaction on the composite surface can also have a positive effect on adhesion. Subsequent studies were carried out at pH 4.

In the headspace and direct immersion mode of the SPME method, the salt degree of the solution has importance for the solubilities of analytes. The solubility of the analytes has been increased by increasing the salt content of the solution, this causes higher extraction efficiency. Therefore, the salt effect was investigated with different concentrations of NaCl solutions (% NaCl (w/v) 0 to 25). As seen in Figure 3.27B, the highest extraction efficiency was obtained with 15% NaCl solution. The extraction efficiency was decreased at higher salt concentrations. The reason could be a high viscosity of the solution, harder mass transfer and so reduction in the extraction affinity. In subsequent experiments, 15% NaCl solution was used.

Another important factor in extraction efficiency is the extraction temperature. The working temperature affects the mass transfer and also has an effect on the extraction time. Therefore, the extraction temperature was studied from 25 °C to 80 °C. As seen in Figure 3.27C, approximately stable extraction efficiency was obtained at 60 °C and above. Subsequent studies were carried out at 60 °C.

The extraction time affects the adhesion of the analytes on the fiber surface. The extraction time was examined from 15 min to 60 min at four different time (Figure

3.27D). There was no major change in extraction efficiency over 40 min. For later studies, the optimum extraction time was applied as 40 min.

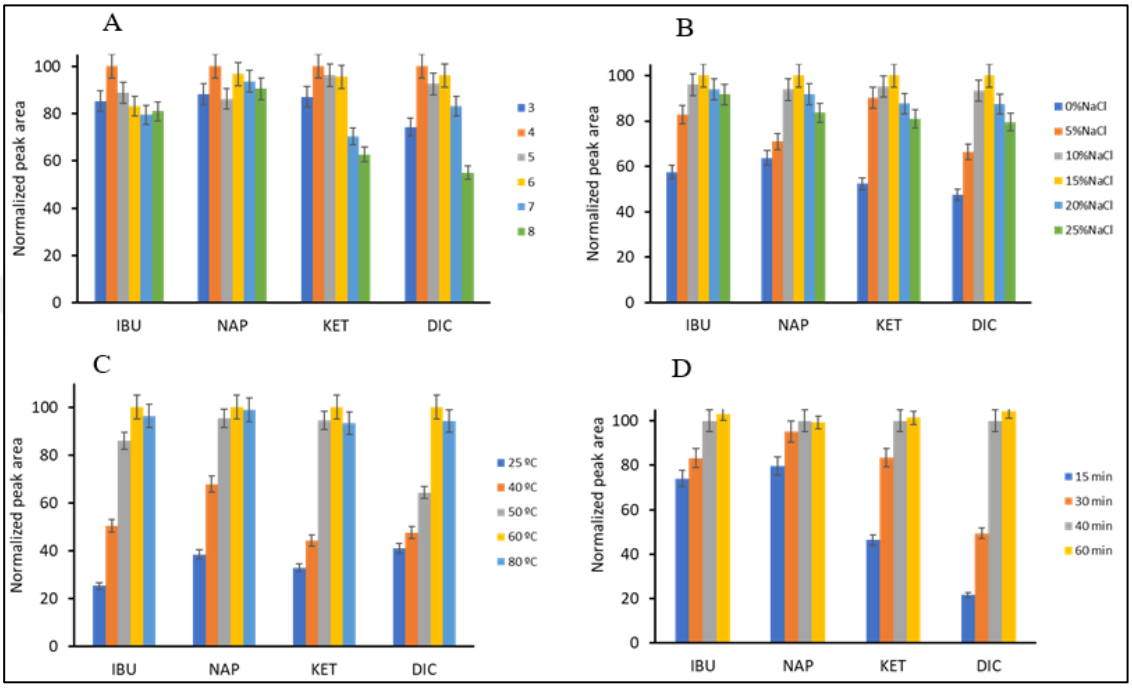



Figure 3.27 Optimizaiton of DI-SPME method using prepared Cu-BDC/MMT fiber, (A) pH, (B) salt effect, (C) extraction temperature and (D) extraction time

### *3.2.3 Optimization of Desorption Conditions for Determination of NSAIDs by Chromatographic Methods*

#### *3.2.3.1 GC/MS*

NSAIDs need to be derivatized and rendered more volatile before their determination by GC/MS. Thus, since the studied NSAID analytes are polar, they were derivatized by trimethyl silane compounds with MSTFA after SPME method in order to increase sensitivity (Rodriguez et al., 2004). Since trimethyl silane compounds are hydrolyzed in aqueous media, the fiber must be dried after SPME method. For the optimization of derivatization conditions, extraction was carried out by mixing the aqueous solution for

40 min at 60 ºC under the conditions of the DI-SPME method. All studies were done in 3 parallels. In derivatization, the drying time of the fiber after SPME (5, 10, 15 min), the amount of derivatizing reagent (40, 50, 60, 75 µL), derivatization temperature (40, 50, 60, 70 ºC) and derivatization time (20, 30, 40 min) were analyzed and optimized (Figure 3.28). Optimum conditions were determined as a result of optimization studies; the drying time was 5 min, the reagent volume was 60 µL, the derivatization time was 30 min, and the derivatization temperature was 60 ºC.

In addition, desorption temperature and desorption time were also optimized in GC/MS analysis. For this purpose, four different desorption temperatures (250, 260, 280 and 300 ºC) followed by 3 different desorption times as 3, 4 and 5 minutes were examined. The highest desorption was obtained at 280 ºC in 5 min desorption time.

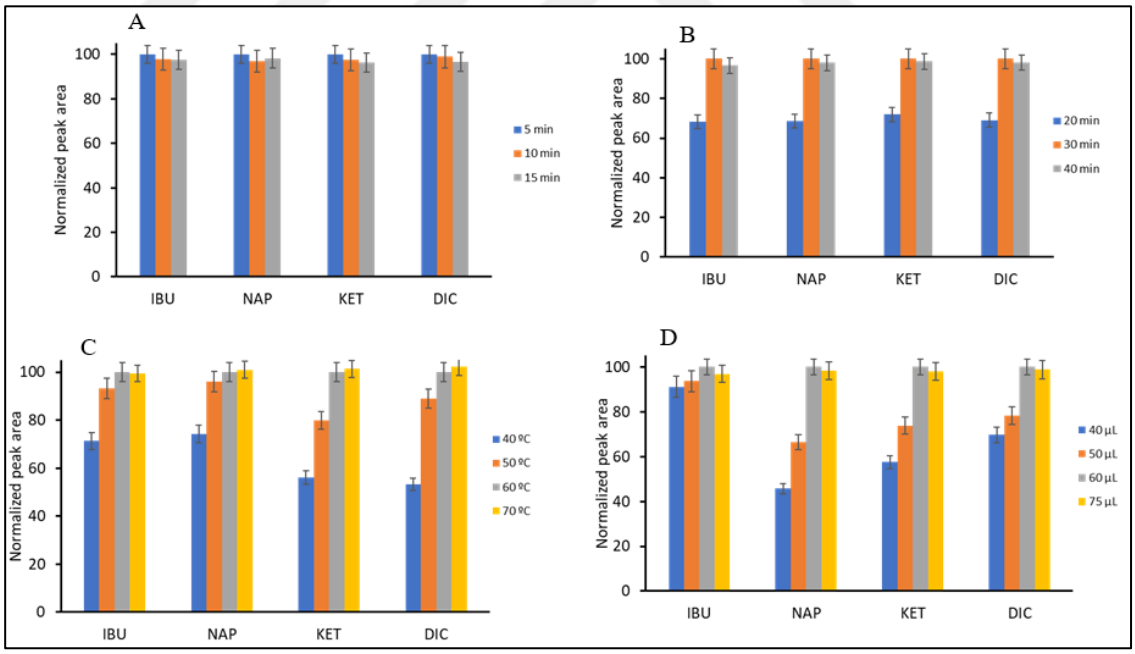



Figure 3.28 Optimization of derivative conditions after DI-SPME method using prepared Cu-BDC/MMT fiber, (A) drying time, (B) derivative time, (C) derivative temperature and (D) reagent volume

*3.2.3.2 HPLC/DAD*

For the determination of NSAIDs by HPLC/DAD method, analytes must be taken into the solution phase. For this purpose, the type of elution solvent, the volume of elution and the time of elution were investigated for desorption of NSAIDs adsorbed onto the fiber surface. For desorption, only desorption studies were carried out with mixtures of MeOH, ACN, MeOH:ACN (50:50), 0.1% TFA in MeOH:ACN (50:50 and 40:60). The highest desorption was obtained with (0.1% TFA in MeOH:ACN (40:60)) (Figure 3.29A). The volume of elution solvent from 0.6 to 1.4 mL and elution time from 5 to 30 min were optimized using vortex. Desorption conditions of NSAID compounds were optimized as 1.2 mL of (0.1% TFA in MeOH:ACN (40:60)) solution over 20 min as seen in Figures 3.29B and 3.29C. Then this eluate was dired under nitrogen atmosphere and diluted with 200 µL of (deionized water: ACN (1:1)) and injected into the HPLC as 20 µL.

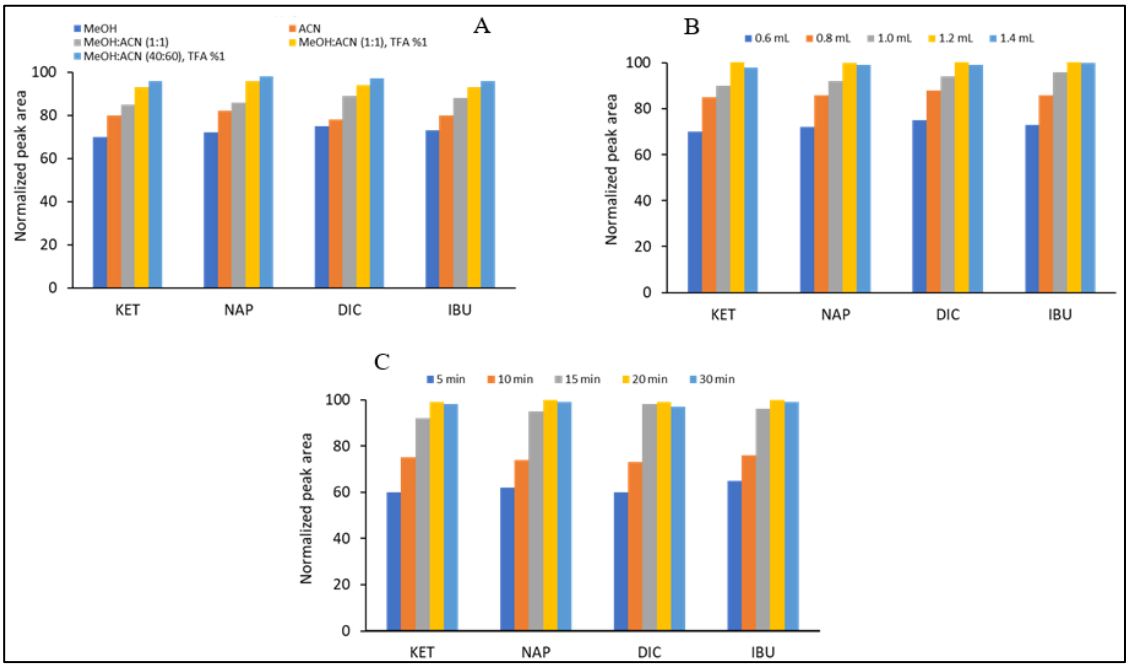



Figure 3.29 Type of elution solvent (A), elution solvent volume (B), and elution solvent time (C) for analysis of HPLC/DAD method after DI-SPME using prepared Cu-BDC/MMT fiber

### *3.2.4 Comparison of Fibers*

In the DI-SPME method, the extraction efficiency of Cu-BDC/MMT composite coated fibers was compared with Cu-BDC coated SPME fiber and MMT coated SPME fiber. In comparison, the determination of NSAIDs was made by HPLC/DAD method. DI-SPME and HPLC/DAD under optimized conditions were applied in the comparison experiment. It was determined that the extraction efficiency of Cu-BDC/MMT composites was higher than Cu-BDC and MMT (Figure 3.30). Among the composites, Cu-BDC/MMT%5 and Cu-BDC/MMT%10 composites containing 5% and 10% MMT showed higher extraction efficiency than the others. Only in MMT coated fiber, only NSAIDs can be attached by electrostatic interaction. There is a possibility of H-bonding of NSAIDs with Cu-BDC coated fiber. On the other hand, it can be stated that there is a higher adsorpiton to the composites with the possibility of both types of interaction and synergistic effect. Subsequent studies were continued with Cu-BDC/MMT%5 as they showed similar extraction efficiency.

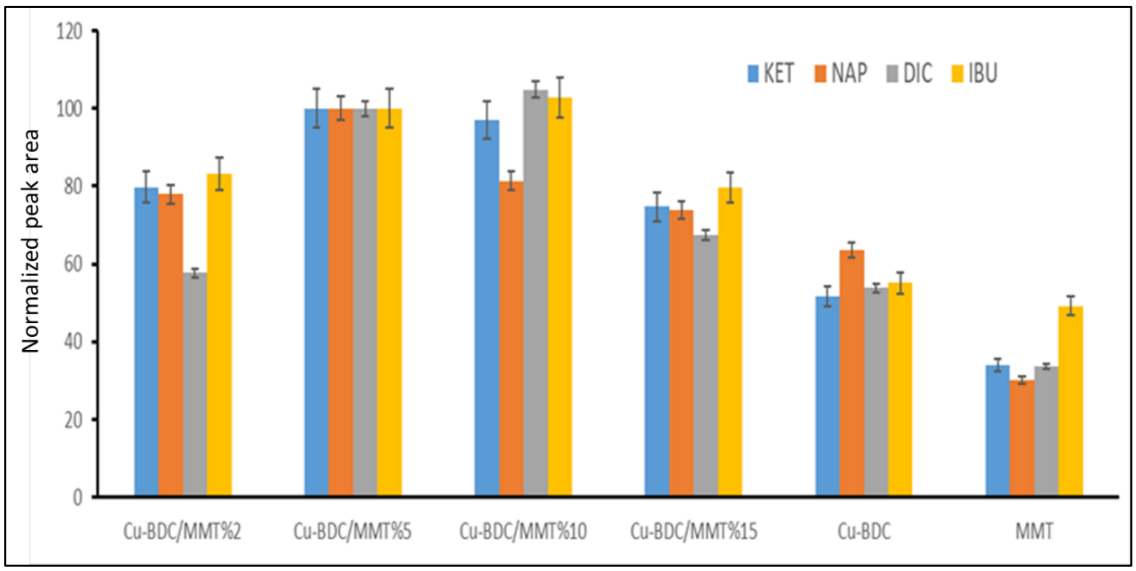



Figure 3.30 Comparison of extraction efficiencies of Cu-BDC/MMT composites, Cu-BDC and MMT by DI-SPME method

### *3.2.5 Method Validation*

Cu-BDC/MMT%5 fiber was used for analytical performance of 4 NSAID compounds by DI-SPME-GC/MS and DI-SPME-HPLC/DAD methods. As analytical performance, linear range, coefficient of determination, limit of detection, precision with a single fiber and from fiber to fiber were examined. For linear range determination, studies were carried out in 3 parallels using aqueous synthetic test solution at 6 calibration points. The results of the validation parameters are given in Tables 3.9 and 3.10. The linear range of all NSAID compounds studied is in the range of 0.25-200 µg/L in HPLC/DAD determination and 0.05-200 µg/L in GC/MS determination, with coefficients of determination over 0.9969 and 0.9982 as $R^2$, respectively. The detection limit values of the four NSAIDs were found in the range of 0.052-0.075 µg/L in the HPLC/DAD method and 0.016-0.018 µg/L in the GC/MS method.

For NSAIDs at concentrations of 1, 5 and 50 µg/L with a single fiber, the repeatability was less than 6.58, 5.48 and 4.47 RSD%, respectively, and the fiber to fiber reproducibility was less than 10.64, 6.61 and 5.93 RSD%, respectively in the HPLC/DAD method. In the GC/MS method, the reproducibility was less than 5.35, 4.54 and 3.25 RSD% for NSAIDs at a concentration of 1, 5 and 50 µg/L with a single fiber, and the reproducibility from fiber to fiber was Less than 8.16, 5.94 and 3.88 RSD%, respectively.

Table 3.9 Analytical performance of Cu-BDC/MMT for NSAIDs by DI-SPME-HPLC/DAD

| **NSAIDs** | **LR (µg/L)** | **$R^2$** | **LOD** | **RSD%, Single fiber** | | | **RSD%, Fiber to fiber** | | |
|---|---|---|---|---|---|---|---|---|---|
| | | | | **1 µg/L** | **5 µg/L** | **50 µg/L** | **1 µg/L** | **5 µg/L** | **50 µg/L** |
| KET | 0.25-200 | 0.9969 | 0.064 | 6.14 | 5.48 | 4.47 | 8.32 | 6.34 | 4.16 |
| NAP | 0.25-200 | 0.9979 | 0.052 | 5.76 | 4.98 | 4.16 | 10.64 | 6.38 | 5.93 |
| DIC | 0.25-200 | 0.9977 | 0.075 | 5.94 | 4.69 | 3.26 | 8.58 | 6.61 | 4.49 |
| IBU | 0.25-200 | 0.9978 | 0.062 | 6.58 | 4.36 | 2.88 | 8.75 | 3.78 | 3.58 |

Table 3.10 Analytical performance of Cu-BDC/MMT for NSAIDs by DI-SPME-GC/MS

| NSAIDs | LR (µg/L) | $R^2$ | LOD | RSD%, Single fiber | | | RSD%, Fiber to fiber | | |
|---|---|---|---|---|---|---|---|---|---|
| | | | | 1 µg/L | 5 µg/L | 50 µg/L | 1 µg/L | 5 µg/L | 50 µg/L |
| KET | 0.05-200 | 0.9987 | 0.016 | 5.25 | 4.54 | 3.24 | 8.16 | 5.94 | 3.24 |
| NAP | 0.05-200 | 0.9983 | 0.018 | 4.46 | 4.18 | 3.25 | 7.50 | 5.38 | 3.88 |
| DIC | 0.05-200 | 0.9988 | 0.017 | 4.34 | 3.59 | 2.06 | 8.58 | 5.92 | 3.32 |
| IBU | 0.05-200 | 0.9982 | 0.016 | 5.35 | 3.86 | 2.28 | 6.87 | 3.45 | 3.42 |

### *3.2.6 Application to Real Samples*

KET, NAP, DIC and IBU compounds were analyzed in tap water, wastewater and drug samples with the developed DI-SPME-HPLC/DAD and DI-SPME/GC/MS methods. Two drug samples were studied, the developed method was applied to each drug sample that was diluted up to 10 µg/L. No NSAIDs were observed in the tap water sample. DIC and IBU drugs were observed in the wastewater sample. In addition, for the accuracy of the method, 5 and 50 µg/L concentrations of synthetic urine solutions, tap water and wastewater samples and 20 and 100 µg/L concentrations of drug samples were added to NSAIDs and their recovery was investigated. The results obtained are given in Tables 3.11 and 3.12. Recoveries in DI-SPME-HPLC/DAD method are in the range of 91.84-98.26% for wastewater, 91.77-96.15% for tap water, 89.36-95.64% for synthetic urine, 91.26-96.26% for pedifen syrup and 92.36-97.25% for Naprosyn plus gel. In the DI-SPME-GC/MS method, the recoveries are in the range of 96.12-99.35% for wastewater, 97.22-99.47% for tap water, 96.68-102.52% for synthetic urine, 98.22-99.24% for Pedifen syrup and 98.24-99.66% for Naprosyn plus gel. Figures from 3.31 to 3.34 show HPLC and GC chromatograms of tap water, wastewater and drug samples with blank and spiked four NSAIDs standards.

Table 3.11 RRs and RSDs % of NSAIDs in synthetic urine solution and water and drug samples by DI-SPME-HPLC/DAD method

| **Samples** | **Added µg/L** | **Found** | **KET** | **NAP** | **DIC** | **IBU** |
|---|---|---|---|---|---|---|
| Wastewater | 0 | µg/L | - | - | < 0,25 | < 0,25 |
| | 5 | RR, RSD (%) | 92.58, 6.53 | 91.84, 5.86 | 92.47, 5.89 | 98.26, 4.96 |
| | 50 | RR, RSD (%) | 96.35, 4.26 | 97.58, 3.47 | 95.55, 4.36 | 96.64, 3.42 |
| Tap water | 0 | µg/L | - | - | - | - |
| | 5 | RR, RSD (%) | 95.52, 4.85 | 94.36, 4.58 | 92.77, 4.74 | 96.15, 4.36 |
| | 50 | RR, RSD (%) | 93.48, 3.48 | 92.88, 3.56 | 91.77, 3.64 | 95.88, 3.24 |
| Synthetic urine | 5 | RR, RSD (%) | 89.36, 5.74 | 92.47, 5.36 | 95.64, 5.47 | 94.47, 4.69 |
| | 50 | RR, RSD (%) | 90.26, 4.39 | 95.63, 3.88 | 94.42, 3.57 | 95.32, 3.48 |
| Pedifen syrup (IBU) | 10* | µg/L | - | - | - | 9.74 |
| | 20 | RR, RSD (%) | 92.69, 5.15 | 93.56, 4.28 | 95.63, 4.88 | 96.26, 3.88 |
| | 100 | RR, RSD (%) | 94.63, 4.89 | 94.68, 5.54 | 91.26, 5.22 | 97.26, 3.44 |
| Naprosyn plus gel (NAP) | 10* | µg/L | - | 9.68 | - | - |
| | 20 | RR, RSD (%) | 96.25, 5.87 | 95.36, 4.84 | 93.26, 4.26 | 97.25, 4.48 |
| | 100 | RR, RSD (%) | 92.36, 4.67 | 94.85, 4.20 | 95.64, 3.52 | 92.47, 4.14 |

* Diluted drug sample

Table 3.12 RRs and RSDs % of NSAIDs in synthetic urine solution and water and drug samples by DI-SPME-GC/MS method

| **Samples** | **Added µg/L** | **Found** | **KET** | **NAP** | **DIC** | **IBU** |
|---|---|---|---|---|---|---|
| Wastewater | 0 | µg/L | - | - | < 0,05 | < 0,05 |
| | 5 | RR, RSD (%) | 96.12, 5.25 | 98.65, 5.21 | 96.35, 4.59 | 98.54, 4.24 |
| | 50 | RR, RSD (%) | 97.44, 4.00 | 97.28, 3.78 | 99.35, 3.52 | 99.26, 3.05 |
| Tap water | 0 | µg/L | - | - | - | - |
| | 5 | RR, RSD (%) | 97.32, 4.26 | 97.25, 4.12 | 99.26, 4.21 | 97.35, 4.02 |
| | 50 | RR, RSD (%) | 98.24, 3.24 | 99.28, 3.24 | 99.27, 3.44 | 99.47, 3.68 |
| Synthetic urine | 5 | RR, RSD (%) | 96.68, 4.24 | 98.65, 4.24 | 100.56, 4.27 | 98.26, 4.20 |
| | 50 | RR, RSD (%) | 98.88, 4.52 | 99.56, 3.44 | 102.52, 3.24 | 98.52, 3.28 |
| Pedifen syrup (IBU) | 10* | µg/L | - | - | - | 9.96 |
| | 20 | RR, RSD (%) | 98.58, 3.24 | 96.88, 3.58 | 97.23, 3.28 | 98.55, 3.34 |
| | 100 | RR, RSD (%) | 99.24, 4.12 | 98.28, 4.25 | 98.66, 4.36 | 98.22, 3.96 |
| Naprosyn plus gel (NAP) | 10* | µg/L | - | 9.98 | - | - |
| | 20 | RR, RSD (%) | 99.36, 3.54 | 98.57, 4.17 | 97.57, 3.94 | 99.34, 3.56 |
| | 100 | RR, RSD (%) | 99.66, 3.27 | 98.25, 3.80 | 98.24, 3.02 | 98.26, 3.25 |

* Diluted drug sample

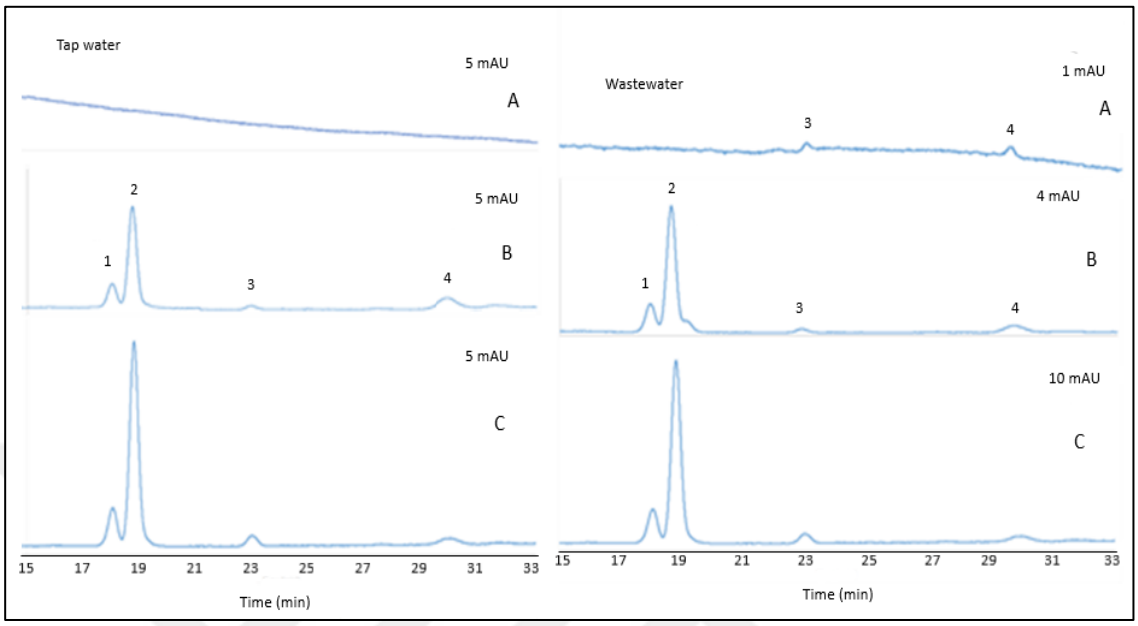



Figure 3.31 HPLC chromatograms of blank (A) and 5 µg/L (B) and 50 µg/L (C) NSAIDs added tap water and wastewater samples (1: KET, 2: NAP, 3: DIC, 4: IBU)

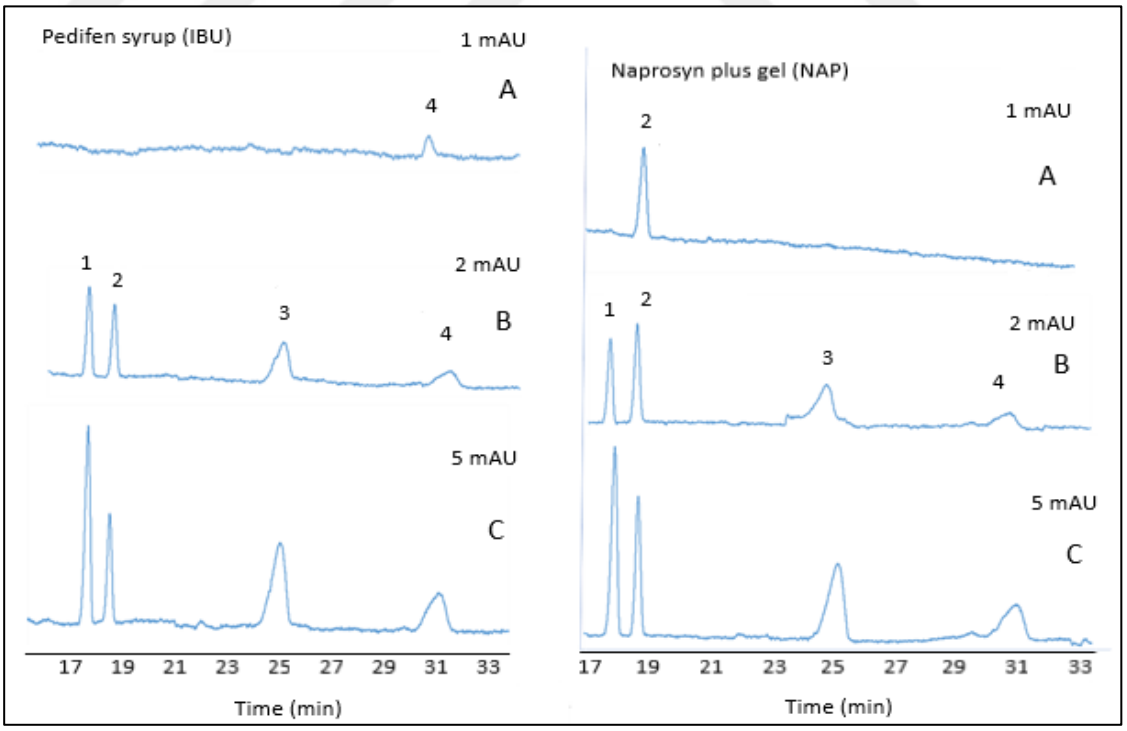



Figure 3.32 HPLC chromatograms of diluted drug sample at 10 µg/L (A) and (20 µg/L (B) and 100 µg/L (C) NSAIDs added drug samples) (1: KET, 2: NAP, 3: DIC, 4: IBU)

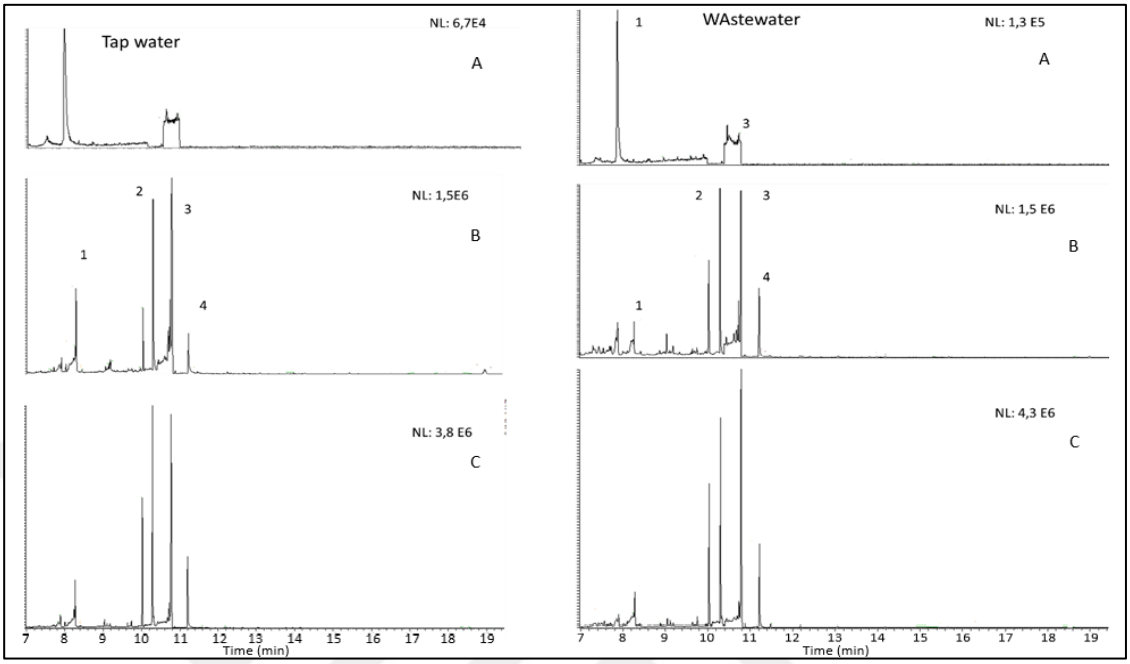



Figure 3.33 GC chromatograms of blank (A) and 5 µg/L (B) and 50 µg/L (C) NSAIDs added tap water and wastewater samples (1: IBU, 2: NAP, 3: KET, 4: DIC)

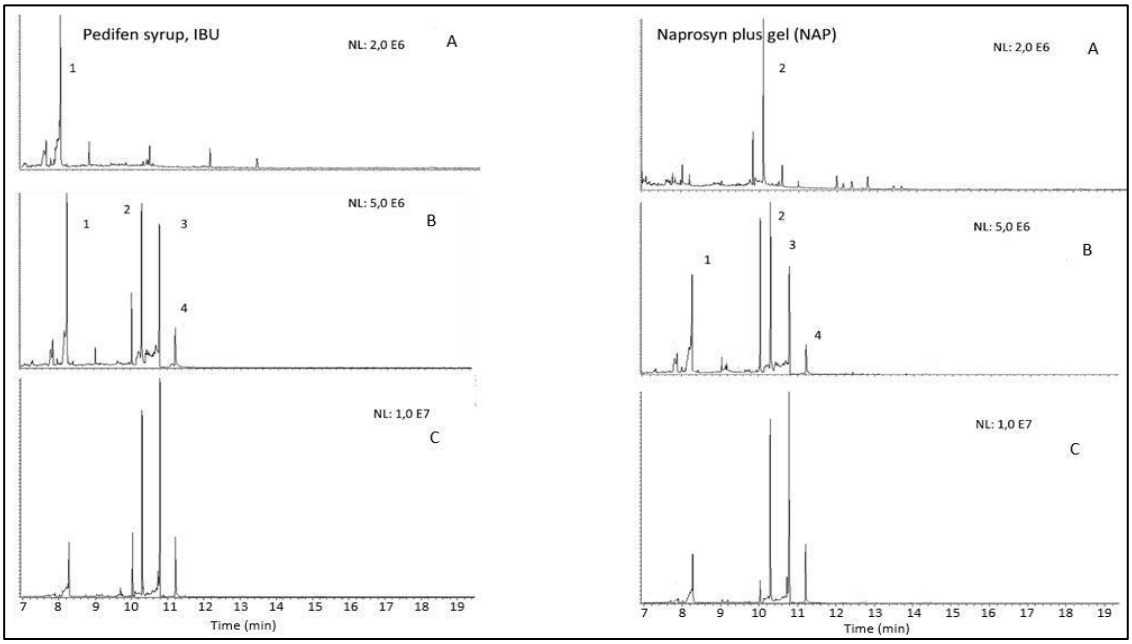



Figure 3.34 GC chromatograms of diluted drug sample at 10 µg/L (A) and (20 µg/L (B) and 100 µg/L (C) NSAIDs added drug samples) (1: IBU, 2: NAP, 3: KET, 4: DIC)

# CHAPTER FOUR
# CONCLUSIONS

In this study, different extraction methods were developed for chromatographic analysis of antibiotics and NSAIDs.

The DMSPE method has been developed for the preconcentration process before the determination of SAs and PENs group antibiotics by HPLC/DAD. MOF-based clay composites (Cu-BTC/MMT) were prepared for the DMSPE method. The FTIR, XRD, TGA, BET and SEM analysis were used for the characterizaiton of the prepared composites. The prepared Cu-BTC/MMT composites having variation in the mass percentage of MMT were evaluated with respect to extraction abilities towards the sulfonamides and penicillins. It resulted that the Cu-BTC/MMT%2 presented the highest extraction capacity. According to the results obtained, it can be concluded that the proposed DMSPE-HPLC/DAD method using a sorbent as Cu-BTC/MMT composite is simple, rapid, susceptible, and repeatable. The application of the proposed method to synthetic urine solution and real milk samples has been successful with high packaging and good reproducibility. It could be possible monitoring of the studied antibiotics in different kinds of milk samples and maybe real urine samples by the developed dispersive micro solid-phase extraction method using the comparably cheaper adsorbent prepared by considering the decisions of the European Communities 2002/657/EC.

In the second part of the study, the DI-SPME method was proposed for the enrichment of NSAIDs. The determinations of the NSAID compounds were performed by HPLC/DAD and GC/MS methods. Cu-BDC/MMT composites (containing different amounts of MMT) were prepared for coating SPME fiber. Characterizations were made by FTIR, TGA, XRD and SEM methods. Of the prepared composites, Cu-BDC/MMT%10 and Cu-BDC/MMT%5 were close to each other and presented better extraction efficiencies than the others. The application of the developed method to synthetic urine solutions and drug, wastewater and tap water samples has succeeded.

High recovery and good reproducibility were achieved in all samples. Better relative recoveries, lower LOD, better RSD% were obtained with GC method compared to HPLC method. When the results are evaluated, it can be suggested that the DI-SPME method developed using SPME fiber prepared with Cu-BDC/MMT composite can be used in the determination of NSAIDs by gas chromatography or liquid chromatography. It can be said that SPME fiber has high reusability, coating material can be prepared easily and relatively cheaply. It can be stated that the proposed SPME method can provide the analysis of NSAIDs with both chromatographic methods quickly, easily, sensitively, with high recovery and high reproducibility.

## REFERENCES


Alalawy, M. D., Socha, B. N., Chavda, B. R., Padariya, T. J., Patel, B. D., Patel, U. H. et al. (2022). Role of secondary ligand on Cd complex of sulfamethizole: synthesis, spectroscopic characterization, Hirshfeld surface analysis and DNA interaction. *Journal of Molecular Structure, 1247*, 131411.

Alampanos, V., Samanidou, V., & Papadoyannis, I. (2019). Trends in sample preparation for the hplc determination of penicillins in biofluids. *Journal of Applied Bioanalysis*, *5*(1), 9-17.

AL-Hashimi, N. N., Aleih, H. A., Fasfous, I. I., & AlKhatib, H. S. (2018). Multi-walled carbon nanotubes as efficient sorbent for the solid bar microextraction of non-steroidal anti-inflammatory drugs from human urine samples. *Current Pharmaceutical Analysis*, *14*(3), 239-246.

Al-Musawi, T. J., Rajiv, P., Mengelizadeh, N., Arghavan, F. S., & Balarak, D. (2021). Photocatalytic efficiency of $CuNiFe_2O_4$ nanoparticles loaded on multi-walled carbon nanotubes as a novel photocatalyst for ampicillin degradation. *Journal of Molecular Liquids, 337*, 116470.

Alshamsan, A., Aleanizy, F. S., Badran, M., Alqahtani, F. Y., Alfassam, H., Almalik, A. et al. (2019). Exploring anti-MRSA activity of chitosan-coated liposomal dicloxacillin. *Journal of microbiological methods, 156*, 23-28.

Altman, R., Bosch, B., Brune, K., Patrignani, P., & Young, C. (2015). Advances in NSAID development: evolution of diclofenac products using pharmaceutical technology. *Drugs*, *75*(8), 859-877.

Alvarez-García, S., & Ramírez-García, J. J. (2021). Sorption Behavior of Dicloxacillin in Zeolites Modified with a Cationic Surfactant at Different pH. *Water, Air, & Soil Pollution*, *232*(4), 1-15.

Amiri, A., & Ghaemi, F. (2017). Carbon nanospheres covalently modified with polydimethylsiloxane on a porous sol–gel support for use in headspace solid-phase fiber microextraction of BTEX. *Microchimica Acta*, *184*(1), 297-305.

Ansari, S., & Karimi, M. (2017). Recent progress, challenges and trends in trace determination of drug analysis using molecularly imprinted solidphase microextraction technology. *Talanta*, *164*, 612-625.

Aqda, T.G., Behkami, S., Raoofi, M., & Bagheri, H. (2019) Graphene oxide-starch -based micro-solid phase extraction ofantibiotic residues from milk samples. *Journal of Chromatography A, 1591*, 7-14.

Aryee, A. A., Han, R., & Qu, L. (2022). Occurrence, detection and removal of amoxicillin in wastewater: A review. *Journal of Cleaner Production*, 133140.

Ashbolt, N. J., Amézquita, A., Backhaus, T., Borriello, P., Brandt, K. K., Collignon, P. et al. (2013). Human health risk assessment (HHRA) for environmental development and transfer of antibiotic resistance. *Environmental health perspectives*, *121*(9), 993-1001.

Attari, S. G., Bahrami, A., Shahna, F. G., & Heidari, M. (2015). Single-walled carbon nanotube/silica composite as a novel coating for solid-phase microextraction fiber based on sol-gel technology. *Journal of analytical chemistry*, *70*(10), 1192-1198.

Babić, S., Horvat, A. J., Pavlović, D. M., & Kaštelan-Macan, M. (2007). Determination of pKa values of active pharmaceutical ingredients. *TrAC Trends in Analytical Chemistry, 26*(11), 1043-1061.

Bacanlı, M., & Başaran, N. (2019). Importance of antibiotic residues in animal food. *Food and Chemical Toxicology, 125*, 462-466.

Baezzat, M. R., Pourghobadi, Z., & Pourghobadi, R. (2021). Nanomolar determination of Penicillin G potassium (PGK) salt using a Carbon Paste Electrode modified with $TiO_2$ nano particles/Ionic Liquids in real samples. *Materials Chemistry and Physics, 270*, 124641.

Barfi, B., Asghari, A., Rajabi, M., Moghadam, A. G., Mirkhani, N., & Ahmadi, F. (2015). Comparison of ultrasound-enhanced air-assisted liquid–liquid microextraction and low-density solvent-based dispersive liquid–liquid microextraction methods for determination of nonsteroidal anti-inflammatory drugs in human urine samples. *Journal of Pharmaceutical and Biomedical Analysis, 111*, 297-305.

Bavandpour, R., Rajabi, M., & Karimi-Maleh, H. (2020). Ultrasensitive electroanalytical sulfisoxazole sensors amplified with Pd-doped ZnO nanoparticles and modified with 1-hexyl-3-methyl imidazolium bis (trifluoromethylsulfonyl) imide. *New Journal of Chemistry, 44*(26), 11125-11130.

Ben, Y., Fu, C., Hu, M., Liu, L., Wong, M. H., & Zheng, C. (2019). Human health risk assessment of antibiotic resistance associated with antibiotic residues in the environment: A review. *Environmental research*, *169*, 483-493.

Bérdy, J. (2012). Thoughts and facts about antibiotics: where we are now and where we are heading. *The Journal of antibiotics*, *65*(8), 385-395.

Bindu, S., Mazumder, S., & Bandyopadhyay, U. (2020). Non-steroidal anti -inflammatory drugs (NSAIDs) and organ damage: A current perspective. *Biochemical pharmacology*, *180*, 114147.

Brouwers, R., Vass, H., Dawson, A., Squires, T., Tavaddod, S., & Allen, R. J. (2020). Stability of β-lactam antibiotics in bacterial growth media. *PloS one*, *15*(7), e0236198.

Bushra, R., & Aslam, N. (2010). An overview of clinical pharmacology of ibuprofen. *Oman medical journal*, *25*(3), 155.

Bylund, D. B., & Enna, S. J. (2008). *xPharm: The Comprehensive Pharmacology Reference*. Elsevier Inc.

Chatzimitakos, T., & Stalikas, C. (2020). Zinc ferrite as a magnetic sorbent for the dispersive micro solid-phase extraction of sulfonamides and their determination by HPLC. *Microchemical Journal*, *155*, 104670.

Chen, T., Cheng, G., Ahmed, S., Wang, Y., Wang, X., Hao, H. et al. (2017). New methodologies in screening of antibiotic residues in animal-derived foods: Biosensors. *Talanta*, *175*, 435-442.

Chiesa, L. M., Nobile, M., Panseri, S., & Arioli, F. (2017). Antibiotic use in heavy pigs: comparison between urine and muscle samples from food chain animals analysed by HPLC-MS/MS. *Food chemistry*, *235*, 111-118.

Dai, X., Jia, X., Zhao, P., Wang, T., Wang, J., Huang, P. et al. (2016). A combined experimental/computational study on metal-organic framework MIL-101 (Cr) as a SPE sorbent for the determination of sulphonamides in environmental water samples coupling with UPLC-MS/MS. *Talanta*, *154*, 581-588.

Dai, Y., Li, M., Liu, F., Xue, M., Wang, Y., & Zhao, C. (2019). Graphene oxide wrapped copper-benzene-1, 3, 5-tricarboxylate metal organic framework as efficient absorbent for gaseous toluene under ambient conditions. *Environmental Science and Pollution Research*, *26*(3), 2477-2491.

Dang, X., Zhao, H., Wang, X., Sailijiang, T., Chen, S., & Quan, X. (2018). Photoelectrochemical aptasensor for sulfadimethoxine using g-$C_3N_4$ quantum dots modified with reduced graphene oxide. *Microchimica Acta*, *185*(7), 1-8.

De Paiva, L. B., Morales, A. R., & Díaz, F. R. V. (2008). Organoclays: properties, preparation and applications. *Applied clay science*, *42*(1-2), 8-24.

Di Corcia, A., & Nazzari, M. (2002). Liquid chromatographic–mass spectrometric methods for analyzing antibiotic and antibacterial agents in animal food products. *Journal of Chromatography A*, *974*(1-2), 53-89.

Díaz, A., & Peña-Alvarez, A. (2017). A simple method for the simultaneous determination of pharmaceuticals and personal care products in river sediment by ultrasound-assisted extraction followed by solid-phase microextraction coupled with gas chromatography–mass spectrometry. *Journal of chromatographic science*, *55*(9), 946-953.

Do, T. L., Ho, T. M. T., Doan, V. D., Le, V. T., & Hoai Thuong, N. (2019). Iron-doped copper 1, 4-benzenedicarboxylate as photo-Fenton catalyst for degradation of methylene blue. *Toxicological & Environmental Chemistry*, *101*(1-2), 13-25.

El-Azazy, M., Ahsan, I., & Bensalah, N. (2022). Electrochemical Analysis of Sulfisoxazole Using Glassy Carbon Electrode (GCE) and MWCNTs/Rare Earth Oxide ($CeO_2$ and $Yb_2O_3$) Modified-GCE Sensors. *Molecules*, *27*(6), 2033.

Es-haghi, A., Hosseininasab, V., & Bagheri, H. (2014). Preparation, characterization, and applications of a novel solid-phase microextraction fiber by sol-gel technology on the surface of stainless steel wire for determination of poly cyclic aromatic hydrocarbons in aquatic environmental samples. *Analytica chimica acta, 813*, 48-55.

Es'haghi, Z., & Esmaeili-Shahri, E. (2014). Sol–gel-derived magnetic $SiO_2/TiO_2$ nanocomposite reinforced hollow fiber-solid phase microextraction for enrichment of non-steroidal anti-inflammatory drugs from human hair prior to high performance liquid chromatography. *Journal of Chromatography B, 973*, 142-151.

European Commission (2002) Comission Regulation of 2002/657/EC, 12 August. Implementing council directive 96/23/EC concerning the performance of analytical methods and the interpretation of results. *Official Journal of the European Communities,* L 221/8-L221/36. 2002

Fallahzadeh, R. A., Mahvi, A. H., Meybodi, M. N., Ghaneian, M. T., Dalvand, A., Salmani, M. H. et al. (2019). Application of photo-electro oxidation process for amoxicillin removal from aqueous solution: Modeling and toxicity evaluation. *Korean Journal of Chemical Engineering, 36*(5), 713-721.

Gaudin, V. (2017). Advances in biosensor development for the screening of antibiotic residues in food products of animal origin–A comprehensive review. *Biosensors and Bioelectronics, 90*, 363-377.

Gawrońska, M., Kowalik, M., & Makowski, M. (2022). Recent advances in medicinal chemistry of ampicillin: Derivatives, metal complexes, and sensing approaches. *TrAC Trends in Analytical Chemistry*, 116691.

Gelband, H., Miller, M., Petrie, Pant, S., Gandra, S., Levinson, J. et al. (2015). The state of the world's antibiotics 2015. *Wound healing southern africa*, *8*(2), 30-34.

Ghambarian, M., Tajabadi, F., Yamini, Y., Behbahani, M., Sobhi, H. R., & Esrafili, A. (2020). An efficient sample preparation method based on dispersive liquid–liquid microextraction associated with back extraction for trace determination of acidic pharmaceuticals. *Arabian Journal of Chemistry*, *13*(1), 1924-1932.

Ghlichloo, I., & Gerriets, V. (2019). *Nonsteroidal anti-inflammatory drugs (NSAIDs)*.

Gu, S., Kang, X., Wang, L., Lichtfouse, E., & Wang, C. (2019). Clay mineral adsorbents for heavy metal removal from wastewater: a review. *Environmental Chemistry Letters*, *17*(2), 629-654.

Guardia, L., Badía, R., Granda-Valdés, M., & Díaz-García, M. E. (2012). Screening of a molecularly imprinted sol–gel library for nafcillin recognition. *Journal of sol-gel science and technology*, *63*(3), 537-545.

Gutiérrez-Serpa, A., Pacheco-Fernández, I., Pasán, J., & Pino, V. (2019). Metal–organic frameworks as key materials for solid-phase microextraction devices—a review. *Separations*, *6*(4), 47.

Habila, I., Saoudi, M., Berrah, F., Benmerad, B., Boudraa, M., Merazig, H. et al. (2021). A new complex of Zinc (II) with sulfamethoxazole ligand: Synthesis, crystal structure, Hirshfeld surface analysis, thermal properties, DFT calculations and antibacterial/antifungal activities. *Journal of Molecular Structure, 1244*, 130903.

Habimana, F., Shi, D., & Ji, S. (2018). Synthesis of Cu-BTC/Mt composites porous materials and their performance in adsorptive desulfurization process. *Applied Clay Science*, *152*, 303-310.

Hagarová, I., & Nemček, L. (2021). Application of Metallic Nanoparticles and Their Hybrids as Innovative Sorbents for Separation and Pre-concentration of Trace Elements by Dispersive Micro-Solid Phase Extraction: A Minireview. *Frontiers in Chemistry*, *9*, 672755.

Hao, S., & Liu, Y. (2022). Constructing and synthesizing optimal Cu-BTC and its application in low-temperature denitration. *Journal of Materials Science*, *57*(3), 1689-1702.

He, Y., Jain, P., & Yalkowsky, S. H. (2010). *Handbook of aqueous solubility data*. CRC press.

Hlabangana, L., & Memeza, S. (2018). Ion-pair isocratic simultaneous determination of broad spectrum antibiotics in environmental samples by HPLC with UV detection. *Environmental Nanotechnology, Monitoring & Management*, *10*, 104-111.

Hrioua, A., Loudiki, A., Farahi, A., Bakasse, M., Lahrich, S., Saqrane, S. et al. (2021). Recent advances in electrochemical sensors for amoxicillin detection in biological and environmental samples. *Bioelectrochemistry*, *137*, 107687.

Injac, R., Kočevar, N., & Štrukelj, B. (2009). Optimized method for determination of amoxicillin, ampicillin, sulfamethoxazole, and sulfacetamide in animal feed by micellar electrokinetic capillary chromatography and comparison with high-performance liquid chromatography. *Croatica Chemica Acta*, *82*(3), 685-694.

Jafari, S., Dehghani, M., Nasirizadeh, N., Baghersad, M. H., & Azimzadeh, M. (2019). Label-free electrochemical detection of Cloxacillin antibiotic in milk samples based on molecularly imprinted polymer and graphene oxide-gold nanocomposite. *Measurement*, *145*, 22-29.

Jalili, V., Barkhordari, A., & Ghiasvand, A. (2020). A comprehensive look at solid phase microextraction technique: A review of reviews. *Microchemical Journal*, *152*, 104319.

Ji, K., Kho, Y., Park, C., Paek, D., Ryu, P., Paek, D. et al. (2010). Influence of water and food consumption on inadvertent antibiotics intake among general population. *Environmental research*, *110*(7), 641-649.

Jia, X., Zhao, P., Ye, X., Zhang, L., Wang, T., Chen, Q. et al. (2017). A novel metal-organic framework composite MIL-101 (Cr)@ GO as an efficient sorbent in dispersive micro-solid phase extraction coupling with UHPLC-MS/MS for the determination of sulfonamides in milk samples. *Talanta*, *169*, 227-238.

Koesukwiwat, U., Jayanta, S., & Leepipatpiboon, N. (2007). Validation of a liquid chromatography–mass spectrometry multi-residue method for the simultaneous determination of sulfonamides, tetracyclines, and pyrimethamine in milk. *Journal of chromatography A*, *1140*(1-2), 147-156.

Kokulnathan, T., Ashok Kumar, E., & Wang, T. J. (2020). Design and in situ synthesis of titanium carbide/boron nitride nanocomposite: Investigation of electrocatalytic activity for the sulfadiazine sensor. *ACS Sustainable Chemistry & Engineering*, *8*(33), 12471-12481.

Kolpin, D. W., Furlong, E. T., Meyer, M. T., Thurman, E. M., Zaugg, S. D., Barber, L. B. et al. (2002). Pharmaceuticals, hormones, and other organic wastewater contaminants in US streams, 1999− 2000: A national reconnaissance. *Environmental science & technology*, *36*(6), 1202-1211.

Kuczyńska, J., & Nieradko-Iwanicka, B. (2021). Future prospects of ketoprofen in improving the safety of the gastric mucosa. *Biomedicine & Pharmacotherapy, 139*, 111608.

Leibovici, L., Paul, M., Garner, P., Sinclair, D. J., Afshari, A., Pace, N. L. et al. (2016). Addressing resistance to antibiotics in systematic reviews of antibiotic interventions. *Journal of Antimicrobial Chemotherapy*, *71*(9), 2367-2369.

Li, C., & Wu, K. (2021). Cu-BTC frameworks based electrochemical sensor for hazardous malachite green in aquaculture. *Analytica Chimica Acta*, *1162*, 338473.

Li, L., Chen, Y., Yang, L., Wang, Z., & Liu, H. (2020). Recent advances in applications of metal–organic frameworks for sample preparation in pharmaceutical analysis. *Coordination Chemistry Reviews*, *411*, 213235.

Li, M., Huang, W., Tang, B., Song, F., Lv, A., & Ling, X. (2019). Preparation of a composite material AC/Cu-BTC with improved water stability and n-hexane vapor adsorption. *Journal of Nanomaterials*, *2019*, 5429264.

Li, W., Wang, R., & Chen, Z. (2018). Zr-based metal-organic framework-modified cotton for solid phase micro-extraction of non-steroidal anti-inflammatory drugs. *Journal of Chromatography a*, *1576*, 19-25.

Li, X., Zhou, H., Qi, F., Niu, X., Xu, X., Qiu, F. et al. (2018). Three hidden talents in one framework: a terephthalic acid-coordinated cupric metal–organic framework with cascade cysteine oxidase-and peroxidase-mimicking activities and stimulus-responsive fluorescence for cysteine sensing. *Journal of Materials Chemistry B*, *6*(39), 6207-6211.

Li, Y., Wu, X., Li, Z., Zhong, S., Wang, W., Wang, A. et al. (2015). Fabrication of $CoFe_2O_4$–graphene nanocomposite and its application in the magnetic solid phase extraction of sulfonamides from milk samples. *Talanta*, *144*, 1279-1286.

Lirio, S., Liu, W. L., Lin, C. L., Lin, C. H., & Huang, H. Y. (2016). Aluminum based metal-organic framework-polymer monolith in solid-phase microextraction of penicillins in river water and milk samples. *Journal of Chromatography A*, *1428*, 236-245.

Liu, H., Fan, H., Dang, S., Li, M., & Yu, H. (2020). A Zr-MOF@ GO-coated fiber with high specific surface areas for efficient, green, long-life solid-phase microextraction of nonsteroidal anti-inflammatory drugs in water. *Chromatographia*, *83*(9), 1065-1073.

Liu, S., Li, S., Yang, W., Gu, F., Xu, H., Wang, T. et al. (2019). Magnetic nanoparticle of metal-organic framework with core-shell structure as an adsorbent for magnetic solid phase extraction of non-steroidal anti-inflammatory drugs. *Talanta*, *194*, 514-521.

Liu, X., Tong, Y., & Zhang, L. (2020). Tailorable yolk-shell $Fe_3O_4$@ graphitic carbon submicroboxes as efficient extraction materials for highly sensitive determination of trace sulfonamides in food samples. *Food chemistry*, *303*, 125369.

Lord, H., & Pawliszyn, J. (2000). Microextraction of drugs. *Journal of Chromatography A*, *902*(1), 17-63.

Madikizela, L. M., & Chimuka, L. (2016). Determination of ibuprofen, naproxen and diclofenac in aqueous samples using a multi-template molecularly imprinted polymer as selective adsorbent for solid-phase extraction. *Journal of pharmaceutical and biomedical analysis*, *128*, 210-215.

Mahmood, T., Saddique, M. T., Naeem, A., Westerhoff, P., Mustafa, S., & Alum, A. (2011). Comparison of different methods for the point of zero charge determination of NiO. *Industrial & Engineering Chemistry Research*, *50*(17), 10017-10023.

Majdinasab, M., Mishra, R. K., Tang, X., & Marty, J. L. (2020). Detection of antibiotics in food: New achievements in the development of biosensors. *TrAC Trends in Analytical Chemistry*, *127*, 115883.

Majdinasab, M., Yaqub, M., Rahim, A., Catanante, G., Hayat, A., & Marty, J. L. (2017). An overview on recent progress in electrochemical biosensors for antimicrobial drug residues in animal-derived food. *Sensors*, *17*(9), 1947.

Malafatti, J. O. D., de Oliveira Ruellas, T. M., Meirelles, M. R., Thomazi, A. C., Renda, C. G., & Paris, E. C. (2021). Nanocarriers of $Eu^{3+}$ doped silica nanoparticles modified by APTES for luminescent monitoring of cloxacillin. *AIMS Materials Science*, *8*(5), 760-775.

Manousi, N., Kabir, A., Furton, K. G., Samanidou, V. F., & Zacharis, C. K. (2022). Exploiting the capsule phase microextraction features in bioanalysis: Extraction of ibuprofen from urine samples. *Microchemical Journal*, *172*, 106934.

Marx, S., Kleist, W., & Baiker, A. (2011). Synthesis, structural properties, and catalytic behavior of Cu-BTC and mixed-linker Cu-BTC-PyDC in the oxidation of benzene derivatives. *Journal of catalysis*, *281*(1), 76-87.

Melis, S. (2007). Ketoprofen. *xPharm: The Comprehensive Pharmacology Reference* (pp. 1-7). Elsevier Inc..

Mestre, A. S., & Carvalho, A. P. (2019). Photocatalytic degradation of pharmaceuticals carbamazepine, diclofenac, and sulfamethoxazole by semiconductor and carbon materials: a review. *Molecules, 24*(20), 3702.

Mirzajani, R., Kardani, F., & Ramezani, Z. (2019). Preparation and characterization of magnetic metal–organic framework nanocomposite as solid-phase microextraction fibers coupled with high-performance liquid chromatography for determination of non-steroidal anti-inflammatory drugs in biological fluids and tablet formulation samples. *Microchemical Journal, 144*, 270-284.

Mitra, S. (2003). *Sample preparation techniques in analytical chemistry*.

Ngangom, B. L., Tamunjoh, S. S. A., & Boyom, F. F. (2019). Antibiotic residues in food animals: Public health concern. *Acta Ecologica Sinica*, *39*(5), 411-415.

Pang, G. F. (2018). *Analytical Methods for Food Safety by Mass Spectrometry: Volume I Pesticides*. Academic Press.

Phuong, N. T., Buess-Herman, C., Thom, N. T., Nam, P. T., Dai Lam, T., & Thanh, D. T. M. (2016). Synthesis of Cu-BTC, from Cu and benzene-1, 3, 5-tricarboxylic acid ($H_3$BTC), by a green electrochemical method. *Green Processing and Synthesis*, *5*(6), 537-547.

Pu, M., Niu, J., Brusseau, M. L., Sun, Y., Zhou, C., Deng, S. et al. (2020). Ferrous metal-organic frameworks with strong electron-donating properties for persulfate activation to effectively degrade aqueous sulfamethoxazole. *Chemical Engineering Journal*, *394*, 125044.

Raich-Montiu, J., Beltrán, J. L., Prat, M. D., & Granados, M. (2010). Studies on the extraction of sulfonamides from agricultural soils. *Analytical and bioanalytical chemistry*, *397*(2), 807-814.

Rainsford, K. D. (2009). Ibuprofen: pharmacology, efficacy and safety. *Inflammopharmacology*, *17*(6), 275-342.

Rocío-Bautista, P., Taima-Mancera, I., Pasán, J., & Pino, V. (2019). Metal-organic frameworks in green analytical chemistry. *Separations*, *6*(3), 33.

Rodrıguez, I., Carpinteiro, J., Quintana, J. B., Carro, A. M., Lorenzo, R. A., & Cela, R. (2004). Solid-phase microextraction with on-fiber derivatization for the analysis of anti-inflammatory drugs in water samples. *Journal of Chromatography A*, *1024*(1-2), 1-8.

Rosset, M., Sfreddo, L. W., Hidalgo, G. E. N., Perez-Lopez, O. W., & Feris, L. A. (2019). Adsorbents derived from hydrotalcites for the removal of diclofenac in wastewater. *Applied Clay Science*, *175*, 150-158.

Sabry, E., Mohamed, H. A., Ewies, E. F., Kariuki, B. M., Darwesh, O. M., & Bekheit, M. S. (2022). Microwave-assisted synthesis of novel sulfonamide-based compounds bearing α-aminophosphonate and their antimicrobial properties. *Journal of Molecular Structure*, 133553.

Safari, M., Shahlaei, M., Yamini, Y., Shakorian, M., & Arkan, E. (2018). Magnetic framework composite as sorbent for magnetic solid phase extraction coupled with high performance liquid chromatography for simultaneous extraction and determination of tricyclic antidepressants. *Analytica chimica acta*, *1034*, 204-213.

Sahebi, H., Konoz, E., Ezabadi, A., Niazi, A., & Ahmadi, S. H. (2020). Simultaneous determination of five penicillins in milk using a new ionic liquid-modified magnetic nanoparticle based dispersive micro-solid phase extraction followed by ultra-performance liquid chromatography-tandem mass spectrometry. *Microchemical Journal*, *154*, 104605.

Salihu, S., Yusof, N. A., Mohammad, F., Abdullah, J., & Al-Lohedan, H. A. (2019). Nickel nanoparticle-modified electrode for the electrochemical sensory detection of penicillin G in bovine milk samples. *Journal of Nanomaterials*, 2019.

Samanidou, V., Michaelidou, K., Kabir, A., & Furton, K. G. (2017). Fabric phase sorptive extraction of selected penicillin antibiotic residues from intact milk followed by high performance liquid chromatography with diode array detection. *Food chemistry*, *224*, 131-138.

Sarafraz-Yazdi, A., Amiri, A., Rounaghi, G., & Eshtiagh-Hosseini, H. (2012). Determination of non-steroidal anti-inflammatory drugs in water samples by solid -phase microextraction based sol–gel technique using poly (ethylene glycol) grafted multi-walled carbon nanotubes coated fiber. *Analytica chimica acta*, *720*, 134-141.

Schlesinger, M., Schulze, S., Hietschold, M., & Mehring, M. (2010). Evaluation of synthetic methods for microporous metal–organic frameworks exemplified by the competitive formation of $[Cu_2(btc)_3(H_2O)_3]$ and $[Cu_2(btc)(OH)(H_2O)]$. *Microporous and Mesoporous Materials*, *132*(1-2), 121-127.

Shafiei-Navid, S., Hosseinzadeh, R., & Ghani, M. (2022). Solid-phase extraction of nonsteroidal anti-inflammatory drugs in urine and water samples using acidic calix [4] arene intercalated in LDH followed by quantification via HPLC-UV. *Microchemical Journal*, *183*, 107985.

Shih, Y. H., Wang, K. Y., Singco, B., Lin, C. H., & Huang, H. Y. (2016). Metal–organic framework–polymer composite as a highly efficient sorbent for sulfonamide adsorption and desorption: effect of coordinatively unsaturated metal site and topology. *Langmuir*, *32*(44), 11465-11473.

Shirani, M., Akbari-Adergani, B., Rashidi Nodeh, H., & Shahabuddin, S. (2020). Ultrasonication-facilitated synthesis of functionalized graphene oxide for ultrasound-assisted magnetic dispersive solid-phase extraction of amoxicillin, ampicillin, and penicillin G. *Microchimica Acta*, *187*(11), 1-11.

Soleimanirad, E., Badameh, A., Raoufi, A., & Ebrahimi, M. (2022). Simultaneous determination of four antibiotics in human urine and hair samples employing a simple and efficient dispersive micro solid-phase extraction-high performance liquid chromatography. *Pharmacological Reports*, 1-14.

Soledad-Rodríguez, B., Fernández-Hernando, P., Garcinuño-Martínez, R. M., & Durand-Alegría, J. S. (2017). Effective determination of ampicillin in cow milk using a molecularly imprinted polymer as sorbent for sample preconcentration. *Food Chemistry*, *224*, 432-438.

Sriram, B., Baby, J. N., Hsu, Y. F., Wang, S. F., Benadict Joseph, X., George, M. et al. (2021). $MnCo_2O_4$ Microflowers anchored on P-doped g-$C_3N_4$ nanosheets as an electrocatalyst for voltammetric determination of the antibiotic drug sulfadiazine. *ACS Applied Electronic Materials*, *3*(9), 3915-3926.

Sule, R., & Mishra, A. K. (2019). Synthesis of mesoporous MWCNT/HKUST-1 composite for wastewater treatment. *Applied Sciences*, *9*(20), 4407.

Sun, X., Xia, Q., Zhao, Z., Li, Y., & Li, Z. (2014). Synthesis and adsorption performance of MIL-101 (Cr)/graphite oxide composites with high capacities of n-hexane. *Chemical engineering journal*, *239*, 226-232.

Sunsandee, N., Ramakul, P., Phatanasri, S., & Pancharoen, U. (2020). Biosorption of dicloxacillin from pharmaceutical waste water using tannin from Indian almond leaf : Kinetic and equilibrium studies. *Biotechnology Reports*, *27*, e00488.

Suresh, K., Minkov, V. S., Namila, K. K., Derevyannikova, E., Losev, E., Nangia, A. et al. (2015). Novel synthons in sulfamethizole cocrystals: structure–property relations and solubility. *Crystal Growth & Design*, *15*(7), 3498-3510.

Tao, X., Pan, P., Huang, T., Chen, L., Ji, H., Qi, J. et al. (2020). In-situ construction of Co $(OH)_2$ nanoparticles decorated urchin-like $WO_3$ for highly efficient degradation of sulfachloropyridazine via peroxymonosulfate activation: Intermediates and DFT calculation. *Chemical Engineering Journal*, *395*, 125186.

Tran, V. A., Nguyen, T. L. H., & Doan, V. D. (2021). Fabrication of $Fe_3O_4$/CuO@ C composite from MOF-based materials as an efficient and magnetically separable photocatalyst for degradation of ciprofloxacin antibiotic. *Chemosphere*, *270*, 129417.

Trucillo, P., Ferrari, P. F., Campardelli, R., Reverchon, E., & Perego, P. (2020). A supercritical assisted process for the production of amoxicillin-loaded liposomes for antimicrobial applications. *The Journal of Supercritical Fluids*, *163*, 104842.

Vardanyan, R., & Hruby, V. (2006). *Synthesis of essential drugs*. Elsevier.

Wang, H., Wang, B., Zhao, Q., Zhao, Y., Fu, C., Feng, X. et al. (2015). Antibiotic body burden of Chinese school children: a multisite biomonitoring-based study. *Environmental science & technology*, *49*(8), 5070-5079.

Wang, W., Saeed, A., He, J., Wang, Z., Zhan, D., Li, Z. et al. (2020). Bio-inspired porous helical carbon fibers with ultrahigh specific surface area for super-efficient removal of sulfamethoxazole from water. *Journal of Colloid and Interface Science*, *578*, 304-314.

Wang, X., Yang, L., Zhang, J., Wang, C., & Li, Q. (2014). Preparation and characterization of chitosan–poly (vinyl alcohol)/bentonite nanocomposites for adsorption of Hg (II) ions. *Chemical Engineering Journal*, *251*, 404-412.

Wang, Y. Q., Yue, Q., Qi, Y., Wang, K., Sun, Q., & Gao, E. Q. (2013). Manganese (II), iron (II), and mixed-metal metal–organic frameworks based on chains with mixed carboxylate and azide bridges: magnetic coupling and slow relaxation. *Inorganic Chemistry*, *52*(8), 4259-4268.

Wojcieszyńska, D., & Guzik, U. (2020). Naproxen in the environment: its occurrence, toxicity to nontarget organisms and biodegradation. *Applied microbiology and biotechnology*, *104*(5), 1849-1857.

Xia, L., Liu, L., Lv, X., Qu, F., Li, G., & You, J. (2017). Towards the determination of sulfonamides in meat samples: A magnetic and mesoporous metal-organic framework as an efficient sorbent for magnetic solid phase extraction combined with high-performance liquid chromatography. *Journal of Chromatography A*, *1500*, 24-31.

Xinbao, L., Yating, H., Ali, F., Nan, S., & Hongkun, Z. (2019). Investigation on Preferential Solvation, Transfer Properties and Solvent Effect of Sulfachloropyridazine in Aqueous Co-solvent Solutions of Some Alcohols. *Journal of Solution Chemistry*, *48*(10), 1413-1435.

Yahaya, N., Mitome, T., Nishiyama, N., Sanagi, M. M., Wan Ibrahim, W. A., & Nur, H. (2013). Rapid dispersive micro-solid phase extraction using mesoporous carbon COU-2 in the analysis of cloxacillin in water. *Journal of Pharmaceutical Innovation*, *8*(4), 240-246.

Yahaya, N., Sanagi, M. M., Mitome, T., Nishiyama, N., Ibrahim, W. A. W., & Nur, H. (2015). Dispersive micro-solid phase extraction combined with high-performance liquid chromatography for the determination of three penicillins in milk samples. *Food Analytical Methods*, *8*(5), 1079-1087.

Yuan, Y., Li, D., Wang, C., Chen, S., Kong, M., Deng, Z. et al. (2019). Structural features of sulfamethizole and its cocrystals: beauty within. *Crystal Growth & Design*, *19*(12), 7185-7192.

Yuvali, D., Narin, I., Soylak, M., & Yilmaz, E. (2020). Green synthesis of magnetic carbon nanodot/graphene oxide hybrid material ($Fe_3O_4$@ C-nanodot@ GO) for magnetic solid phase extraction of ibuprofen in human blood samples prior to HPLC-DAD determination. *Journal of pharmaceutical and biomedical analysis*, *179*, 113001.

Zeynizadeh, B., Rahmani, S., & Tizhoush, H. (2020). The immobilized Cu nanoparticles on magnetic montmorillonite (MMT@ $Fe_3O_4$@Cu): As an efficient and reusable nanocatalyst for reduction and reductive-acetylation of nitroarenes with $NaBH_4$. *Polyhedron*, *175*, 114201.

Zhang, H. Y., Zhang, Z. R., Yang, C., Ling, L. X., Wang, B. J., & Fan, H. L. (2018). A Computational Study of the Adsorptive Removal of $H_2S$ by MOF-199. *Journal of Inorganic and Organometallic Polymers and Materials*, *28*(3), 694-701.

Zhang, M., Zeng, J., Wang, Y., & Chen, X. (2013). Developments and trends of molecularly imprinted solid-phase microextraction. *Journal of chromatographic science*, *51*(7), 577-586.

Zhang, R., Sun, P., Boyer, T. H., Zhao, L., & Huang, C. H. (2015). Degradation of pharmaceuticals and metabolite in synthetic human urine by UV, UV/$H_2O_2$, and UV/PDS. *Environmental science & technology*, *49*(5), 3056-3066.

Zhang, X., Zhang, D., Zhao, T., Chen, L., & He, K. (2020). Development and application of a novel immunoaffinity test column assay for visual detection of cloxacillin residues in animal-derived food samples. *Journal of Food Measurement and Characterization*, *14*(4), 1884-1891.

Zhao, X., Lü, L., Zhu, M., Liu, H., He, J., & Zheng, F. (2021). Development of hydrophilic magnetic molecularly imprinted polymers for the dispersive solid-phase extraction of sulfonamides from animal-derived samples before HPLC detection. *Journal of Separation Science*, *44*(12), 2399-2407.

Zhou, L., Yang, X., Ji, Y., & Wei, J. (2019). Sulfate radical-based oxidation of the antibiotics sulfamethoxazole, sulfisoxazole, sulfathiazole, and sulfamethizole: the role of five-membered heterocyclic rings. *Science of the Total Environment*, *692*, 201-208.

Zhu, L., Shi, Z., Deng, L., & Duan, Y. (2021). Efficient degradation of sulfadiazine using magnetically recoverable $MnFe_2O_4$/δ-$MnO_2$ hybrid as a heterogeneous catalyst of peroxymonosulfate. *Colloids and Surfaces A: Physicochemical and Engineering Aspects*, *609*, 125637.

Zuo, L., He, R., Wang, L., & Wei, Y. (2022). Phosphorescence aptasensing system for sulfadimethoxine with petal-like $MoS_2$ nanosheets for signal amplification. *Sensors and Actuators B: Chemical, 360*, 131639.